

Magnetostratigraphy of the Lower Carboniferous



Bc. Tereza Kameníková

This dissertation is submitted for the

Masters by Research degree

April 2020

Lancaster Environment Centre

Declaration

This thesis has not been submitted in support of an application for another degree at this or any other university. It is the result of my own work and includes nothing that is the outcome of work done in collaboration except where specifically indicated. Many of the ideas in this thesis were the product of discussion with my supervisor Dr Mark Hounslow.

Excerpts of this thesis have been published in the following conference manuscripts and academic publications.

Kamenikova, T., Hounslow, M. W., Sprain, C., et al. (2019) 'Extracting Lower Carboniferous Magnetisations from Troublesome UK Limestones', in 27th IUGG General Assembly.

Kamenikova, T., Hounslow, M. W., van der Boon, A., Sprain, C. and Biggin, A. J. (2019) 'Magnetostratigraphy of Cumbrian Lower Carboniferous: Meathop Quarry', in Lancaster Environment Centre postgraduate conference.

Kamenikova, T., Hounslow, M. W., van der Boon, A., Sprain, C., Wójcik, K., et al. (2019) 'Tournaisian-Viséan magnetostratigraphy: new data from British and Polish limestones', in 3rd International Congress on Stratigraphy, p. 206.

Bc. Tereza Kameníková

Lancaster University, UK

Acknowledgements

Thank you to Dr Vassil Karloukovski, Courtney Sprain, Annique van der Boon and rest of the Liverpool team for your help and patience.

Thank Alex Wild, Ondrej Sysel and Ondrej Kozel for your help, patience, support and understanding.

Abstract

Geomagnetic polarity reversals studied by magnetostratigraphy have been described well in the Cenozoic and Mesozoic, unfortunately, there are still many data gaps in the Palaeozoic where the magnetostratigraphic record is not easy to correlate or is unknown. One of those is during the Carboniferous System.

The magnetostratigraphy of Carboniferous rocks is quite complicated, since overprints produced during the Kiaman Superchron (late Carboniferous-mid Permian) tend to be the strongest components and primary remanence very weak or completely overprinted.

This study focused on sediments from S. Cumbria, in North-West England. The studied limestones were on the western edge of the Craven Basin and the NE fringe of the Irish Sea Basin. Two localities in South Cumbria were sampled, the Martin Limestone Formation in Meathop Quarry (50 m profile) and Urswick Limestone Fm in Trowbarrow Quarry (183m) together covering the lower and upper Visean, with a gap in the middle Visean. The sedimentation rate is approx. 30 kyrs/m.

Detailed profiles were hand sampled at ~one-meter intervals, conducted with magnetic susceptibility sampling at ~25 centimetres intervals. For paleomagnetic measurements, most samples were thermally demagnetized up to 300-400°C and then AF (alternating field) demagnetization was used. This best differentiated the original magnetic signal from the later Kiaman overprint, and limited thermal alteration. For the time correlation, biostratigraphy using foraminifera was used for Meathop Quarry and carbon isotopes for Trowbarrow Quarry.

Results show a Carboniferous dual polarity magnetisation clearly distinguished from the younger Kiaman component. The first detailed magnetostratigraphy through a part of the Visean is presented. The dominant carrier of remanence is magnetite at Meathop Quarry

(over 40% of samples) with 7 reversals. At Trowbarrow Quarry, magnetite is dominant in the reversed polarity samples (50% of samples) and hematite for normal polarity samples (over 35% of samples), showing 18 reversals. These results fill a gap in magnetostratigraphic research providing the first detailed magnetostratigraphic study of the Lower Carboniferous in Europe.

Key words

Magnetostratigraphy, Carboniferous, Earth dynamo, Visean, Magnetic field, Geomagnetism, Depositional magnetism, Limestones, Cumbria, Craven Basin

Contents

1 INTRODUCTION	22
2 LITERATURE REVIEW	24
2.1 THE GEOMAGNETIC FIELD	24
2.1.1 <i>Secular and palaeosecular variations</i>	26
2.1.2 <i>Apparent polar wander</i>	28
2.1.3 <i>Magnetic reversals</i>	29
2.1.4 <i>Geological and Geomagnetic polarity time scale</i>	29
2.1.5 <i>Magnetism and its types</i>	32
2.1.6 <i>Magnetization in sediments and limestones</i>	33
2.1.7 <i>Existing magnetostratigraphic data for the Mississippian</i>	35
2.1.8 <i>Geological background</i>	39
2.1 MISSISSIPPIAN IN NORTHERN ENGLAND	41
2.2 BIOSTRATIGRAPHY OF THE UNITS IN SOUTH CUMBRIA AND NORTH LANCASHIRE	47
2.2.1 <i>Conodont zonation</i>	47
2.2.2 <i>Foraminifera zonation</i>	50
2.2.3 <i>Brachiopod zonation and Coral zonation</i>	52
2.3 THE CARBON ISOTOPE STRATIGRAPHY	53
3 METHODS	55
3.1 LOCATION AND AREAS OF SAMPLING	55
3.1.1 <i>Meathop Quarry</i>	58
3.1.2 <i>Trowbarrow Quarry</i>	61
3.2 SAMPLING AND SAMPLE PREPARATION	67
3.2.1 <i>Fieldwork sampling</i>	67
3.2.2 <i>Laboratory sample preparations</i>	68
3.3 MEASUREMENTS	73
3.3.1 <i>Susceptibility sample measurements</i>	73
3.3.2 <i>Palaeomagnetic measurements</i>	73
3.3.3 <i>Biostratigraphical analysis of Foraminifera</i>	75
	11

3.3.4 <i>Isotopic measurements</i>	76
3.4 DATA PROCESSING	77
3.4.1 <i>GM4 edit software</i>	77
3.4.2 <i>Remasoft software</i>	77
4 RESULTS	79
4.1 MEATHOP QUARRY	79
4.1.1 <i>Sedimentary description</i>	90
4.1.2 <i>Microfossil biostratigraphy</i>	91
4.1.3 <i>Magnetostratigraphy, magnetic susceptibility and mineral origin of the magnetism</i>	93
4.2 TROWBARROW QUARRY	104
4.2.1 <i>Geological features and logs</i>	104
4.2.2 <i>Magnetostratigraphy, magnetic susceptibility and mineral origin of the magnetism</i>	110
5 DISCUSSION	124
5.1 FILLING "THE GAP"	124
5.2 REVERSAL FREQUENCY	126
6 CONCLUSION	127
7 REFERENCES	129

List of Equations

EQUATION 1 GAUSS LAW FOR MAGNETISM. UPPER EQUATION STATES THAT CHANGE IN THE ELECTRIC FLUX DENSITY D EQUALS THE VOLUMETRIC ELECTRIC CHARGE DENSITY. THE LOWER EQUATION SAYS THAT THE CHANGE OF MAGNETIC FLUX DENSITY B IS 0 (SLEEP AND FUJITA, 1997). 25

EQUATION 2 GEOCENTRIC AXIAL DIPOLE EQUATION. H_h IS HORIZONTAL COMPONENT OF MAGNETIC FIELD, M IS MAGNETIC DIPOLE, Λ GEOGRAPHIC LATITUDE, AND R_e IS EARTH RADIUS (BUTLER, 1992). 26

List of Figures

FIGURE 1 VIZUALIZATION OF THE BAR MAGNET IN CENTRE OF THE EARTH (LANG, 2010).	25
FIGURE 2 THE CHANGE OF MAGNETIC DECLINATION IN LONDON IN THE PAST 5 CENTURIES (GEOLOGICAL SURVEY OF CANADA, 2018).	27
FIGURE 3 VISUALIZATION OF APPARENT POLAR WANDER, WITH CONNECTION TO ORIGINAL PALEOMAGNETIC INCLINATION (KHATTAK, 2018).	28
FIGURE 4 GEOMAGNETIC POLARITY TIMESCALE OF THE YOUNGEST 2.5M A (MEGA ANNUM = MILLION YEARS AGO). BLACK PARTS ARE NORMAL POLARITY, WHITE ONES REVERSED (<i>ICS - CHART/TIME SCALE</i> , 2019).	31
FIGURE 5 BURROWS PRODUCED BY BIOTURBATION, TROWBARROW QUARRY IN CUMBRIA, UK.	35
FIGURE 6 THE PALEOMAGNETIC REVERSAL RATES OVER TIME. THERE IS A SIGNIFICANT GAP IN THE LOWER AND MIDDLE CARBONIFEROUS (HOUNSLOW, DOMEIER AND BIGGIN, 2018).	36
FIGURE 7 PALEOMAGNETIC STRATIGRAPHY CHART FOR CARBONIFEROUS OF BRITISH ISLES, PRE REMAGNETISATION (WHITE) (PALMER ET AL., 1985), RED MARKS THE VISEAN. AND MAGNETOSTRATIGRAPHIC CHART WITH PRESENT DATA (BLACK IS NORMAL AND WHITE REVERSED POLARITY) (OGG ET AL., 2008).	38
FIGURE 8 CHRONOSTRATIGRAPHIC CHART OF THE CARBONIFEROUS (COHEN ET AL., 2018).	40
FIGURE 9 GEOLOGY OF THE ARNSIDE AREA (THOMPSON AND POOLE, 2018).	42
FIGURE 10 GEOLOGICAL MAP OF THE CARBONIFEROUS SEDIMENTS IN THE AREA FROM CUMBRIA TO THE NORTH PENNINES (WATERS ET AL., 2012).	43
FIGURE 11 GEOLOGICAL SUCCESSION ON SOUTH CUMBRIA AND NORTH LANCASHIRE (ADAMS ET AL., 1990).	44
FIGURE 12 THE CARBONIFEROUS REGIONAL AND INTERNATIONAL STAGES WITH LITHOSTRATIGRAPHIC UNITS OF CUMBRIA AND ADJACENT PART OF NORTHERN ENGLAND (WATERS ET AL., 2017).	45
FIGURE 13 MAP OF THE SILVERDALE DISTURBANCES, MAPPING THE STUDIED OF TROWBARROW QUARRY – MARKED BY THE WHITE CIRCLE (THOMPSON AND POOLE, 2018)	46
FIGURE 14 LIVING CONODONT ANIMAL, VISUALIZATION (BONADONNA, 2018).	48
FIGURE 15 CONODONT FOSSILS (<i>CONODONT COLLECTION, NATURAL HISTORY MUSEUM</i> , 2018).	48
FIGURE 16 THE CONODONT ALTERATION INDEX (CAI) COMPARATION WITH CONODONT COLOUR AND BURRIAL TEMPERATURE (<i>SENCKENBERG WORLD OF BIODIVERSITY</i> , 2018).	49
FIGURE 17 FORAMINIFERA FROM THE LOWER URSWICK LIMESTONE (DINATIAN) (ATHERSUCH AND STRANK, 1989).	50
FIGURE 18 FAUNAL ZONATIONS OF DINATIAN (RILEY, 1993).	52

FIGURE 19: VARIATIONS OF $\delta^{13}\text{C}$ (CARBONATE CARBON) WITHIN THE CARBONIFEROUS (SALTZMAN AND THOMAS, 2012).	
THE STRONG NEGATIVE $\delta^{13}\text{C}$ EXCURSION IN THE LATE VISEAN IS THE TARGET IN TROWBARROW QUARRY.	54
FIGURE 20 GEOLOGY MAP OF THE NORTH-WEST OF UK, THE STUDIED AREA IS MARKED BY BLACK RECTANGLE (DEAN, BROWNE, WATERS, & POWELL, 2011).	55
FIGURE 21 LOCATION OF STUDIED AREA. ON TOP MAP, IS AREA OF CUMBRIA VISIBLE IN YELLOW RECTANGLE. ON BOTTOM MAP IS CUMBRIA AREA WITH LOCATION OF STUDIED MEATHOP QUARRY IN YELLOW ELLIPSE AND TROWBARROW QUARRY IN BLUE ELLIPSE (GOOGLE MAPS, 2019).	56
FIGURE 22 PALEOGEOGRAPHIC MAP. THE STUDIED AREA IN CARBONIFEROUS (440MA AND 420 MA), MARKED WITH RED DOT – LEFT COLUMN FIGURE. TODAYS GEOGRAPHICAL SETTING VISUALISED AS ORIGINAL SOURCE CONTINETS (AVALONIA AND LAURENTIA). STUDIED AREA (RED DOT) – TOP FIGURE. BOTH FIGURES (SMIT ET AL., 2018).	57
FIGURE 23 LOCATION OF BRITAIN (RED DOT) IN EARLY CARBONIFEROUS 356 MA (SCOTESE, 2002).	58
FIGURE 24 <i>MEATHOP QUARRY ENTRANCE OUTCROP. AS IT IS POSSIBLE TO SEE, THE QUARRY IS EASILY ACCESSIBLE DUE WAY OF MINING IN THIS LOCATION, THEY LEFT SECTIONS STEP-LIKE. EACH STEP IS ABOUT METER HIGH.</i>	59
FIGURE 25 <i>PICTURE ON TOP SHOWS THE MEATHOP QUARRY WALL IN THE ENTRANCE AREA. THE WALL ITSELF APPEAR STEPS LIKE, IT IS REFLECT THE WAY HOW LIMESTONES WERE MINED IN THE HISTORY. PICTURE IN THE MIDDLE (SOUTH WEST VIEW) AND BOTTOM (NORTH WESTERN VIEW) SHOWS THE AREA SURROUNDINGS.</i>	60
FIGURE 26 TROWBARROW QUARRY, THE ENTRANCE.	61
FIGURE 27 MAP OF THE TROWBARROW QUARRY BY (AONB UNIT, 2009). DIRECTION OF SAMPLING IS SHOWED BY THE RED ARROWS. ONES WITH DOTTED LINES ARE PLACES WHICH WERE SKIPPED DUE THE SAME LITHOLOGY AS PREVIOUSLY SAMPLED AREA (DUE HE VERTICAL BEDDING). ALL SAMPLED AREA HAS OVER 170M, SAMPLING TOOK ABOUT 3 WEEKS OF WORK.	62
FIGURE 28 TROWBARROW QUARRY MAIN SITE.	63
FIGURE 29 TROWBARROW QUARRY SITE WITH VISIBLE VERTICAL BEDDING.	63
FIGURE 30 TOP LEFT OVERALL VIEW OF VERTICAL BEDDING. TOP RIGHT SPACE IN BETWEEN 2 OUTCROPS, DUE THE WEATHERED-OUT SHALE, SPACE HAS ABOUT 4M. BOTTOM LEFT, SIGNATURE RED LIMESTONES, RED COLOUR IS DUE PALEO SOIL HORIZON ABUNDANT IN THIS PART, IT IS ENRICHED BY HAEMATITE. BOTTOM RIGHT, ALREADY SAMPLED AREA (WHITE DOTS).	64
FIGURE 31 DIVERSITY OF THE TROWBARROW QUARRY. ON TOP, IT IS VISIBLE, THAT SOME AREAS WERE NOT EASILY ACCESSIBLE.	65

- FIGURE 32 ON TOP CAN BE SEEN A DENSITY OF SAMPLING IN THE QUARRIES. EACH SMALL WHITE SPOT IS APPROX. 25 CM FROM EACH OTHER, THERE WAS THE SUSCEPTIBILITY SAMPLE TAKEN FROM. BIG WHITE SPOT IS HAND SAMPLE FOR PALEOMAGNETIC MEASUREMENTS. THOSE ARE 1 M FROM EACH OTHER. 66
- FIGURE 33 THE BALANCING DEVICE, USED FOR MEASURING DIP AND BALANCING THE SAMPLES BEFORE PLASTERING. DEVICE HAS AIR BUBBLE IN THE WATER CAPSULE, AND MOVING POINTING ARROW, SHOWING THE DIP ON SCALE FROM 0 TO 180 DEGREES. ON THE RIGHT SIDE, IS THIS DEVICE USED IN FIELD, TO MARK THE SAMPLES AND MEASURE THE DIP AND STRIKE (PHOTO: MARK HOUNSLOW) 69
- FIGURE 34 ON THE LEFT SIDE IS PLUG OF LENGTH 5 CM, COMING AS A RESULT OF THE DRILLING PROCESS. THIS PLUG IS CUT FOR SMALLER PIECES, IN ORDER TO GET A FINAL SAMPLE. ON TOP RIGHT IS A CUBE SAMPLE, THIS TYPE OF SAMPLES IS ACHIEVED BY THE DIRECT CUTTING ON A ROCK SAW. THE DIMENSIONS ARE 2,5x2,5x2,5 CM. THIS METHOD IS USED FOR SAMPLES WHICH ARE FRACTURED OR HAVING ANY OTHER DEFECT AND CANNOT BE DRILLED. BOTTOM RIGHT, PICTURE OF RAPID 2G SAMPLE TABLE. 70
- FIGURE 35 PLASTERED SAMPLE: SAMPLE WAS FIRST BALANCED WITH THE BALANCING DEVICE IN THE ALUMINIUM TRAIL (GREY BASKET). THIS WAS STABILIZED IN ORIGINAL POSITION WITH OLD PLASTER WEDGES. THEN WE MIXED DENTAL PLASTER WITH WATER AND POUR IT IN TO THE EMPTY SPACES. AFTER HARDENING, FOLLOWING DAY, WE DRAW THE ARROWS, FOR EASIER ORIENTATION OD THE CORE, ONCE DRILLED. 71
- FIGURE 36 SUSCEPTIBILITY SAMPLES: A) SMALL CHIPS OF SAMPLES WERE PUT TO THE PLASTIC BAG AND MARKED WITH SAMPLE NUMBER. PREPARATION, IT WAS WASHED AND CRUSHED TO MIX OF SMALL GRAINS AND DUST. B) THIS WAS ROLLED TO SMALL CIGAR AND SEALED WITH CLEAR TAPE. 72
- FIGURE 37 THE EXAMPLE OF EXTRACTED DATA FROM REMASOFT SOFTWARE, SPECIMEN FROM TROWBARROW QUARRY, PART OF THE URSWICK LIMESTONE, SAMPLE 102. THE SPECIMEN SHOWS THE KIAMAN OVERPRINT IN STEPS 200°C, 250°C AND 300°C. AFTER THIS DEMAGNETIZATION CONTINUES TO IS THE NORMAL CARBONIFEROUS POLARITY UNTIL THE HEATING STEP 600°C WHERE SAMPLE ACQUIRES THE THERMAL ALTERATION (THIS IS DOCUMENTED BY THE INCREASE OF MAGNETIC SUSCEPTIBILITY). 78
- FIGURE 38 ORIGINAL MEATHOP QUARRY LOG, WITH CORELATED LEVELS OF THE STAGES , USED AS A PRELIMINARY INFORMATION FOR OUR CREATION OF THE LOG (LEVISTON, 1979). 79
- FIGURE 39 FOSSILS FOUND IN LOWER SECTION OF MEATHOP QUARRY. THESE WERE MOSTLY RESIDUALS OF BIOCLASTS OF BRACIOPODS AND CORALS IN LIMESTONE FORMING LAYERS OF WEATHERED OUT MATERIAL EASILY VISIBLE IN THE OUTCROP. 80
- FIGURE 40 CONTINUOUS EROSION CONTACT CORRESPONDING WITH LOCATION OF SAMPLE MQ38. 81

FIGURE 41 LAMINATED LIMESTONE WITH WEATHERED OUT FOSSIL BIOCLASTS. THOSE PHOTOGRAPHS ARE SHOT IN AREA OF SAMPLE MQ40.	82
FIGURE 42 LAMINATED SEDIMENTS OF STROMATOLITIC ORIGIN. THIS AREA IS IN BETWEEN SAMPLE MQ 41 AND MQ42.	83
FIGURE 43 FOSSILS FOUND IN TOP SECTION AROUND METER 50 OF MEATHOP QUARRY. MOSTLY RESIDUALS OF BIOCLASTS OF CORALS IN LIMESTONES FORMING LAYERS OF WEATHERED OUT MATERIAL EASILY VISIBLE IN THE OUTCROP AND NEPTUNE VEINS FILLED WITH DOLOSTONES.	84
FIGURE 44 THE KEY FOR AND LOG PRODUCED BY OUR LOCALITY DESCRIPTION, LITHOLOGICAL DESCRIPTION AND BEDDING MEASUREMENTS.	89
FIGURE 45 UPPER: MEATHOP QUARRY: THE DATASET OF PRESENCE AND ABSENCE OF FORAMINIFERA ASSEMBLAGES. BOTTOM: THE ZONATION OF FORAMINIFERA BY (KALVODA AND ET AL., 2011).	92
FIGURE 46 SHOWS THE STUDIED SECTION MEATHOP QUARRY WITH SURROUNDING AREAS SAMPLED FOR SIMILAR PROJECTS CORRESPONDING WITH TIME.	93
FIGURE 47 RESULTS OF MAGNETOSTRATIGRAPHIC MEASUREMENTS FORM MEATHOP QUARRY. BLACK STANDS FOR NORMAL POLARITY AND WHITE FOR REVERSED POLARITY. GREY COLOUR SHOWS UNCERTAINTY OF POLARITY.	96
FIGURE 48 SAMPLE MQ50.1. UPPER: PROJECTIONS IN GEOGRAPHIC COORDINATES AND TILT CORRECTED ON THE LOWER PART. ON EACH, THE RIGHT SIDE IS A ZIJDERVELD PROJECTION. IN THE STEREOSCOPIC PROJECTION IS A STRONG KIAMAN COMPONENT (RED CIRCLE) AND THEN FURTHER DEMAGNETIZATION TRENDS TOWARDS THE PRIMARY DIRECTION OF NORMAL POLARITY (GREEN CIRCLE). LEFT CHART SHOWS THE INTENSITY FOR THE DIFFERENT DEMAGNETISATION STEPS. RIGHT SIDE: THE MAGNETIC SUSCEPTIBILITY FOR EACH STEP.	97
FIGURE 49 SAMPLE MQ37.1. SEE (FIG 48) FOR DETAILS. IN THE STEREOSCOPIC PROJECTION IS A STRONG KIAMAN COMPONENT (RED CIRCLE) AND THEN A FURTHER DEMAGNETIZATION TRENDS TOWARDS THE PRIMARY DIRECTION OF NORMAL POLARITY (GREEN CIRCLE).	98
FIGURE 50 SAMPLE MQ13.2. SEE (FIG 48) FOR DETAILS. IN THE STEREOSCOPIC PROJECTION IS A STRONG KIAMAN COMPONENT (RED CIRCLE) AND THEN FURTHER DEMAGNETIZATION TOWARDS THE PRIMARY DIRECTION OF REVERSE POLARITY (BLUE CIRCLE).	99
FIGURE 51 SAMPLE MQ3.1. SEE (FIG 48) FOR DETAILS. IN THE STEREOSCOPIC PROJECTION IS A STRONG KIAMAN COMPONENT (RED CIRCLE) AND THEN FURTHER DEMAGNETIZATION TOWARDS THE PRIMARY DIRECTION OF REVERSE POLARITY (BLUE CIRCLE).	100
FIGURE 52 PERCENTAGE CONTRIBUTION OF DIFFERENT MINERALS TO INFERRED POLARITY. NORMAL POLARITY SPECIMENS HAVE A SLIGHTLY HIGHER ABUNDANCE OF MAGNETITE AS A MAGNETIC CARRIER THAN THE REVERSED POLARITY.	101

FIGURE 53 SUMMARY OF MEATHOP QUARRY MAGNETIC SUSCEPTIBILITY (LEFT), NRM INTENSITY (MIDDLE) AND MAGNETIC POLARITY (RIGHT) ON METER SCALE. BOTTOM -6M IS EQUAL TO 0. THERE WERE MEASURED 4 DIFFERENT SPECIMENS FOR EACH SAMPLE, WHICH HAS THE DIFFERENT COLOUR AND SHAPE CODE.	103
FIGURE 54 ORIGINAL TROWBARROW QUARRY LOGS FROM (HORBURY, 1987) WHICH WERE USED AS A PRELIMINARY INFORMATION FOR LOGGING.	105
FIGURE 55 TREE ROOT STRUCTURES IN TROWBARROW QUARRY, THIS SITE IS EXCEPTIONAL FOR OCCURRENCE OF THIS STRUCTURES, WHICH ARE PERFECTLY VISIBLE DUE THE VERTICAL BEDDING. THIS PART IS PROTECTED, AND IT IS USED AS A CLIMBING WALL, SO THE LIGHT MARKS ARE FROM CLIMBING CHALK.	106
FIGURE 56 BURROWS IN TROWBARROW QUARRY ARE VISIBLE IN MULTIPLE PLACES, MAINLY THE TOP PART OF THE QUARRY.	107
FIGURE 57 AREA WITH QUITE BIG BURROWS, VERY WELL VISIBLE THE 2D ARCHITECTURE IN THE WALL. THOSE BURROWS OF DIFFERENT SIZES ARE VISIBLE IN MULTIPLE PLACES IN THE TOP SECTION OF THE QUARRY.	108
FIGURE 58 RICH FOSSIL FAUNA, AREA WITH QUITE BIG FOSSILS OF BRACHIOPODS AND OTHER CLASTIC RESIDUALS.	109
FIGURE 59 SHOWS THE STUDIED SECTION TROWBARROW QUARRY, WITH SURROUNDING AREAS SAMPLED FOR SIMILAR PROJECTS CORRESPONDING WITH TIME.	110
FIGURE 60 SAMPLE TQ1.1. SEE (FIGURE 48) FOR DETAILS. IN THE STEREOSCOPIC PROJECTION IS VISIBLE A DEMAGNETIZATION TREND, TOWARDS INFERRED KIAMAN REMAGNETISATION (RED CIRCLE).	111
FIGURE 61 SAMPLE TQ154.1. SEE (FIGURE 48) FOR DETAILS. IN THE STEREOSCOPIC PROJECTION IS A DEMAGNETIZATION TREND TOWARDS EXPECTED REVERSED POLARITY (BLUE CIRCLE).	112
FIGURE 62 SAMPLE TQ34.4. SEE (FIGURE 48) FOR DETAILS. IN THE STEREOSCOPIC PROJECTION IS VISIBLE A DEMAGNETIZATION TREND, TOWARDS EXPECTED NORMAL POLARITY (GREEN CIRCLE).	113
FIGURE 63: SAMPLE TQ13.1. SEE (FIGURE 48) FOR DETAILS. STEREOSCOPIC PROJECTION SHOWS A PARTIAL DEMAGNETIZATION TREND TOWARDS NORMAL POLARITY (GREEN CIRCLE).	114
FIGURE 64 SAMPLE TQ106.2. SEE (FIGURE 48) FOR DETAILS. STEREOSCOPIC PROJECTION SHOWS A STRONG KIAMAN COMPONENT (RED CIRCLE), WITH NO EVIDENCE OF A PRIMARY CARBONIFEROUS COMPONENT.	115
FIGURE 65 SUMMARY OF DATA FROM TROWBARROW QUARRY, LEFT COLUMN IS LOG AND LITHOLOGIES, NEXT COLUMN IS MAGNETIC SUSCEPTIBILITY. NEXT COLUMN IS NRM INTENSITY, AND NEXT IS SPECIMEN POLARITY CLASSIFICATION (BLACK STANDS FOR NORMAL POLARITY, WHITE FOR REVERSED POLARITY AND GREY FOR UNCERTAIN POLARITY. FAR RIGHT COLUMN IS RESULTS FROM CARBON ISOTOPES ANALYSIS. ORANGE IS FOR, $\delta^{18}\text{O}$ AND BLUE, $\delta^{13}\text{C}$.	118

FIGURE 66 MEAN PALEO DIRECTIONS OF THE TROWBARROW QUARRY: A) TILT-CORRECTED DIRECTIONS, B) INSITU DIRECTIONS (KAMENIKOVA <i>ET AL.</i> , 2019).	120
FIGURE 67 THE RESULTS OF ISOTOPE MEASUREMENTS. PINK CURVE MARKS OUR ¹³ C RESULTS COMPARED WITH GLOBAL ISOTOPIC CURVE FOR UPPER VISEAN (SALTZMAN AND THOMAS, 2012).	122
FIGURE 68 PERCENTAGE CONTRIBUTION OF DIFFERENT MINERALS TO POLARITY. NORMAL POLARITY SPECIMENS HAVE LOWER ABUNDANCE OF MAGNETITE AS A MAGNETIC CARRIER THAN THE REVERSED POLARITY.	123

1 Introduction

This work is focused on filling a gap in magnetostratigraphic research. The main motivation for doing this work is a deeper understanding the early Carboniferous magnetic field, and how frequently the magnetic field was reversing, which that will contribute in the longer term to theories of geodynamo evolution.

The Carboniferous ranges from 358.9 Ma (± 0.4) (mega-annum, million years) to 298.9 Ma (± 0.15) Ma, but with the tectonically active Permian and later the Mesozoic era, it is not a surprise that from a geological perspective, and especially the paleomagnetic view, we have problems in understanding the Carboniferous magnetic field. This is the motivation for this research, to fill a gap in palaeomagnetic knowledge and understand the detailed magnetostratigraphy in the Visean of the Lower Carboniferous.

(Palmer, Perry and Tarling, 1985; Torsvik *et al.*, 1989; Opdyke and Divenere, 2004) and others have attempted to develop a magnetostratigraphy of the Visean previously, a task that has proven problematic in finding suitable rocks which can be studied for this purpose. Previous Carboniferous magnetostratigraphic research can be divided into two main parts. Authors who have been doing research pre-1990's were not fully aware of the secondary remagnetisation of the studied material. The magnetic signal was not then original but originated in the later period when the rocks were biased by regional or local changes as precipitation of new minerals, veining, dolomitization etc. or simply viscous remagnetisation by present day field, due to the long term exposure of the studied material to present date field without shielding. Evidence of remagnetisation became abundant during the 1980's and since the late 1980's it became clear that paleomagnetic research data were affected (van der Voo and Torsvik, 2012). Then confidence of data prior to this

realization (Khramov and Rodionov, 1981; Palmer, Perry and Tarling, 1985) is questioned. The post remagnetisation realization datasets like (Hounslow *et al.*, 2004; Opdyke, Giles and Utting, 2014; Iosifidi *et al.*, 2019), those data fill the gap of the gap in paleomagnetic knowledge of Carboniferous.

Finding non remagnetised Carboniferous material for paleomagnetic research is difficult hence the studied material, limestones from S. Cumbria and North Lancashire seem like suitable untested rocks which maybe able to keep the original information about the palaeomagnetic field in the Visean.

South Cumbria seems to have suitable properties for the research as a primary strong magnetic signal which may be has not been remagnetized in a later time period. The succession of the Visean in Cumbrian is continuous without large hiatus (sedimentation gaps). At some places, we can see paleosols which indicate the small hiatuses but probably not major enough to make the limestones unsuitable for magnetostratigraphic research.

Magnetostratigraphic methods, in addition to carbon isotopic measurements and biostratigraphic-foraminiferal research form a solid combination supporting the magnetostratigraphy and adding the value of absolute time to calibrate any changes.

This research will contribute to the gap in knowledge about this period, helping those researchers who work on the palaeomagnetic field, adding to models to understand it better.

2 Literature review

2.1 The geomagnetic field

The geomagnetic field of the Earth was already known in ancient China (Dunlop and Özdemir, 1997), where compasses had been used as a tool used for navigation on ships for centuries. In the late 1600's, the first observations were made that the Earth's magnetic field changed direction, and that it was continually changing. Since then, navigation charts have been continually updated to reflect this. Two centuries later, C. F. Gauss defined a law (Equation 1 Gauss law for Magnetism. Upper equation states that change in the electric flux density D equals the volumetric electric charge density. The lower equation says that the change of Magnetic flux density B is 0 (**Sleep and Fujita, 1997**). Gauss suggested that the Earth's magnetic field is produced by processes interior to our planet (Sleep and Fujita, 1997).

The magnetic field of the Earth has the overall character of an axial dipole, the reason why it is possible to distinguish clearly between the North and South magnetic poles (Dunlop and Özdemir, 1997), a field configuration like that produced by a bar magnet (Figure 1 Visualization of the bar magnet in centre of the Earth (Lang, 2010)). The average magnetic poles align when averaged out over 200 – 300 000 years (Merrill, 2010) with the geographic poles. This configuration of the earth field is known as the geocentric axial dipole (GAD), (Equation 2), (Kodama, 2013).

$$\nabla \cdot \mathbf{D} = \rho_V$$

$$\nabla \cdot \mathbf{B} = 0$$

Equation 1 Gauss law for Magnetism. Upper equation states that change in the electric flux density \mathbf{D} equals the volumetric electric charge density. The lower equation says that the change of Magnetic flux density \mathbf{B} is 0 (Sleep and Fujita, 1997).

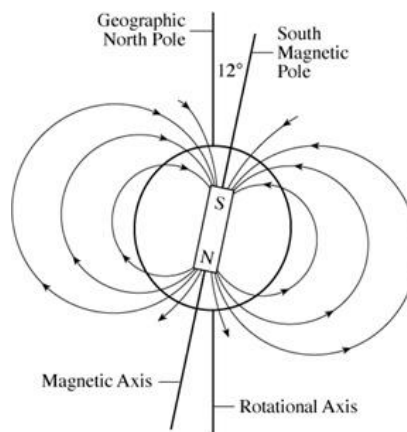


Figure 1 Vizualization of the bar magnet in centre of the Earth (Lang, 2010).

The geomagnetic field can be divided into two parts, known as internal and external. The internal or main field is associated with the fluid motions in the outer core of the earth. The external field is produced in the upper atmosphere, by the interaction of solar wind (high speed charged particles coming out of a Sun) with atmospheric ionized gas (Sleep and Fujita, 1997).

Palaeomagnetists are concerned with only the internal magnetic field, and this thesis will focus on that.

The fluid in the outer core of the Earth, generating in the magnetic field is composed of iron and nickel in a liquid state and some less dense components. The convection motion

of those liquids is regulated by the buoyancy of the liquids, their interaction with the magnetic field and the spin of Earth, creating a self-sustaining dynamo. (Tauxe, 2005).

$$H_h = \frac{M \cos \lambda}{r_e^3}$$

Equation 2 Geocentric Axial Dipole equation. H_h is horizontal component of magnetic field, M is magnetic dipole, λ geographic latitude, and r_e is Earth radius (Butler, 1992).

2.1.1 Secular and palaeosecular variations

The geomagnetic field is characterized by two properties, direction, specified as inclination- declination and intensity. Over short periods of days to years the intensity and direction at any spot on the earth's surface changes slightly (Dunlop and Özdemir, 1997). Location dependent, secular variation (SV), characterizes the geomagnetic field, constantly changing nature, and palaeosecular variation (PSV) is when this variation is historical (Tauxe, 2002).

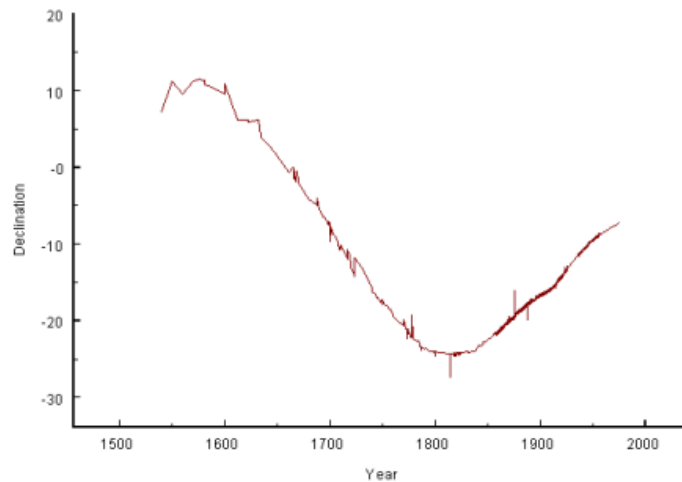


Figure 2 The change of magnetic declination in London in the past 5 centuries (Geological Survey of Canada, 2018).

Secular variation is important for archaeomagnetic dating since regional changes can distinguish between some age intervals over the last few 1000 years. As a result of long term observations from 1600 AD, researchers, noticed that London’s declination angle moved west a total of 14 degrees until early 1800 AD (Figure 2; Opdyke and Channell, 1996).

Due to the rotation of the Earth and the slightly differing angular velocities of Earth’s core and lithosphere, the drift of magnetic field declination has a main direction of westward movement. However, despite that fact, the drift of secular variation is not uniform, some regions demonstrate a slow eastward movement also (Opdyke and Channell, 1996).

Due to the interaction of the mantle which moves very slowly and the outer core, the magnetic field is not stable but changes with time and position on the earth’s surface, that causes the long term change of the magnetic field (Dunlop and Özdemir, 1997).

2.1.2 Apparent polar wander

Apparent polar wander describes the apparent motion of the GAD pole when movements of tectonic plates occur on the earth's surface. The tectonic movements are often references with respect to the geographical North Pole. Seen from a single place on a slowly moving tectonic plate, it seems that an observation of the GAD pole is performing a slow progressive movement, thus the name 'apparent polar wander path' (APWP). The data which contribute to defining the APWP are determined by fossilised magnetisation (palaeomagnetism) produced in near surface crustal materials. This has enabled paleomagnetists to track the motions of continents over many hundreds of millions of years into the Pre-Cambrian (Figure 3; Tauxe, 2002).

Accurate plate reconstructions based on palaeomagnetism depend on two main conditions, firstly, the age of the sampled material (or accurately the age of its magnetisation) must be known to within a few million years. Secondly, there must be

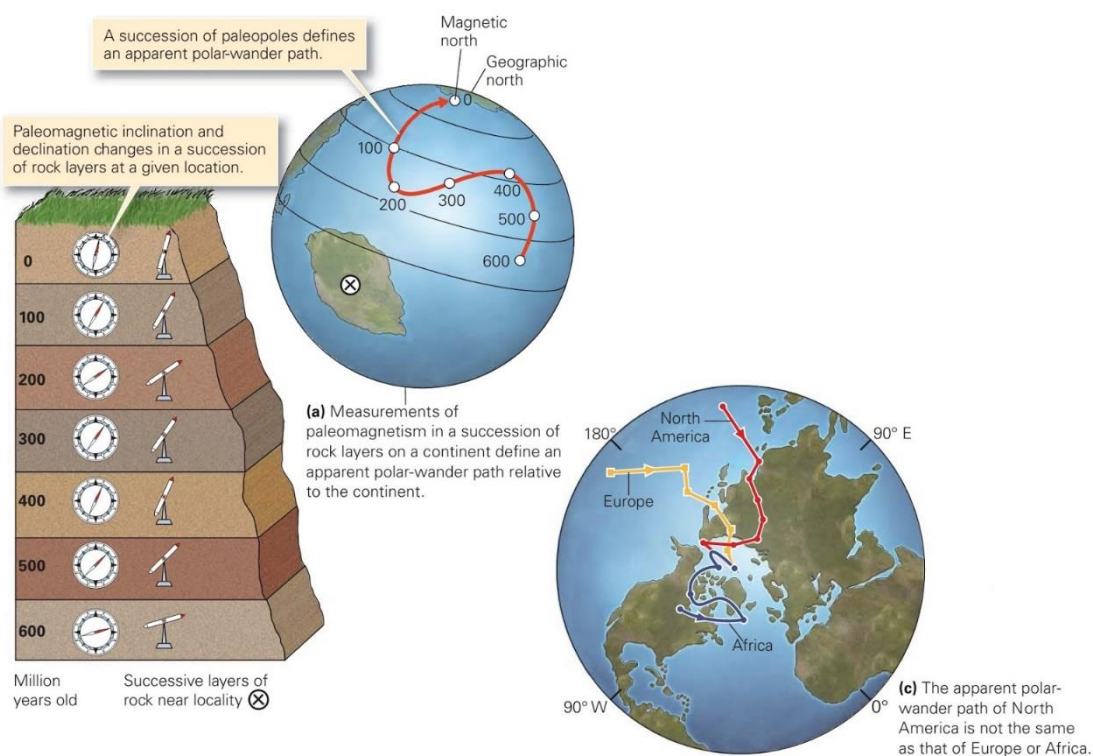


Figure 3 Visualization of Apparent polar wander, with connection to original paleomagnetic inclination (Khattak, 2018).

enough individually oriented samples (to average out orientation errors, and cover enough age window) to define the direction to within a few degrees uncertainty and to average out secular variation (McElhinny, 1973; Van der Voo, 1993; Tauxe *et al.*, 2010).

2.1.3 Magnetic reversals

The geomagnetic axial dipole field may not be stable over extended periods, exceeding a few tens of kiloyears, when reversals of the poles of the GAD can occur, producing a magnetic field reversal, and change in field polarity. The GAD North pole moves to the south, and roughly aligns with the south geographic pole, a state which is deemed a reverse polarity. When the GAD North pole is aligned with the North geographic pole, this is known as normal polarity. The time interval (transition) between reversed and normal polarity states, when the GAD pole is wandering (moving across the hemisphere) is of the order of a few 1000 years (Clement, 2004).

Magnetic excursions occur on shorter timescales than reversals. During a magnetic excursion, the GAD poles wander to a position away from the geographic pole but not going to a complete reversal. Instead, the GAD pole returns to its usual position after some time. The definition of an excursion is commonly based on virtual geomagnetic poles (VGPs), which are the apparent pole of a single studied sample or horizon. When the VGP differs more than 45° from the average GAD pole, this may constitute a geomagnetic excursion (Tauxe *et al.*, 2010).

2.1.4 Geological and Geomagnetic polarity time scale

The geological timescale is a large succession of Stages, which provide the chronostratigraphic definition of geological time (Tauxe, 2002). The lowest formal unit

for chronostratigraphic subdivision is the Stage, with stages grouped into Periods, Series and Eons. The smallest unit of time duration is a chron, which may allow subdivision of stages into many chronostratigraphic intervals. Methods of measuring time, such as radioactive isotopes, biostratigraphy, geomagnetic polarity, Milankovitch cyclicality are alternative ways of correlating the stage boundaries, and intervals within them to other rocks around the world (Lowrie, 2007).

The Geomagnetic polarity time scale (GPTS) (Figure 4) is the past succession of palaeomagnetic normal and reverse magnetochrons, often with age of chrons based on radiometric dating (Tauxe *et al.*, 2010).

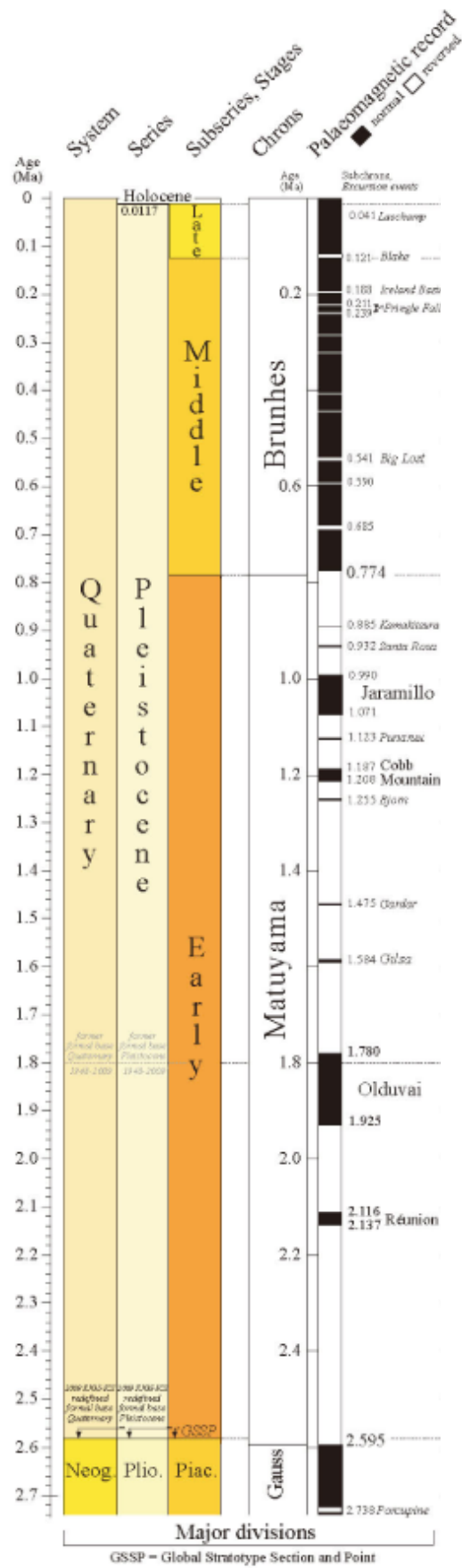


Figure 4 Geomagnetic polarity timescale of the youngest 2.5M a (mega annum = million years ago). Black parts are normal polarity, white ones reversed (*ICS - Chart/Time Scale, 2019*).

2.1.5 Magnetism and its types

Rocks can acquire a remanent magnetisation in several different ways. The remanent magnetisation of a rock, when collected, is referred to as the natural remanent magnetisation (NRM). The NRM is most often a combination of magnetisation components the rock has acquired, both of primary origin or secondary origin. Primary magnetisations are acquired when the rock was formed, and this component is usually the most important one for paleomagnetists since it is expected to coincide with the formation age of the rock. A secondary remanence component (a total or partial remagnetisation) is acquired after the rock was formed, such as during deformation and heating during orogeny, or growth of new magnetic minerals. Types of magnetisation processes are:

Thermo-remanent magnetization (TRM) is acquired during the cooling of the remanence-carrying minerals below its Curie temperature. The Curie temperature is specific for different kinds of ferromagnetic minerals, which experience a sharp change (enhancement) in their ability to carry a remanence, while exposed to an ambient magnetic field. For ferrimagnetic magnetite (Fe_3O_4) the Curie temperature is close to 580°C . For ferromagnetic and antiferromagnetic minerals (such as haematite) this temperature is called the Néel temperature. As a result of temperatures changes below or at the Curie/Neel temperature, magnetisation blocking (while cooling) and unblocking (while heating) of the magnetic moments occurs, which either fixes or demagnetises the remanence held in the ferromagnetic minerals (Dunlop & Özdemir, 1997).

A Chemical remanent magnetization (CRM) is formed during the growth of new magnetic grains or during insitu alteration of already existing magnetic (or nonmagnetic) minerals to new ferromagnetic minerals (e.g. during oxidation in soils or weathering etc.). The formation of the CRM happens below the Curie temperature and in the ambient magnetic field at a particular blocking volume (Dunlop & Özdemir, 1997).

A Depositional remanent magnetization (DRM) is acquired by sedimentary rocks. Magnetic particles, already magnetized and freed from the igneous bodies, will during the deposition process, move and turn, and align themselves to the earth's magnetic field, like a needle in a compass (Tauxe et al., 2006).

Post-depositional remanent magnetization (pDRM)) is achieved after the DRM, in sedimentary rocks. Modification of the sediment fabric and particle packing during compaction and activity of organisms leads to realignment of existing magnetic particles in the earth field, leading to production of a pDRM (Kent, 1973).

Viscous remanent magnetization (VRM) is a process whereby particles naturally lose their magnetisation, through intrinsic thermal processes and acquire a new magnetisation in the ambient field. The process is dependent on the stability of the particles remanence, which is in part particle size dependent. VRM is enhanced during heating as a thermoviscous remanent magnetization (TVRM) (Worm and Jackson, 1988).

2.1.6 Magnetization in sediments and limestones

Limestones are sedimentary deposits that can form in various environments. Calcium carbonate (CaCO_3) in the form of calcite or aragonite is their primary mineral. The CaCO_3 can be formed by chemical precipitation from saturated solution (travertine), but most often limestones are of biological origins in marine settings, where limestones are built up of skeletal parts of marine organisms (King, 2018).

Calcium carbonate is diamagnetic and does not preserve remanent magnetism. The DRM in limestones is mainly derived from clastic particles of iron oxides, hydroxides or authigenic minerals (eg. magnetic Fe-sulphides) (Lowrie and Heller, 1982). Carbonates

may also have a ferrimagnetism produced by magnetotactic bacteria, where the dominant magnetic carrier is magnetite (Stolz et al., 1986; Kopp and Kirschvink, 2008).

Clastic deposits contain micron to submicron-sized detrital Fe-oxides eroded from metamorphic or volcanic rocks (Lovlie, et al., 1971). CaCO₃ formation in seawater is usually in warm environments, often at shallow depths, in subtropical and tropical seas and environments which produces lime muds which are, depending on the distance from shore, enriched by clastic deposits (including aeolian) that include ferromagnetic minerals (Lovlie et al., 1971).

Once the sediment is deposited, burial and compaction process starts, producing physical and chemical processes (such as limestone) which continues with the lithification (Bathurst, 1971). During and after lithification the remanence could be changed due to acquisition of later CRM (such as dolomite).

Remanent magnetization can also be acquired post-depositionally due to bacteria producing magnetite, as a by product of the consumption of organic material at shallow depths. Bottom and benthic organisms feed on this material causing bioturbation, which mixes the sediment in all directions, on the order of a few centimetres to one meter. At a micro-scale this complicates pDRM acquisition due to the smearing of the signal between sediment layers (Figure 5). Bioturbation also changes the alignment of magnetic particles during sedimentation, and the remanence is not likely to be a DRM but a pDRM (Lowrie and Heller, 1982). This process is not limited to limestones but also to the other sediments.

The most abundant carriers of remanence in ancient limestones are thought to maghemite, magnetite, hematite and goethite (Lowrie and Heller, 1982).



Figure 5 Burrows produced by bioturbation, Trowbarrow Quarry in Cumbria, UK.

2.1.7 Existing magnetostratigraphic data for the Mississippian

The Earth's magnetic field during the Late Carboniferous is characterised by a long period of reverse polarity, the 'Kiaman Superchron', also called Permian-Carboniferous Reversed Superchron (PCRS; Figure 6). The PCRS is a significant magnetostratigraphic marker, the beginning of which is likely to be ~ 317 to 320 Ma (Opdyke *et al.*, 2000; Hounslow *et al.*, 2016). The PCRS lasted around 50-60 million years, from the Westphalian to mid Permian (Irving and Parry, 1963; Opdyke, 1995; Hounslow and Balabanov, 2018). The Kiaman superchron is the longest known superchron (Hounslow *et al.*, 2018), and is important for broad correlation in late Palaeozoic stratigraphy (Opdyke and Channell, 1996).

The polarity of the Earth's magnetic field during the Mississippian is still poorly known (Opdyke and Channell, 1996). Significant intervals within the early Visean lack data (Khramov and Rodionov, 1980; Molostovskii, *et al.*, 2007).

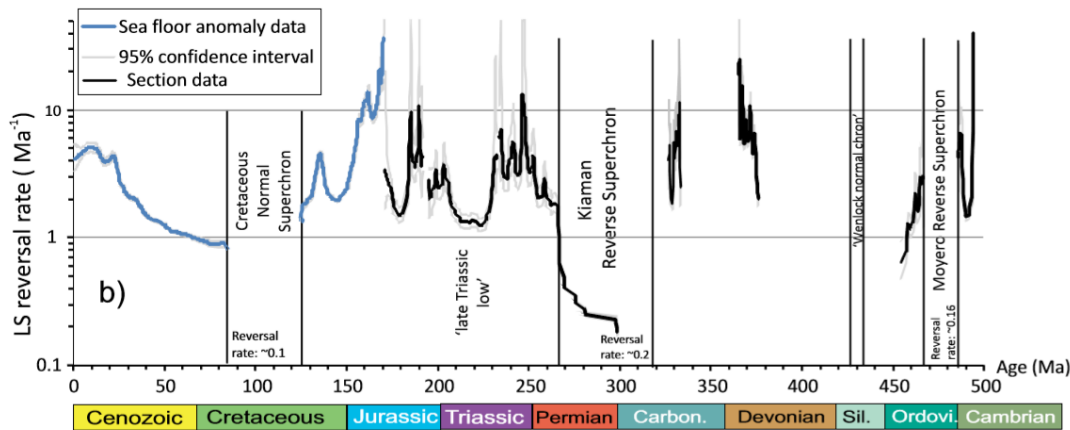


Figure 6 The paleomagnetic reversal rates over time. There is a significant gap in the lower and middle Carboniferous (Hounslow, Domeier and Biggin, 2018).

2.1.7.1 Russia

A wide variety of Carboniferous sediments were studied in Russia in the 1960's and 1970's, mainly from the Donets Basin and the southern Urals (Khramov, 1963; Khramov *et al.*, 1974; Khramov and Rodionov, 1981). Unfortunately, the correlation between palaeomagnetic data from Russia and the rest of the world is unclear because the scientists were unaware of the concept of remagnetisation which was discovered later (Hounslow *et al.*, 2004). In 1992, (Smethurst and Khramov, 1992) observed the reverse polarity overprinting of the upper Devonian and lower Carboniferous sediments on the Russian platform.

2.1.7.2 America

Further palaeomagnetic research of Carboniferous sediments was undertaken in North America, but most of the platform carbonates were later shown to be remagnetized (Roy and Morris, 1983; McCabe and Elmore, 1989). The most fruitful research was done in Mauch Chunk Formation in Pennsylvania, Maringouin Peninsula in New Brunswick and Nova Scotia (Divenere and Opdyke, 1990, 1991b, 1991a; Opdyke and Channell,

1996; Opdyke *et al.*, 2000, 2014). Studies showed mixed polarities during the late Visian and early Pennsylvanian (Divenere and Opdyke, 1991a; Opdyke and Channell, 1996).

2.1.7.3 Europe

The situation in Europe is similarly complicated as in the rest of the world. During the late Devonian to early Permian, the Variscan orogeny took place. The area of central and western Europe was folded and extended from a northerly directed compression (according to the position of the continents now). The rock basement during the Variscan orogeny was extensively folded in some directions and extended in others, directions are dependent to the directions of the tectonic stresses at the time (Woodcock and Strachan, 2012). This tectonism lead to the overprinting of primary magnetisations in the Carboniferous in large areas of Europe (Thominski *et al.*, 1993; Zegers *et al.*, 2003).

However, some Carboniferous sediments likely still maintain their original paleomagnetic signal, in areas that were away from Variscan deformation fronts. These areas are in Britain (Besly and Turner, 1983), carbonates from Cumbria (Northern England, Lancashire) and lavas from Kinghorn Volcanic formation (Scotland) (Torsvik *et al.*, 1989) and Derbyshire (Piper *et al.*, 1991).

2.1.8 Geological background

2.1.8.1 Regional Geology of Northern England

The oldest rocks from the evolution of Great Britain can be found in the North West of Scotland. The Lewisian gneiss with age about 2.7Ga (Giga annum-billion years). In the Proterozoic, they formed the North West Highlands in Scotland and beginning at ~450 Ma the Caledonian orogeny took place. The North of Scotland, remained on the Laurentinian continent at that time, with southern Britain on the edge of Gondwana.

In the **Cambrian**, the sea level rose, and sandstones were deposited in Northern Scotland and England. In the Ordovician, the microcontinent Avalonia was formed, consisting now of fragments from Southern England, parts of NW America and Newfoundland. During the **Ordovician**, the Lake District saw volcanic activity, triggered by subduction of the Iapetus oceanic plate under the continental margin of Avalonia. The remains of this are now the Borrowdale Volcanics. In the late **Silurian**, the Caledonian Orogeny had begun forming mountain belts in Scotland due to the continental collision of Avalonia with Baltica. In Northern England, this resulted in the deposits of sandstones of the Kirkby Moor Fm and slates of the Bannisdale Fm. At the beginning of the **Devonian**, the orogeny continued. Areas were uplifted, the mountain Ben Nevis in Scotland was formed as well. Due to the northward drift of the continent from southern latitudes, the climate changed producing desert-like conditions in the Devonian. The erosion became fast and by the end of Devonian, Caledonian mountains were significantly eroded. Many granitic intrusion, such as the Shap Granite in the Lake District, also occurred during the early and mid Devonian (Woodcock and Strachan, 2012; Thompson and Poole, 2018).

By the **Carboniferous** (Figure 8), Britain was situated around the equator and was covered by the shallow seas of the Rheic Ocean. During the Visean widespread carbonate deposition took place, which today can be found in the Pennines, Derbyshire, Wales and SW England. In Scotland, North England and Wales, the deposits of swamps and

rainforests are found as coal deposits in the Pennsylvanian. By the end of Carboniferous, the Variscan orogeny took place as a result of the collision of Laurussia and Gondwana (Rowe et al. 1998; Woodcock and Strachan, 2012; Thompson and Poole, 2018).

System	Series (NW Europe)	Stage (NW Europe)	Series (ICS)	Stage (ICS)	Age (Ma)
Permian					younger
Carboniferous	Silesian	Stephanian	Pennsylvanian	Gzhelian	298.9–303.7
		Westphalian		Kasimovian	303.7–307.0
				Moscovian	307.0–315.2
		Bashkirian		315.2–323.2	
	Namurian	Serpukhovian	323.2–330.9		
	Dinantian	Visean	Mississippian	Visean	330.9–346.7
		Tournaisian		Tournaisian	346.7–358.9
Devonian					older

Figure 8 Chronostratigraphic chart of the Carboniferous (Cohen et al., 2018).

In the early **Permian**, the continuing Variscan orogeny, and northward motion of Britain, produced in North England arid desert conditions in a mountainous regime (Woodcock and Strachan, 2012; Thompson and Poole, 2018).

The **Triassic** is important because of the production of hematite deposits on the fringes of the Irish Sea Basin. The genesis of the hematite deposits is unclear, but it is assumed that the iron was transported during the desert-like conditions in the Permian and Triassic sediments, with groundwater producing iron ore deposits (Crowley et al., 2014).

2.1 Mississippian in Northern England

The Tournaisian-Visean is widely developed in South Cumbria and the Pennines (Figure 9, Figure 10), with two major groups: the Ravenstonedale Group and Great Scar Limestone Group. Ravenstonedale Group is Middle Tournaisian to around the Tournaisian-Visean boundary in age (Dean *et al.*, 2011). The age of the Great Scar Limestone Group is from the Tournaisian-Visean boundary to the late Visean (Figure 11) (Dean *et al.*, 2011; Waters *et al.*, 2012). These groups provide us with a continuous record for a possible palaeofield signature.

The Ravenstonedale Group is presented by a sequence of mudstones deposited by the influx of fine detritus from the Caledonian source area to the north and argillaceous limestones produced in a shallow seawater environment fringing upland areas (Gawthorpe, Gutteridge and Leeder, 1989; Ebdon *et al.*, 1990; Fraser *et al.*, 1990).

The Great Scar Limestone Group was deposited during the early Chadian upto the Asbian-Brigantian boundary. The Martin Limestone Formation (Figure 11) from late Courceyan to mid-Chadian, is composed mainly of pure carbonate mudstones, but in some parts of west Cumbria has several generations of dolomitization. The greatest recorded thickness is 135 m (Rose *et al.*, 1977) and the top of the formation is a possible disconformity (Adams and Cossey, 1981).

During the early Arundian, palaeosols were formed, with the maximum thickness of 2 m, deposited unevenly on the Martin Limestone Fm, in Levens Estuary area (Adams and Cossey, 1981). The succession continues with the Red Hill limestone Fm (Figure 11), consisting of peloidal grainstone with extensive bioturbation and occurrence of rounded faecal pellets. The average thickness of these deposits is around 60m (Thomas *et al.*, 2005). The overlying Dalton Formation (Figure 11) lies conformably on the Red Hill

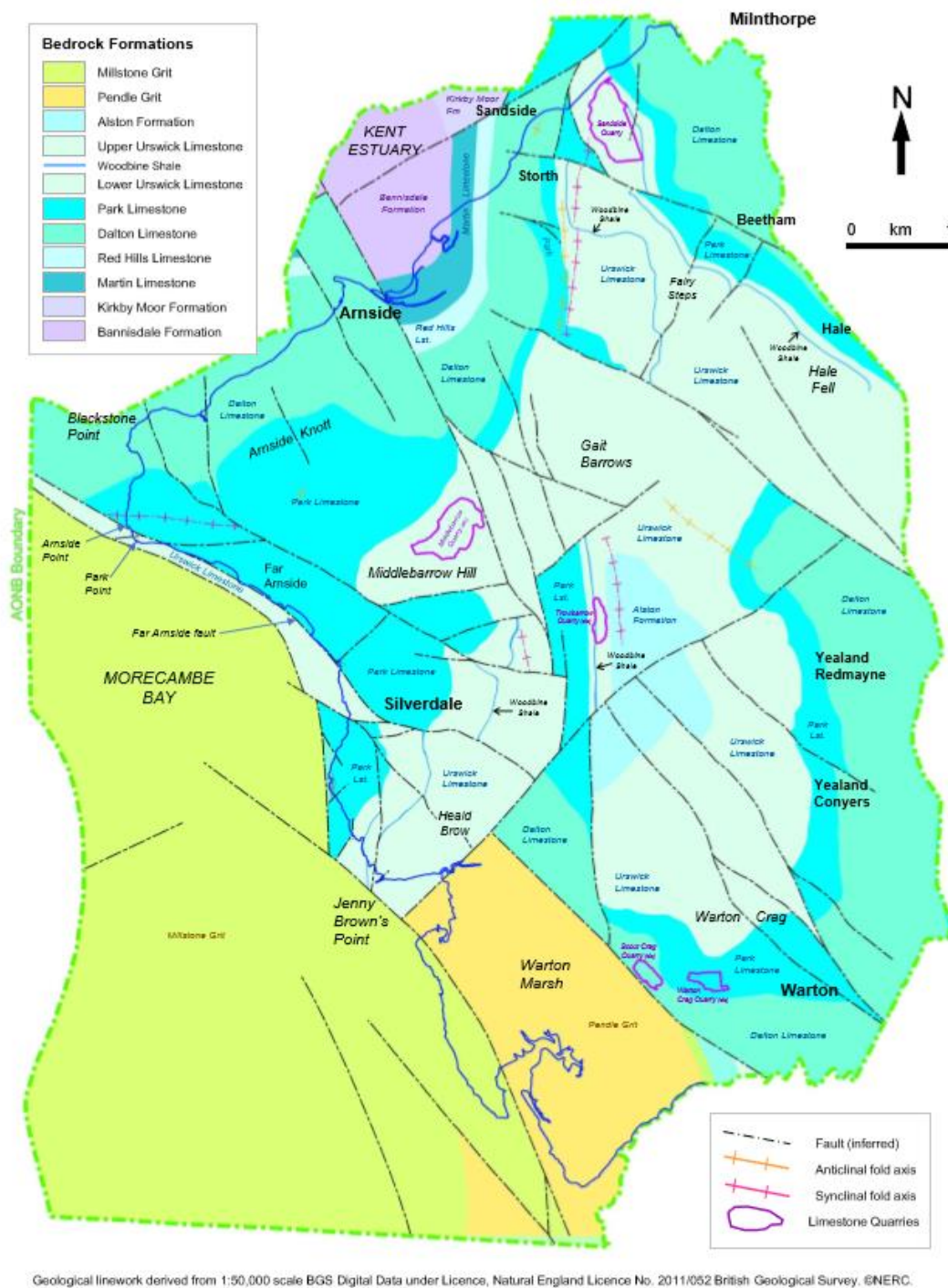


Figure 9 Geology of the Arnside area (Thompson and Poole, 2018).

limestone (Thomas *et al.*, 2005). It is a crinoidal packstone, well-bedded, and divided into 3 divisions in west Cumbria. The lower part has small reefs, the middle part interbedded marine mudstone and siltstone and the upper part consists of packstone and grainstone (Dean *et al.* 2011). The thickest recorded sequence is 255m (Rose *et al.*, 1977). In South Cumbria, the Dalton Formation can be divided into five units separated by two mudstone

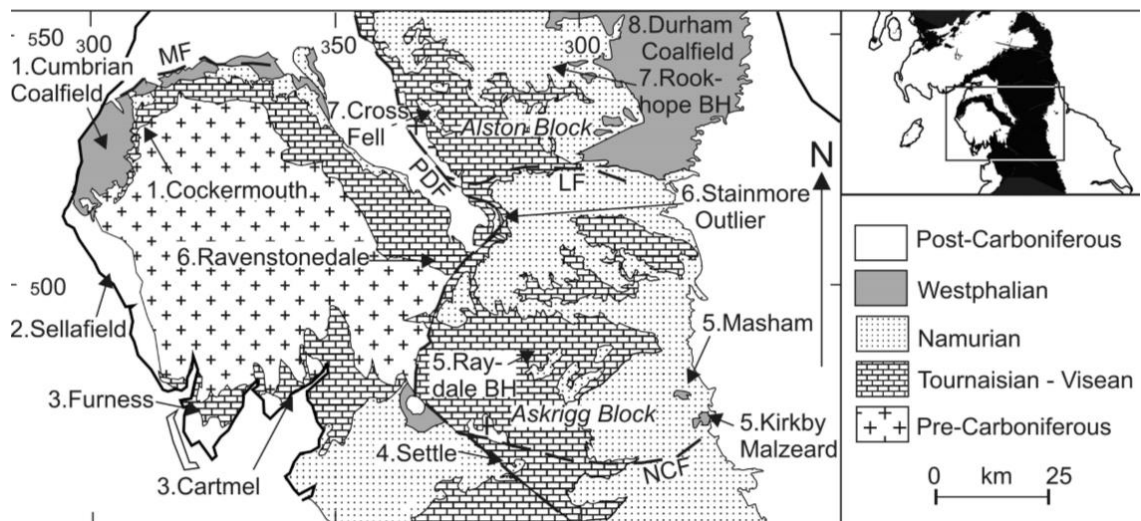


Figure 10 Geological map of the Carboniferous sediments in the area from Cumbria to the North Pennines (Waters et al., 2012).

units. The mudstone units equate to the mid-division further west, and the 5th uppermost unit, of packstones, is often dolomitised (Adams, Horbury and Abdel Aziz, 1990).

The Park Limestone Fm (Figure 11), has an average thickness of 125m and is composed by bioclastic and peloidal grainstone. Bedding is not normally present, it is heavily bioturbated (Adams, Horbury and Abdel Aziz, 1990). The carbonate grains are angular and the sediment has a lack of fine-grained matrix which indicates a strong regular current in the area (Rose *et al.*, 1977).

The uppermost part of the Great Scar Limestone Group (Figure 11, Figure 12) is the Urswick Limestone Fm, of Asbian age. The Urswick Limestone Formation (Thomas *et al.*, 2005) is a bioclastic grainstone and packstone with pseudobreccias and reddened karstic surfaces with palaeosols. The lower part of the formation is thickly bedded (Thomas *et al.*, 2005). The depositional cycles in the Urswick Limestone Fm were controlled by small glacio-eustasy sea-level changes triggered by glaciations on Gondwana, coordinated with a period of slow and steady subsidence in the area (Horbury, 1989). In the Urswick Limestone Fm, during the Quaternary an evolution of paleokarst is

apparent, mainly by large sinkholes, scarps and limestone pavements (Thomas *et al.*, 2005).

The Carboniferous sediments are gently folded and faulted. The main phases that affected these sediments are an early Carboniferous extensional phase, creating the Carboniferous basins and a late Carboniferous to early Permian (transpression) associated with the Variscan Orogeny. Further extensional fault reactivation followed in the Permian-Triassic and the Neogene. The major faults are oriented NNW to SSE and they transverse the whole studied area (Thomas *et al.*, 2005). As seen in (Figure 13), the area of Silverdale is tectonically disturbed, by Silverdale Disturbance (Thompson and Poole, 2018), a major monocline.

	Stage (George et al 1976)	Lithostratigraphical Unit (Rose & Dunham 1977)
Dinantian	Brigantian	Gleaston Fm (80-180m)
	Asbian	Urswick Lst (120-160m)
	Holkerian	Park Lst (120m)
	Arundian	Dalton Beds (110-255m)
		Red Hill Oolite (60m)
	Chadian	Martin Lst (0-135m)
	Courseyan	Basement Beds (0-250m)

Figure 11 Geological succession on south Cumbria and north Lancashire (Adams et al., 1990).

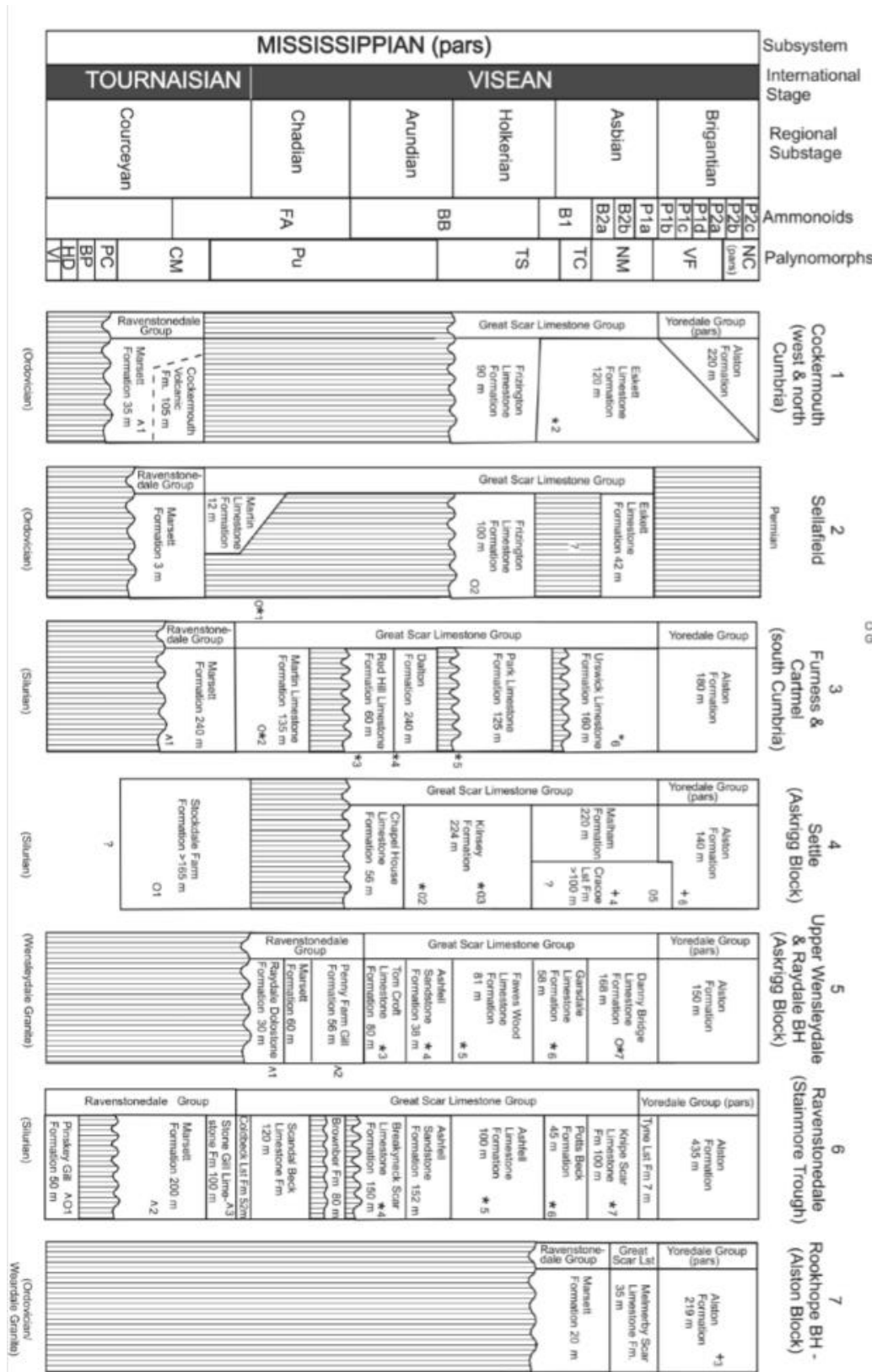


Figure 12 The Carboniferous regional and international stages with lithostratigraphic units of Cumbria and adjacent part of Northern England (Waters et al., 2017).

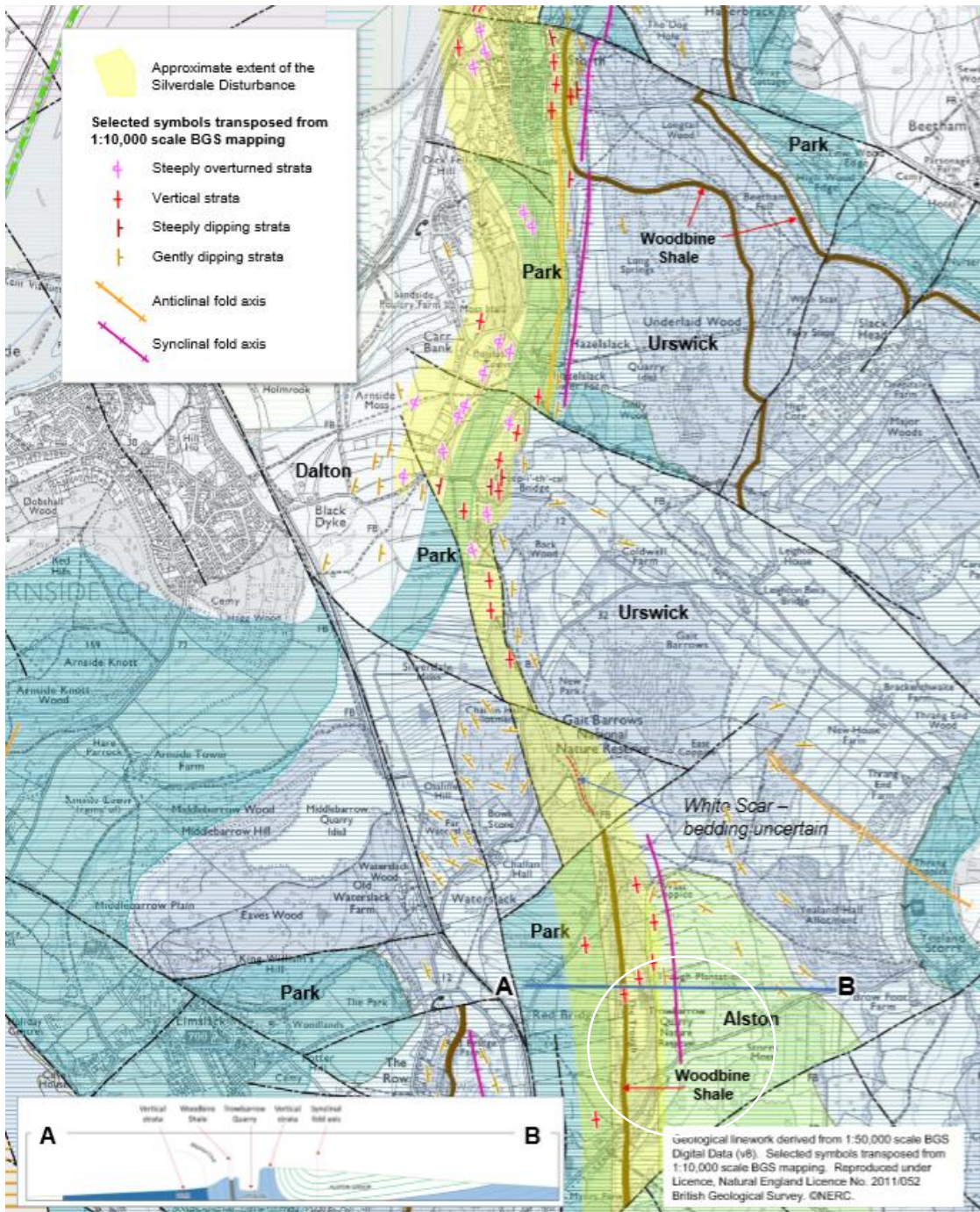


Figure 13 Map of the Silverdale disturbances, mapping the studied of Trowbarrow Quarry – marked by the white circle (Thompson and Poole, 2018)

2.2 Biostratigraphy of the units in south Cumbria and north Lancashire

The first biostratigraphical description in this area was attempted by (Garwood, 1907, 1913, 1916). He described the faunal sequence in Carboniferous limestones in Cumbria and southern Lake District. The following work (Ramsbottom, 1973) set the correlations in between the authors. Ramsbottom divided the Dinantian series to six major cycles (further divided to eleven mesothems) defined by regressive top and transgressive base. Lately divided mesothems were defined again by transgressive and regressive boundaries associated with biostratigraphical shift. This work set the correlation and context both at national scale and locally (including surrounding areas).

The next detailed sedimentological study was attempted by (Horbury, 1989) who studied the Morecambe bay and Cumbria and bring insight to glacioeustatic cyclicity and changes driven by local tectonism.

The significant biostratigraphy markers in this area are conodonts, foraminiferas, brachiopods and corals (Riley, 1993).

2.2.1 Conodont zonation

Conodonts are phosphatic elements of the feeding apparatus of the conodont animal (agnathan chordates), having eel like body (Figure 15 and Figure 14) and are found in sediments from the early Palaeozoic to latest Triassic, and in some parts of this interval, provide the highest resolution biostratigraphic chronology (Sweet and Donoghue, 2001). Once this material is heated, it changes its colour and microstructure and may recrystallize. The conodont Colour Alteration Indices (CAIs) (Figure 16) is based on these changes (Epstein, Epstein and Harris, 1977; Rejebian, Harris and Huebner, 1987). It reflects the burial history and maximum temperature reached during burial. The best-

preserved fragments in the Carboniferous come from hemipelagic calcareous shales and turbidites, although they occur in platform carbonates also (Riley, 1993).

In the Craven Basin, the CAI values vary from 2 to 3.5, with the highest values on the southwest of the basin and the lowest values in the north (Burnett, 1987; Armstrong and Purnell, 1993). Conodonts from black shales tend to have higher CAI than those from limestones.



Figure 14 Living conodont animal, visualization (Bonadonna, 2018).

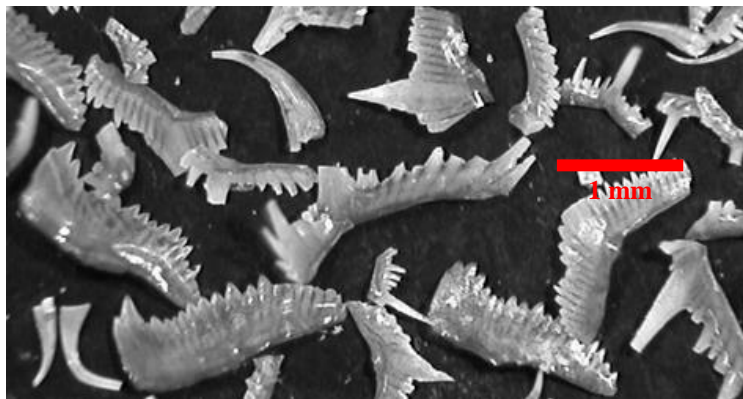


Figure 15 Conodont fossils (*Conodont collection, Natural History Museum, 2018*).

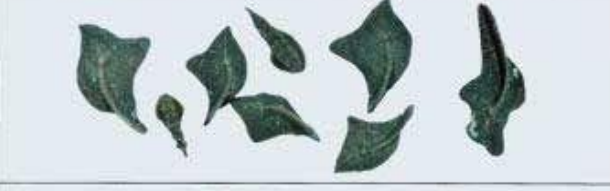
CAI	Naturally altered conodonts from field samples (Rheinisches Schiefergebirge and Montagne Noire)	Temperature range
1		<50°-80°
2		60°-140°
3		110°-200°
4		190°-300°
5		300° - 480°
6		360° - 550°

Figure 16 The Conodont alteration index (CAI) comparison with conodont colour and burrial temperature (*SENCKENBERG world of biodiversity*, 2018).

2.2.2 Foraminifera zonation

Foraminiferas are microscopic calcareous marine organisms, first found in the early Cambrian (Figure 17). They are abundant usually in all marine environments as either benthic or planktonic forms (Postgraduate Unit of Micropalaeontology, 2002). The base of the Visean is defined as the first appearance of foraminifera *Eoparastaffella simplex* within the *Eoparastaffella ovalis*-*Eoparastaffella simplex* lineage (Kalvoda *et al.*, 2012).

All foraminifera species in the European Visean were benthic, with the richest association in environments on mid ramps and platforms. Some were re-deposited after their death due to turbidite flows into the basinal area or tempestite episodes (Riley, 1993). British Visean regional biostratigraphy (Fig. 17), is represented, by six foraminifera zones (Cf1 - Cf6), (Riley, 1993).



Figure 17 Foraminifera from the Lower Urswick limestone (Dinatian) (Athersuch and Strank, 1989).

2.2.2.1 Significant foraminifera assemblages of the Visean

Courseyan: The most typical foraminiferas are *Endothyra Danica*, *Lugtoniamonilis*, *Palaeospiroplectamina mellina* and *Spinoendothyra mitchelli* (Waters *et al.*, 2011).

Chadian: Characterised mainly of *Eotuberitina eritlingerae*, Cf. *Glomispinella* sp., Cf. *Quasiendothyra* sp. (Ramsbottom and Aithenhead, 1981). **Arundian** limestones are partially dolomitized, but mainly characterized by corals such as *Dorlodotia briarti*, *Lithostrotion minus* and *Syringopora*. Important Arundian foraminifera are *Glomodiscus* sp., *Eoparastaffella simplex* and *Eoparastaffella restricta* (Strank, 1982). **Holkerian:** Foraminiferal species are mainly *Koskinotextularia* sp., *Nibelia Nibelis*, *Bogushella* sp., *Eostaffella parastruvei*, *Archaeodiscus stilus* and *Pletogyranopsis convexa* (Strank, 1982). **Asbian:** The Holkerian type foraminifera faunas continue to the basal part of the Asbian (Strank, 1982). **Brigantian:** These limestones were strongly dolomitized, but the most prominent species are *Archaeodiscus* sp., *Endothyra* sp., *Euxinita efremovi*, *Palaeotextularia longiseptata*, *Pseudoammodiscus volgensis* and *Pseudotaxis eominima* (Cózar and Somerville, 2016).

2.3 The Carbon isotope stratigraphy

Carbon is naturally recycled at the Earth surface from the atmosphere to the ocean, surface and back to the atmosphere - this is the carbon cycle. Atmospheric CO₂ is naturally dissolved in the ocean water to keep the balance. This dissolved CO₂ accumulates at the bottom of the ocean as organic carbon and inorganic carbonate through the activity of organisms (Berner, 1990). This dissolving/precipitating process is greatly influence by the partial pressure in the atmosphere and the fluctuations of global temperature. The carbon cycle between the ocean and atmosphere occurs at the time periods up to 1 kyr (Saltzman and Thomas, 2012). However, the major source of the carbon is not the atmospheric CO₂ but mainly terrestrial soils and carbonate dissolution (Mook and Tan, 1991).

The inorganic ¹³C isotope is fractionated (with respect to C¹²) during carbonate formation in the oceans, a process which is dependent on the temperature, and its relative storage in other carbon reservoirs. In any particular carbon source the ratio between C¹² and C¹³ stored (¹³C/¹²C) is expressed as the δ¹³C value. Although the δ¹³C is incompletely known in the Carboniferous, the best estimate of its changes is shown in (Figure 19). Changes in δ¹³C largely reflect global modifications in carbon storage patterns, although other factors are involved (Saltzman, 2003).

The biproduct of the δ¹³C mass spectroscopy measurements is a δ¹⁸O value, since these measurements are performed on CO₂ liberated from CaCO₃ disassociation. δ¹⁸O is a palaeotemperature indicator, due the heaviness of this isotope over the ¹⁶O and ¹⁷O, the ¹⁸O which occurs more in deep and cold waters. The higher abundance of this isotope can signify a colder climate since there is preferential storage in ice caps, so that δ¹⁸O in the Quaternary reflects ice volume- so it may be important in the Carboniferous also, since this interval; also had ice caps in Gondwana (Fielding *et al.*, 2008).

$\delta^{13}\text{C}$ is measured on a mass spectrometer. This ratio is then compared with the standard, which is established on the fossil Pee Dee Belemnite (PDB), which is a ratio $^{13}\text{C}/^{12}\text{C}$ of 0.01118 (Miller and Wheeler, 2012). This value of $\delta^{13}\text{C}$ was established as reference zero. Nowadays the PDB standard is no longer available. However, new standards were created as NBS-19 or VPDB (Vienna pee dee belemnite), for some the ratios were recalculated to correspond with the original standard PDB (Brand *et al.*, 2014).

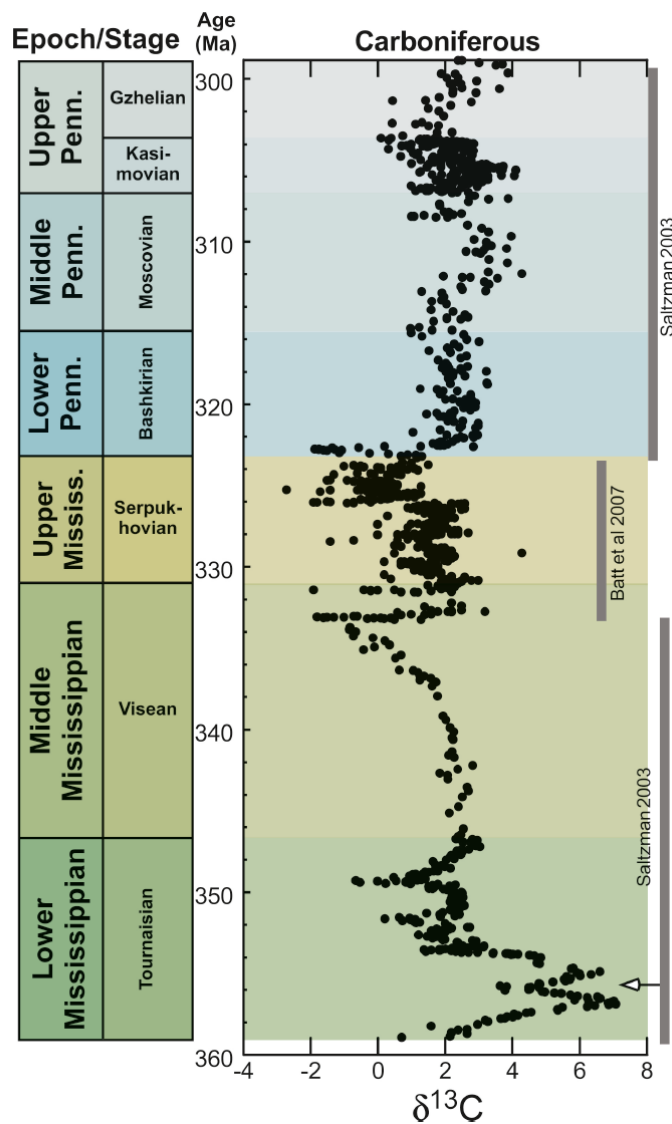


Figure 19: Variations of $\delta^{13}\text{C}$ (carbonate carbon) within the Carboniferous (Saltzman and Thomas, 2012). The strong negative $\delta^{13}\text{C}$ excursion in the late Visean is the target in Trowbarrow Quarry.

3 Methods

3.1 Location and areas of sampling

The studied area is situated in NW England, south of the Lake District in Cumbria (Figure 20 and Figure 21). The paleogeographic map (Figure 22 and Figure 23) shows the position of the studied area in early Carboniferous, positioned at the border of two micro continents Avalonia and Laurentia (Smit *et al.*, 2018). During the Visean, Baltica, Avalonia and Laurentia were approaching, the Avalonia was in extension over the Visean continuing to the onset of post-rift thermal subsidence (Kombrink *et al.*, 2008). By the late Visean the Dinantian basin was deepening and at the southern margin (Leeder and Hardman, 1990; Kombrink *et al.*, 2008), the clastic sedimentation begun.

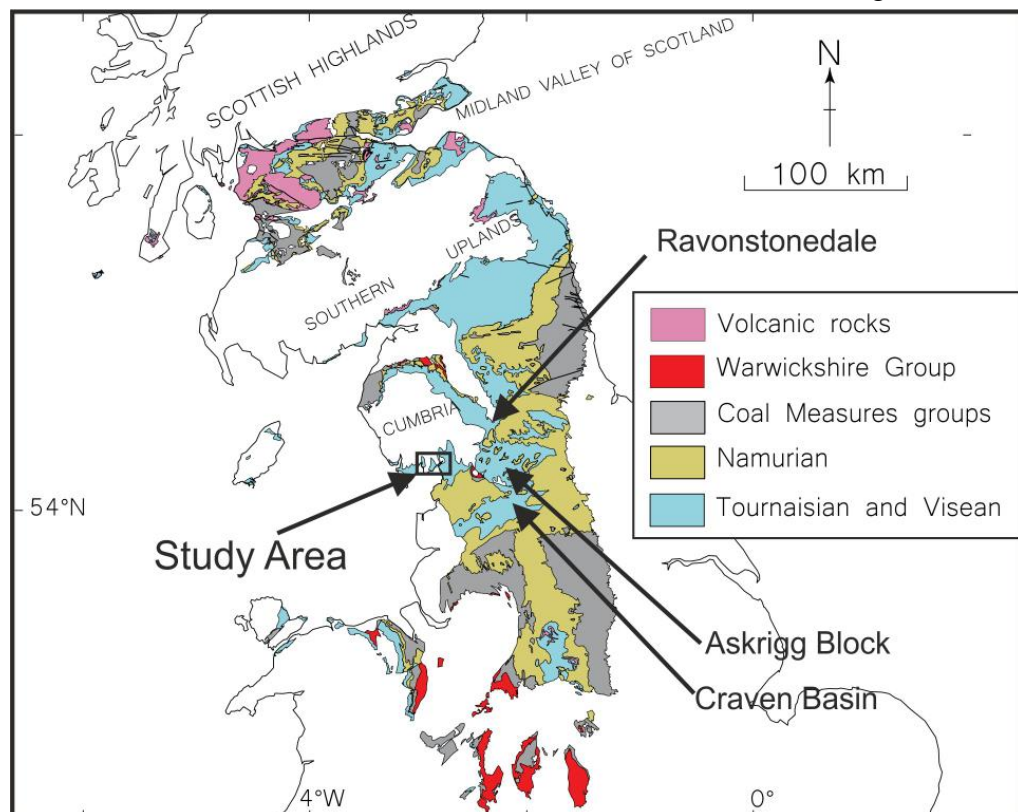


Figure 20 Geology map of the North-West of UK, the studied area is marked by black rectangle (Dean, Browne, Waters, & Powell, 2011).



Figure 21 Location of studied area. On top map, is Area of Cumbria visible in yellow rectangle. On bottom map is Cumbria area with location of studied Meathop Quarry in yellow ellipse and Trowbarrow Quarry in blue ellipse (Google Maps, 2019).

The collision of the microcontinents ended by the end of Westphalian (Arthaud and Matte, 1977). This location is dominated by two estuaries, merging south into Morecambe Bay. Geologically, this is the fringe of the NE corner of the Craven Basin, and also

fringing the Irish Sea Basin, continuing to the south into North Wales and West to the Shores of Ireland. This study sampled two locations Meathop Quarry and Trowbarrow Quarry.

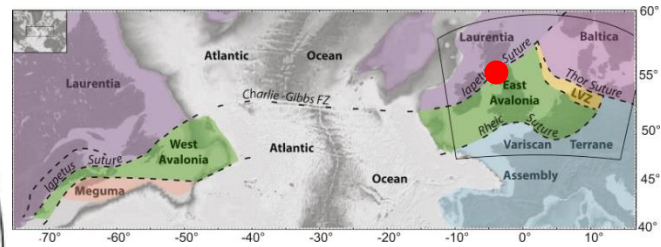
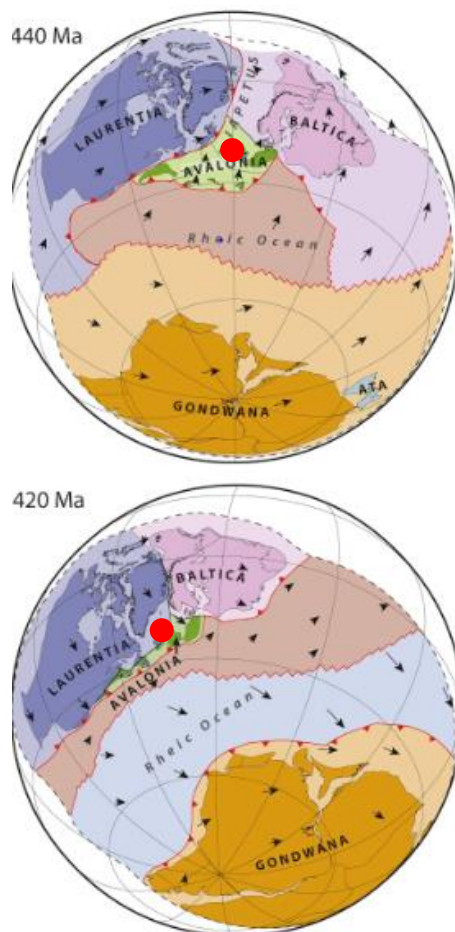


Figure 22 Paleogeographic map. The Studied area in Carboniferous (440Ma and 420 Ma), marked with red dot – left column figure. Today's geographical setting visualised as original source continents (Avalonia and Laurentia). Studied area (red dot) – top figure. Both figures (Smit et al., 2018).

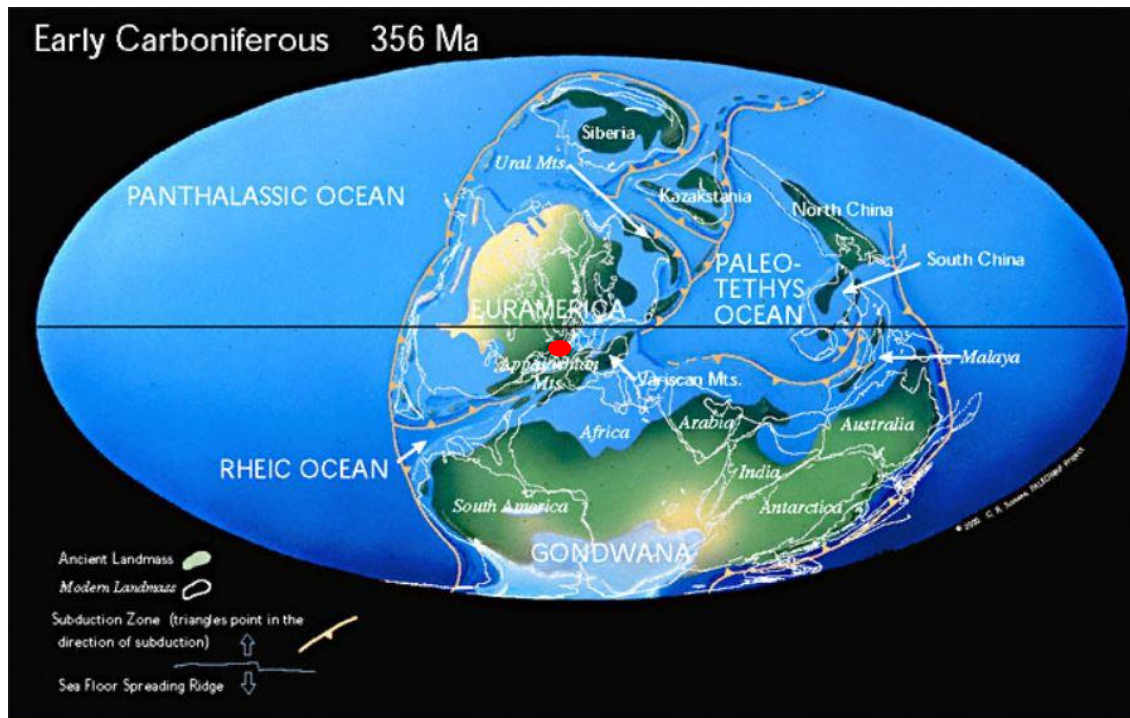


Figure 23 Location of Britain (red dot) in Early Carboniferous 356 Ma (Scotese, 2002).

3.1.1 Meathop Quarry

This is an old quarry and since 1984, was designated as a Site of Special Scientific interest of Great Britain (*Meathop Woods and Quarry | Protected Planet, 2019*). The locality is surrounded by a golf course, farmed land and the River Kent estuary.

3.1.1.1 Geology

Meathop Quarry contains a sedimentary succession of limestones and dolostones with rich fossil fauna in some parts. The previous mining works created steps like sections, so that all parts of the succession are accessible (Figure 24, Figure 24, Figure 25). The length of the sampled profile is 50 m, the bottom 40 m is part of the regional division of the Marset Formation but locally referred to the Martin Limestone Fm. Above this level is a hiatus, with the top 10 m being part of the Red Hill Limestone Fm (Waters *et al.*, 2012).

The location of the Meathop Quarry is Latitude: 54°12',18.48N and Longitude: 2°52'20,61W. The bottom part of the quarry is surrounded by a road, where we took the first sample close to the road level- sample MQ6. We continued towards the top in intervals of ~1m taking palaeomagnetic samples. Also each 20 cm between the magnetostratigraphic samples a chip of rock for cyclostratigraphy - susceptibility measurements was taken. A total of 53 samples were collected for palaeomagnetic measurements and 136 samples for susceptibility.



Figure 24 *Meathop Quarry entrance outcrop. As it is possible to see, the quarry is easily accessible due way of mining in this location, they left sections step-like. Each step is about meter high.*



Figure 25 *Picture on top shows the Meathop Quarry wall in the entrance area. The wall itself appear steps like, it is reflect the way how limestones were mined in the history. Picture in the middle (south west view) and bottom (north western view) shows the area surroundings.*

3.1.2 Trowbarrow Quarry

This locality was a previously active quarry until 1959, but today it is under the management of the Arnside/Silverdale AONB Landscape trust and is treated as a local nature reserve (Thompson and Poole, 2018) (Figure 26 and Figure 28). For this reason, the drilling of samples directly was not allowed on this site and only hand sampling was allowed (Figure 27).

This quarry has about 170 m of limestones with near-vertical bedding, as it is within the Silverdale disturbance/monocline and has in part overturned bedding. The limestone locally has different size of calcite veins and palaeo-karstic development with palaeosols in some parts. It seems that Urswick Limestone has up to four different veining systems which are intersecting each other. Those veins have different colours, two directions with the black veining, one with red to brownish coloured veining and white calcite veining with small grains of calcite, the calcite grainsize seems to be variable.



Figure 26 Trowbarrow Quarry, the entrance.

There are many places with burrows and faunal remains, mainly branchiopod faunas with

solitary and colonial corals and many more. Its microfaunal remains, are mainly foraminifera and calcareous algae.

Trowbarrow Quarry's environment can be seen on (Figure 28, Figure 29, Figure 30, Figure 31, Figure 32), GPS location is Latitude: 54°10',33.36N and Longitude: 2°47'47,74W.

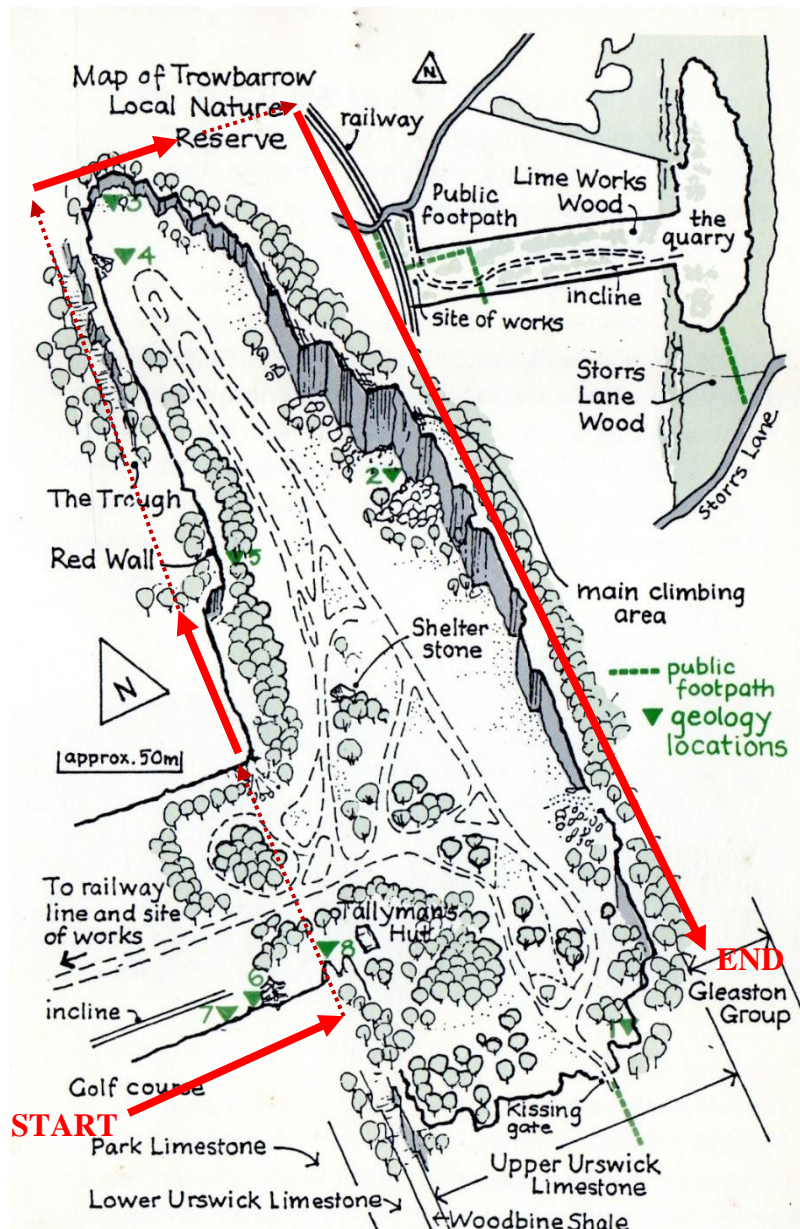


Figure 27 Map of the Trowbarrow Quarry by (AONB Unit, 2009). Direction of sampling is shown by the red arrows. Ones with dotted lines are places which were skipped due to the same lithology as previously sampled area (due to the vertical bedding). All sampled area has over 170m, sampling took about 3 weeks of work.



Figure 28 Trowbarrow Quarry main site.



Figure 29 Trowbarrow Quarry site with visible vertical bedding.



Figure 30 Top left overall view of vertical bedding. Top right space in between 2 outcrops, due the weathered-out shale, space has about 4m. Bottom left, signature red limestones, red colour is due paleo soil horizon abundant in this part, it is enriched by haematite. Bottom right, already sampled area (white dots).

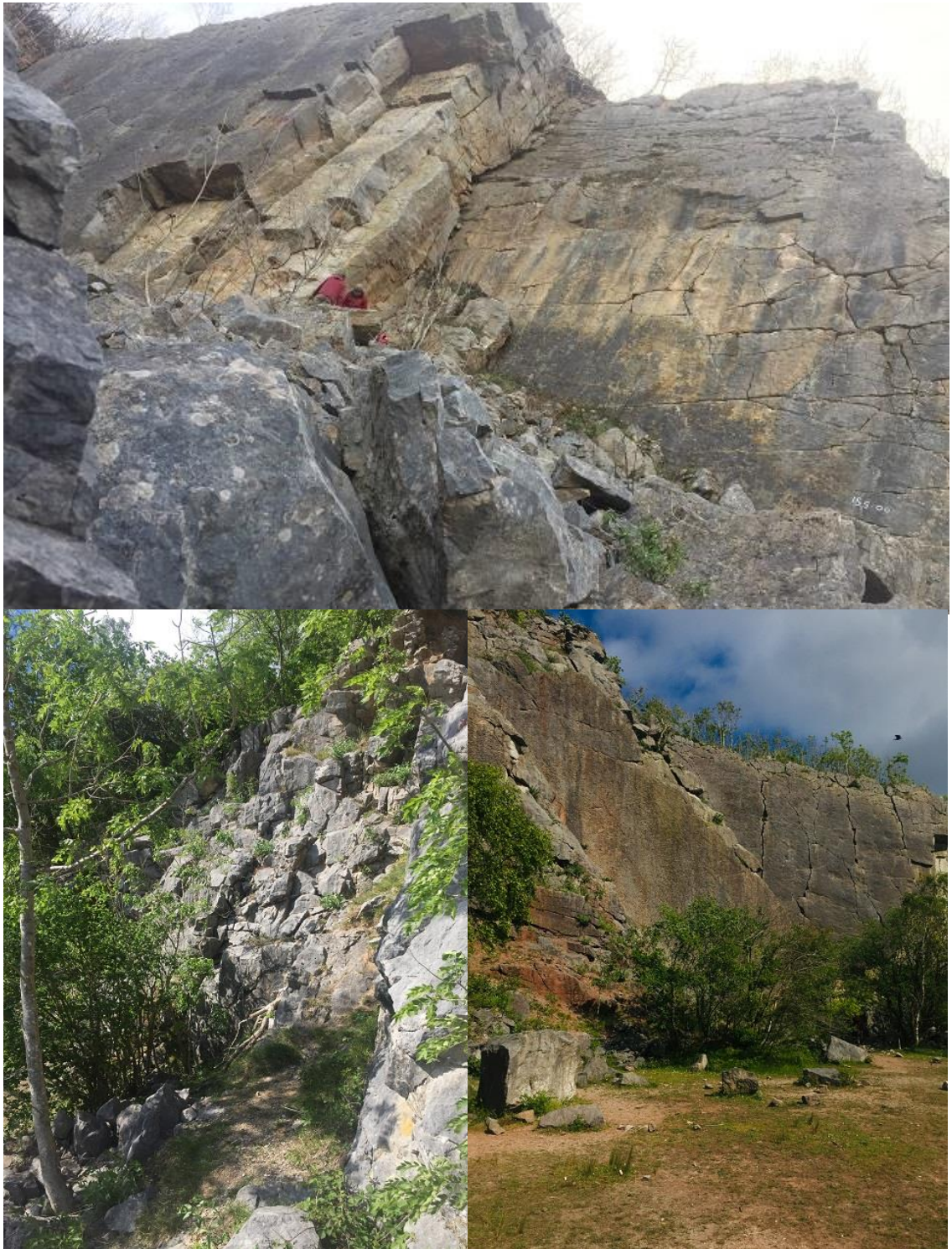


Figure 31 Diversity of the Trowbarrow Quarry. On top, it is visible, that some areas were not easily accessible.



Figure 32 On top can be seen a density of sampling in the quarries. Each small white spot is approx. 25 cm from each other, there was the susceptibility sample taken from. Big white spot is hand sample for paleomagnetic measurements. Those are 1 m from each other.

Bottom figure shows the vertical bedding in the Trowbarrow Quarry, sometimes the terrain wasn't exactly easily accessible. This is quite extensive rock fall which was triggered by winter de-icing.

3.2 Sampling and sample preparation

3.2.1 Fieldwork sampling

Because of the authorization from the landowners and managers, the lack of a rock drill, we choose the hand sampling method, a type of sampling which is more challenging and sample preparation more time consuming, then if we would be able to drill cores in the outcrop. However, importantly, residual samples were also available for other techniques such a foraminiferal assessment.

3.2.1.1 Hand samples

On the site, we took a hand sample each meter, approximately 20x20x20 cm large. First, we used an angle grinder with a diamond cup-wheel to flatten the surface of a rock and then with an orientation staff and geological compass, we took the strike and dip of the surface, and drew the square footprint of the staff and marked the sample number and location code. Then we took the sample out with chisel and hammer and packed them into the plastic bags also with a number and location code.

3.2.1.2 Susceptibility samples

We took a small ~30-80 g sample every 20-25 cm for measurement of magnetic susceptibility (MS). These MS specimens came from rock areas, which were unweathered. With a tungsten chisel and hammer, we chipped pieces into a small plastic bag, which was marked with the number of the closest previous hand sample, letter a to f (a-sample lowest stratigraphically) and location code.

All samples were drawn onto the log of the site with the distances and lithological description of the site.

3.2.2 Laboratory sample preparations

Samples were taken to the Lancaster University sample preparation laboratory, where all samples were described to identify the key lithological detail of each.

3.2.2.1 Hand samples

Hand samples were unpacked and mounted into aluminium trays (Figure 35), re-oriented with the orientation device (Figure 33) to an exactly horizontal position (0 degrees dip), locked in this position with a dental plaster cast. This cast was left to dry for about two days. Then they were marked with co-parallel orientation arrows on the surface to ensure that the orientation was transferred to the plug when plugging.

The plaster-cast samples were loaded and taken to the Geomagnetic laboratory of the University of Liverpool and there they were plugged on a vertical diamond drilling machine. The drilling produced 2 to 3 plugs about 7 cm long and 2.5 cm in diameter from each sample, producing at least 3 good specimens from each sample. The plugs were marked along the long side with arrows to maintain the correct orientation for further magnetic measurements.

All plugs (Figure 34) were taken back to Lancaster University, where they were cut on the rock saw into lengths of 2.5 cm per specimen.

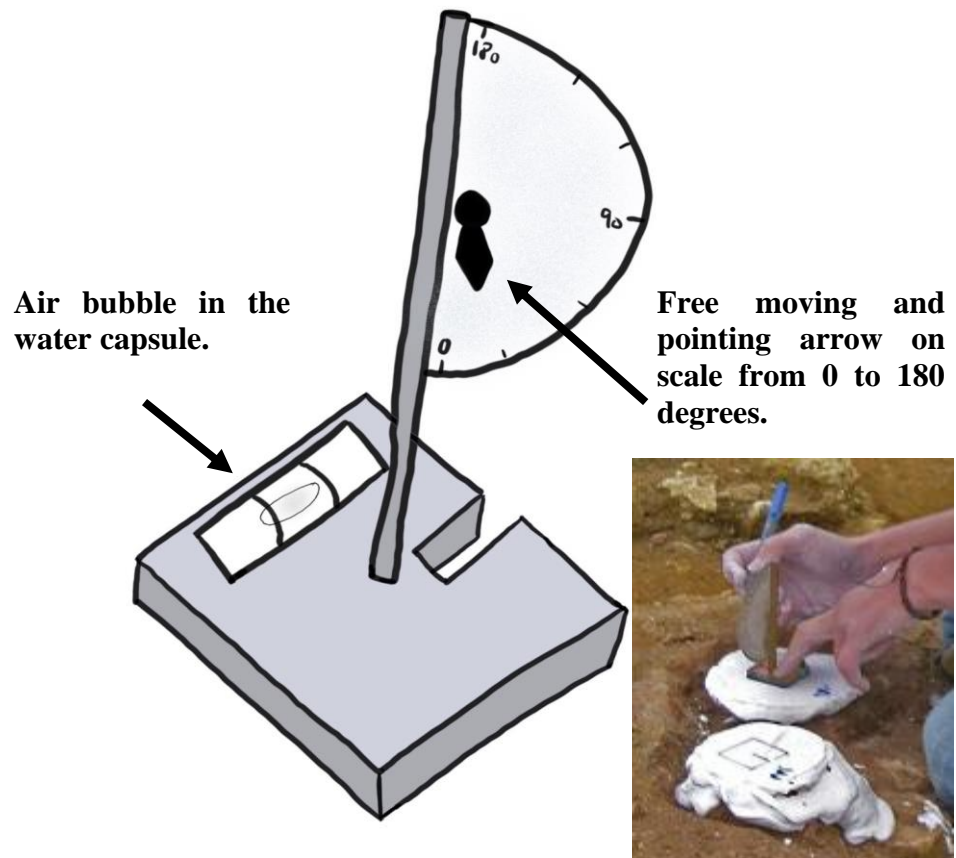


Figure 33 The balancing device, used for measuring dip and balancing the samples before plastering. Device has air bubble in the water capsule, and moving pointing arrow, showing the dip on scale from 0 to 180 degrees. On the right side, is this device used in field, to mark the samples and measure the dip and strike (Photo: Mark Hounslow)



Figure 34 On the left side is plug of length 5 cm, coming as a result of the drilling process. This plug is cut for smaller pieces, in order to get a final sample. On top right is a cube sample, this type of samples is achieved by the direct cutting on a rock saw. The dimensions are 2,5x2,5x2,5 cm. This method is used for samples which are fractured or having any other defect and cannot be drilled. Bottom right, picture of Rapid 2G sample table.

The drilling technique is a quite fast and effective method, but some fractured samples needed to be cut by hand on the rock saw, because the rotating head of the drilling machine tended to destroy such fractured samples. For the samples, which needed this special treatment on the rock saw, we obtained 2.1x2.1x2.1 cm cubes which were marked with an arrow following the original sample orientation arrow.

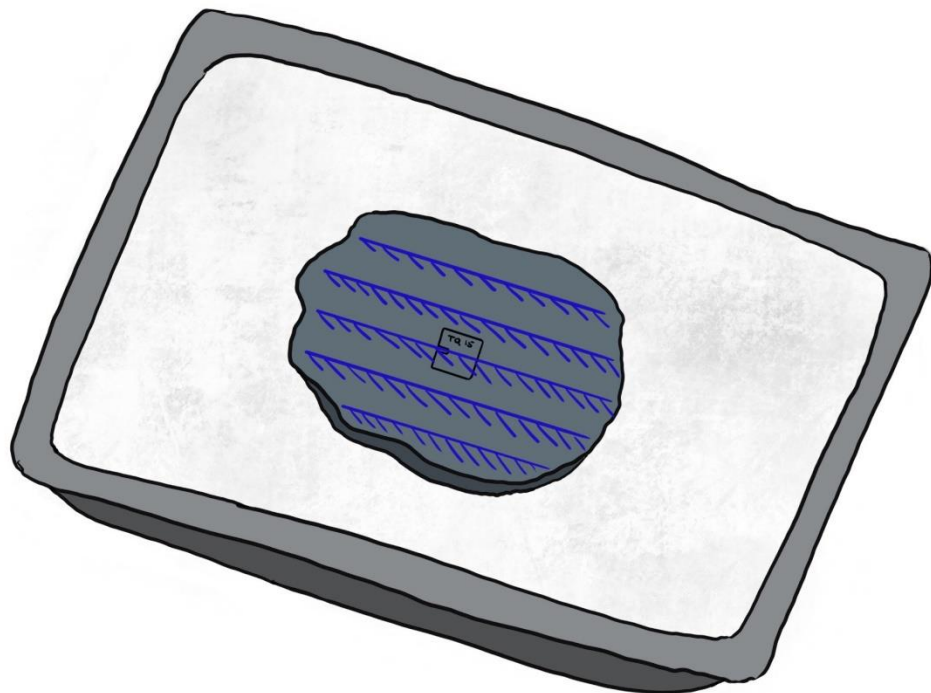


Figure 35 Plastered sample: Sample was first balanced with the balancing device in the aluminium tray (grey basket). This was stabilized in original position with old plaster wedges. Then we mixed dental plaster with water and pour it in to the empty spaces. After hardening, following day, we draw the arrows, for easier orientation of the core, once drilled.

3.2.2.2 Susceptibility samples

These samples were washed with a brush to get rid of any soil particles which might be mixed in the samples. They were then crushed on a mechanical jaw crusher. Approximately 30 g of the crushed sample was inserted into small plastic bags and rolled as an 'MS cigar' (Figure 36). Those 'cigars' were marked with the number, letter a to f and location code. All samples were weighed, and the mass of the empty plastic bag was subtracted to get the sample mass, to normalise the susceptibility.

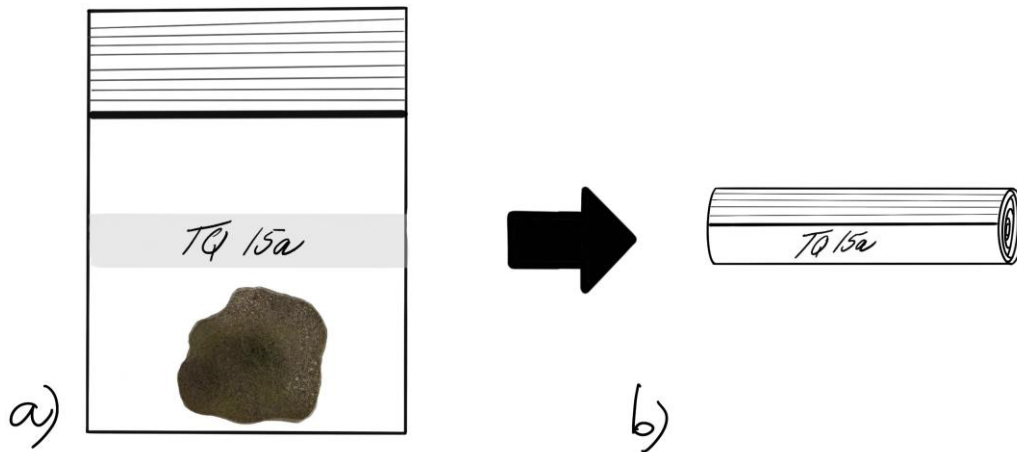


Figure 36 Susceptibility samples: a) Small chips of samples were put to the plastic bag and marked with sample number. Preparation, it was washed and crushed to mix of small grains and dust. B) This was rolled to small cigar and sealed with clear tape.

3.3 Measurements

3.3.1 Susceptibility sample measurements

Susceptibility samples and one plug from each hand sample were taken to Liverpool University to Geomagnetic laboratory. We used an AGICO Kappa Bridge device to obtain high-resolution magnetic susceptibility (χ_{lf}) measurements (in m^3/kg). Measured bulk susceptibility is a result of all mineral grain susceptibility contributions in sample, mostly dominated by ferromagnetic grains (Butler, 1992).

All samples were weighed, and the weight was inserted into the software. Each sample was measured 3 times to obtain a reliable average. These measurements were used for a magnetic susceptibility (MS) curve for each site to complement the log and aid in later cyclostratigraphy (Dearing, 1994; Lecoanet, Lévêque and Segura, 1999).

3.3.2 Palaeomagnetic measurements

The NRM measurement following by alternating field demagnetization (AF) and thermal demagnetization (TD) was used as measurement technique. The NRM measured on superconducting magnetometer, measures the magnetic moment in sample coordinates in three directions X, Y and Z. 2G magnetometer has for each direction own coil in which the sample is measured. Each coil is calibrated together with the magnetic shielding to provide clean magnetic ambient for the sample measurement to avoid external magnetic and geomagnetic field (Butler, 1992).

During the demagnetization, the remanence is gradually removed. During AF demagnetization, performed on Rapid 2G magnetometer, the alternating field increase removing gradually the remanence, providing way how to remove remanence with

control (Stephenson, 1981). For thermal demagnetisation was used Magnetic Measurements thermal demagnetizer (MMTD), the remanence is gradually removed with increase of the temperature as it is unblocking magnetic domains (Butler, 1992).

The nature of the samples causing during AF demagnetization gyromagnetic remanence (GRM), which will be always produced as some magnetic grains are naturally aligning together. AF demagnetization cannot perfectly demagnetize those grains causing then the problematic GRM. In order to get rid of the GRM, samples need to be Tumble AF demagnetized on Tumble demagnetizer, where sample is slowly rotating during the increase of the alternating field (Stephenson, 1981).

3.3.2.1 Paleomagnetic sample measurements

Samples were thermally demagnetised in a Magnetic Measurements MMTD with a 3-stage controllable temperature oven from room temperature to 700°C. A maximum temperature of 250°C or 300°C or 350°C or 400°C or 450°C or 650°C, was used for each sample, followed by 5 mT to 10 mT steps of AF demagnetisation. The first sample measurement was the NRM at 2G magnetometer followed by heating to 100°C, 200°C and continuing in the steps of 100°C (or 50°C depending on the character of the sample) up to the maximum temperature (this was decided on behalf of the data acquired on 2G magnetometer after each heating step), with MS measurement at each heating step. All specimens were processed in batches of 12 to 15 since this is as many as the thermal demagnetiser could take.

The maximum temperature of heating was decided by the MS rise (the encreasement of the magnetic susceptibility signifies the thermal alteration gain during the last heating step, this was various to each sample due its slightly different mineralogy) measured during the heating-induced alteration of the specimens, or in some cases the dominance

of a haematite remanence. The combined technique (i.e. thermal followed by AF demagnetisation) for demagnetizations were used because of the rise in MS. Specimens containing a hematite remanence were heated to higher temperatures such as 650°C. The dolomitic samples were heated to 250°C or 300°C at most, as suggested also by other studies (Langereis *et al.*, 1989; Kirschvink *et al.*, 2008).

The remanence was measured on RAPID 2G magnetometer after each demagnetisation step (Kirschvink *et al.*, 2008), together with susceptibility measurement (MS) on a Bartington MS1-D susceptibility meter (Dearing, 1994).

After thermal demagnetisation, static alternating field (AF) demagnetization on the RAPID 2G magnetometer was used on most specimens. AF steps were dependent on the maximum temperature of the heating. For low maximum temperatures, up to 350°C, AF demagnetization was used in steps 5mT, 10mT, 15mT, 20mT and then in steps by 10mT up to 100mT.

For some higher maximum heating temperatures, from 400°C to 650°C, AF demagnetization were also used in steps 5mT, 10mT, 15mT, 20mT and then in steps 10mT up to 50mT. For these higher temperatures, this was to attempt to remove the viscous remanence acquired by the thermally altered specimen. Most of the specimens were treated to the GRM correction procedure of (Stephenson, 1981), at 30 mT and higher fields.

3.3.3 Biostratigraphical analysis of Foraminifera

For magnetostratigraphic correlation in an absolute time scale, foraminiferal biostratigraphy was used. This was co-work with Charles University in Prague with Katarina Holcova and Matic Rifl.

3.3.3.1 Sample preparation

For the Meathop Quarry 17 samples were chosen from the residual palaeomagnetic samples, corresponding to important stratigraphy levels, where could bioclasts could be expected. These samples were cut into smaller sizes 10 to 5cm long and send to Charles University. They then cut the thin sections and polished them for microscopy.

3.3.3.2 Sample detection

Samples were taken by Matic Rifl for analysis under the polarising microscope Motic BA310Pol. They were evaluated for abundances of identifiable grains and their areal coverage in each thin section. Sedimentary structures and textures were also broadly identified as well. The classification of foraminifera was done according to (Kalvoda *et al.*, 2012; Vachard and Arefifard, 2015).

3.3.4 Isotopic measurements

25 samples of roughly equal spacing within the 170 m were chosen for carbon isotopes, avoiding palaeosols. Samples were firstly cleaned with brush under the running water to get rid of all soil and other non-original organic material. Samples were then crushed to fine dust, one by one by using the cylindrical Tema mill. Those samples were transported to the clear plastic bags to not to contaminate the samples.

Then the samples were weighted to the small sampling tubes for the Mass spectroscopy method. Carbonate carbon isotopes from bulk carbonate $\delta^{13}\text{Carb}$ were determined on the samples by liberation with phosphoric acid. Produced gases were passed under He (to provide inert atmosphere) through chemical traps to remove sulphur, excess oxygen and water. Nitrogen was separated from CO_2 by temperature programmed desorption. The

isotopic composition of the resultant purified CO₂ was then measured using an Isoprime100 Isotope mass spectrometer. Carbon isotope ratios are reported as delta values $\delta^{13}\text{C}$ in per mil relative to the international VPDB scale. Analytical precision (1σ) is estimated to be better than $\pm 2.492\%$ for $\delta^{13}\text{C}_{\text{carb}}$ based on the replicate analysis of pure, well-mixed, organic compounds used as laboratory calibration materials.

The measurements were then compared with standards LSVEC (standardised lithium carbonate), NBS18 (carbonatite standard) and IAEA-CO-1 (natural carbonatite standard).

3.4 Data processing

3.4.1 GM4 edit software

For data processing the GM4edit software was used, developed by Mark Hounslow. Datasets were loaded into GM4edit as the 2G SAM files, which extracted the RMG data for each specimen. Then the susceptibility data were manually entered into the specimen information and saved as rs3 and gm4 format files.

3.4.2 Remasoft software

The rs3 files were loaded into Remasoft 3.0 software from AGICO.Inc. and the stereo plots and Zijderveld diagrams in geographic and tilt corrected coordinates were produced. Those two plots were extracted into a Word document for visual analysis of the demagnetisation information (Figure 37).

The information from each specimen was also summarised into an Excel file, to constrain a list of magnetic polarities and other information for each specimen from each sample.

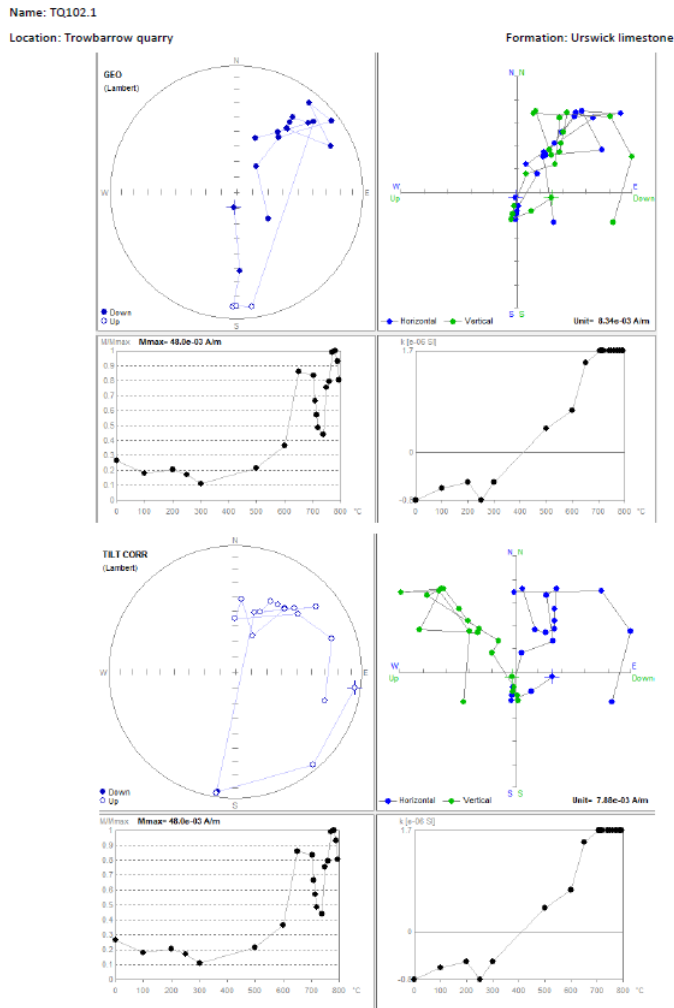


Figure 37 The example of extracted data from Remasoft software, specimen from Trowbarrow Quarry, part of the Urswick limestone, sample 102. The specimen shows the Kiaman overprint in steps 200°C, 250°C and 300°C. After this demagnetization continues to is the Normal Carboniferous polarity until the heating step 600°C where sample acquires the thermal alteration (this is documented by the increase of magnetic susceptibility).

The most abundant lithologies in the section were grainstones, packstones, wackestone, calcareous mudstones, dolomites, clastic shale or mudstones. Most abundant macrofossils were brachiopods, solitary and colonial corals, gastropods, roots. Also burrows and algal remain. There were also sedimentary structures visible as parallel lamination, cross-bedding, ripple lamination, channels, (lenticular, graded, nodular bedding), stromatolites and bioturbation.

Examples of features and macrofossils are visible on (Figure 39, Figure 40, Figure 41, Figure 42, Figure 43).

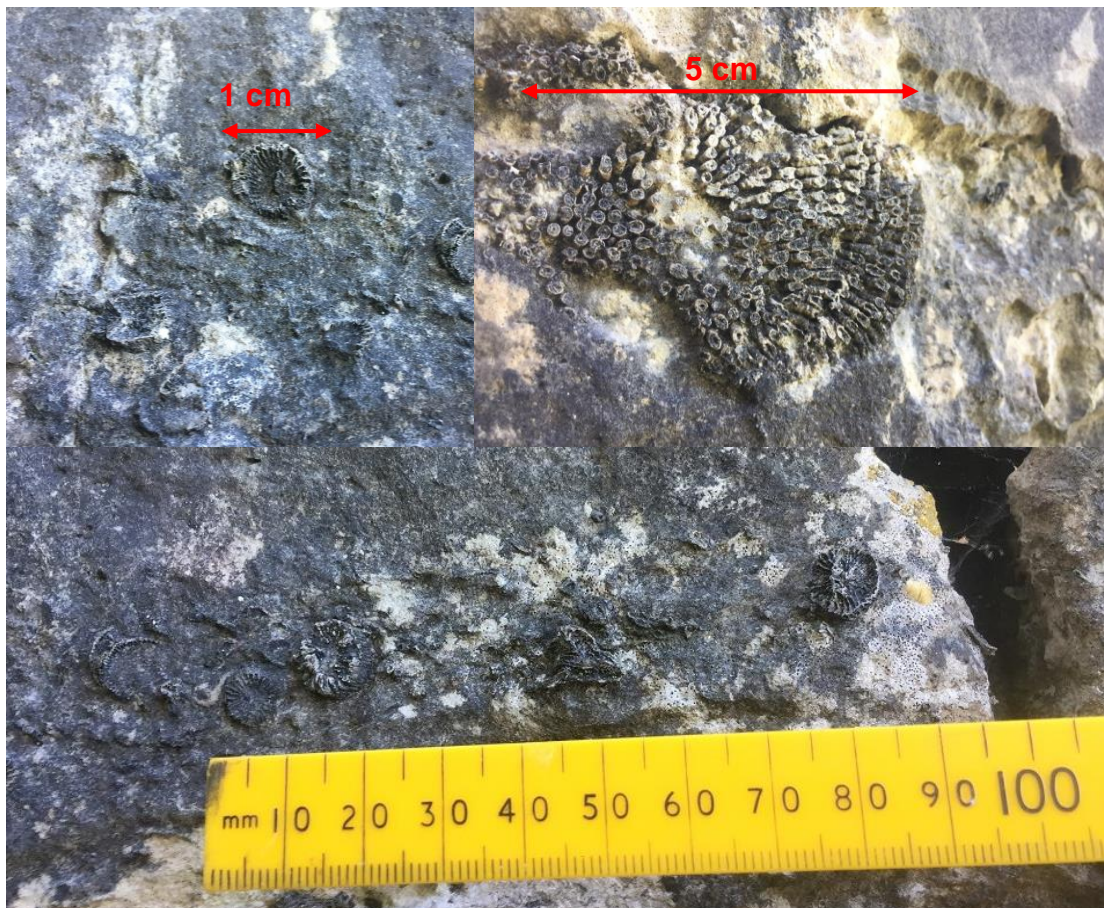


Figure 39 Fossils found in lower section of Meathop Quarry. These were mostly residuals of bioclasts of brachiopods and corals in limestone forming layers of weathered out material easily visible in the outcrop.



Figure 40 Continuous erosion contact corresponding with location of sample MQ38.



Figure 41 Laminated limestone with weathered out fossil bioclasts. Those photographs are shot in area of sample MQ40.

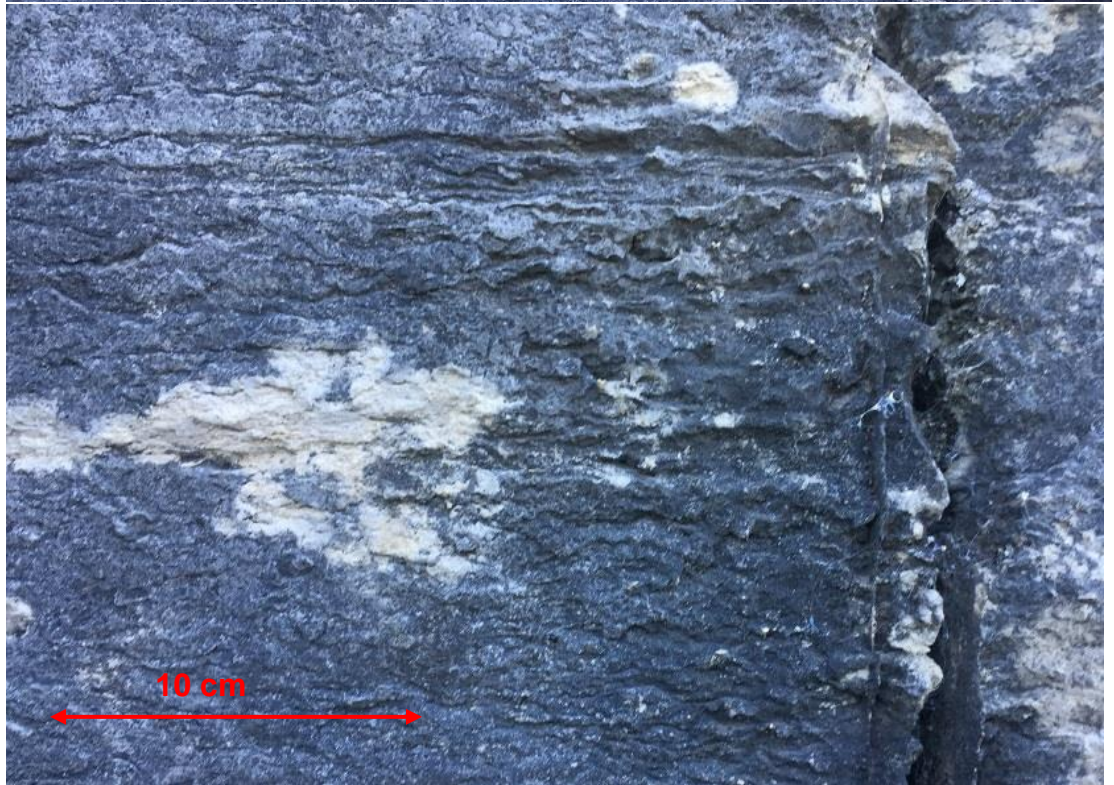


Figure 42 Laminated sediments of stromatolitic origin. This area is in between sample MQ 41 and MQ42.



Figure 43 Fossils found in top section around meter 50 of Meathop Quarry. Mostly residuals of bioclasts of corals in limestones forming layers of weathered out material easily visible in the outcrop and Neptune veins filled with dolostones.

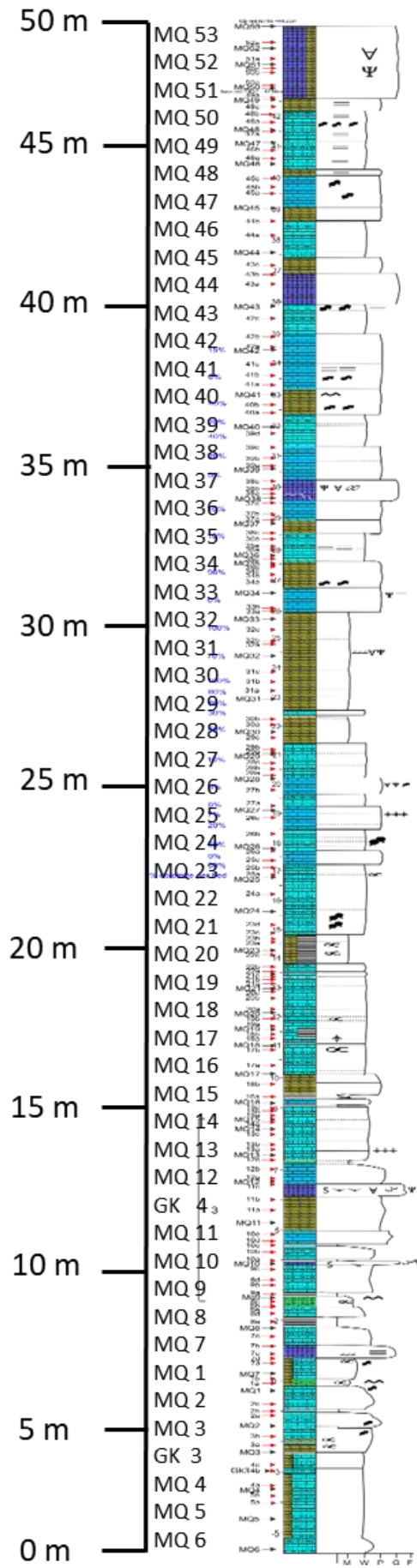


Figure 44

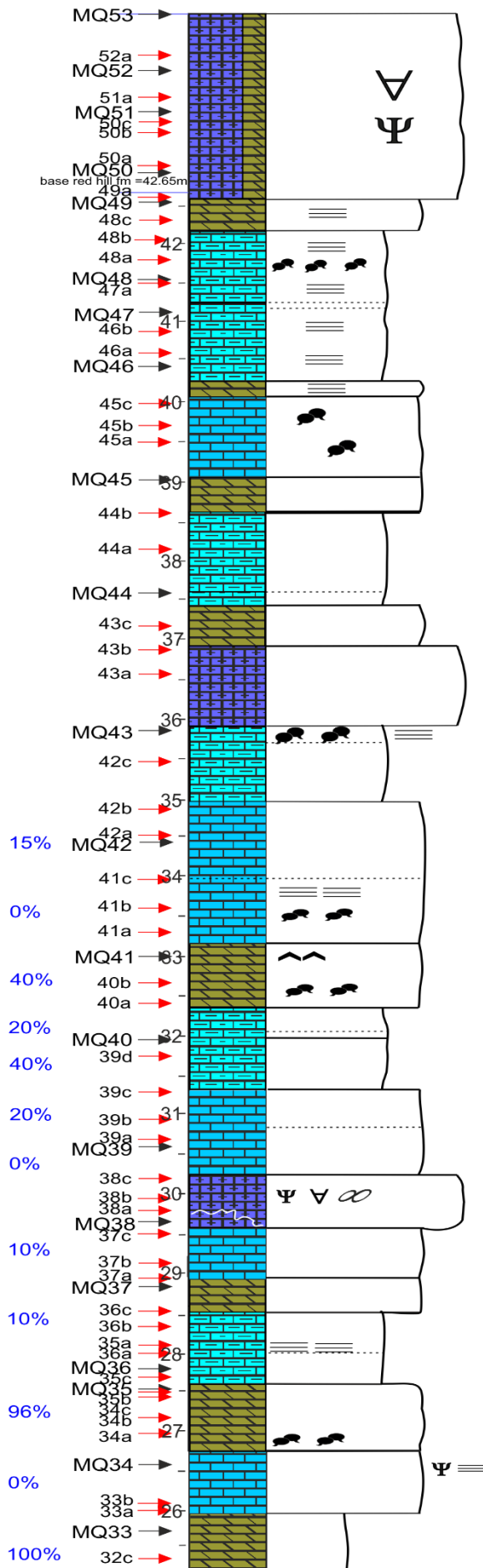


Figure 44

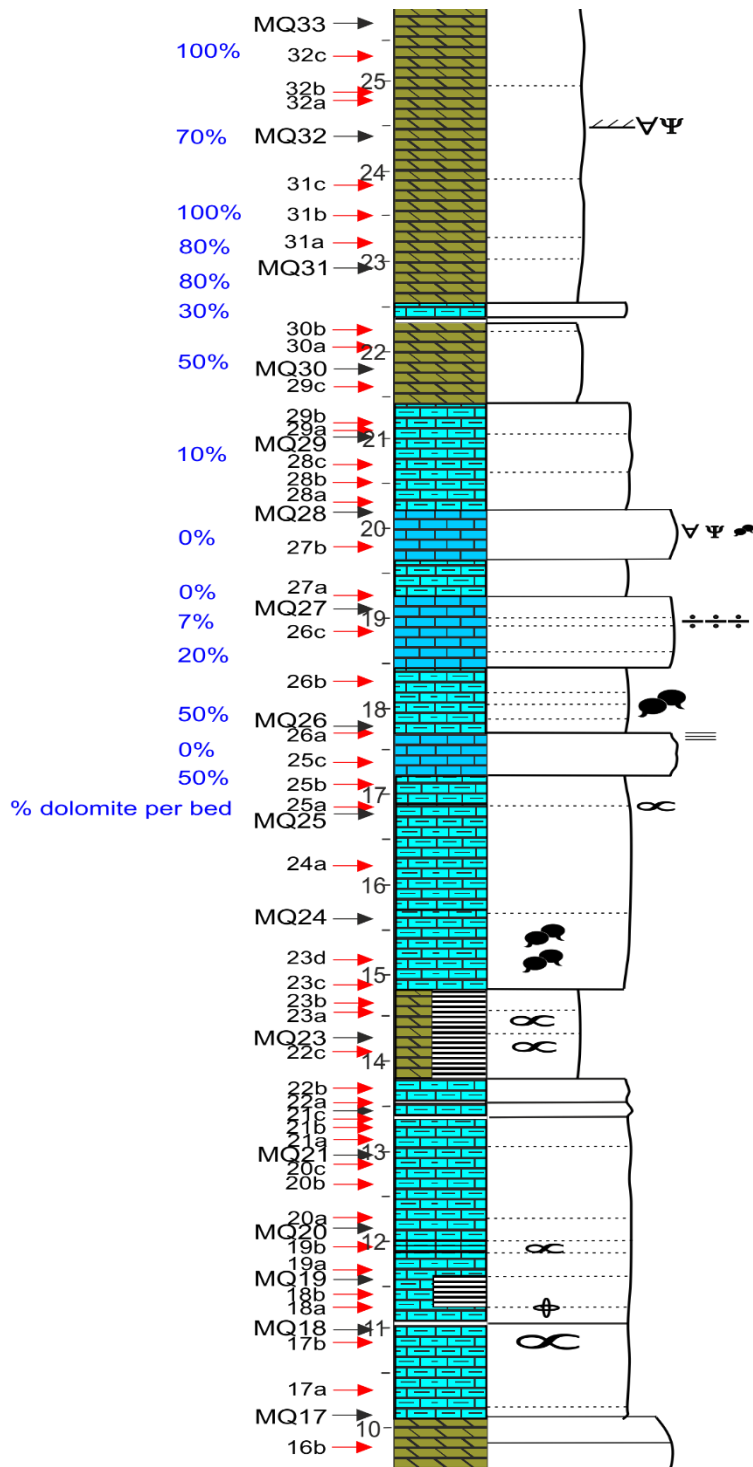


Figure 44

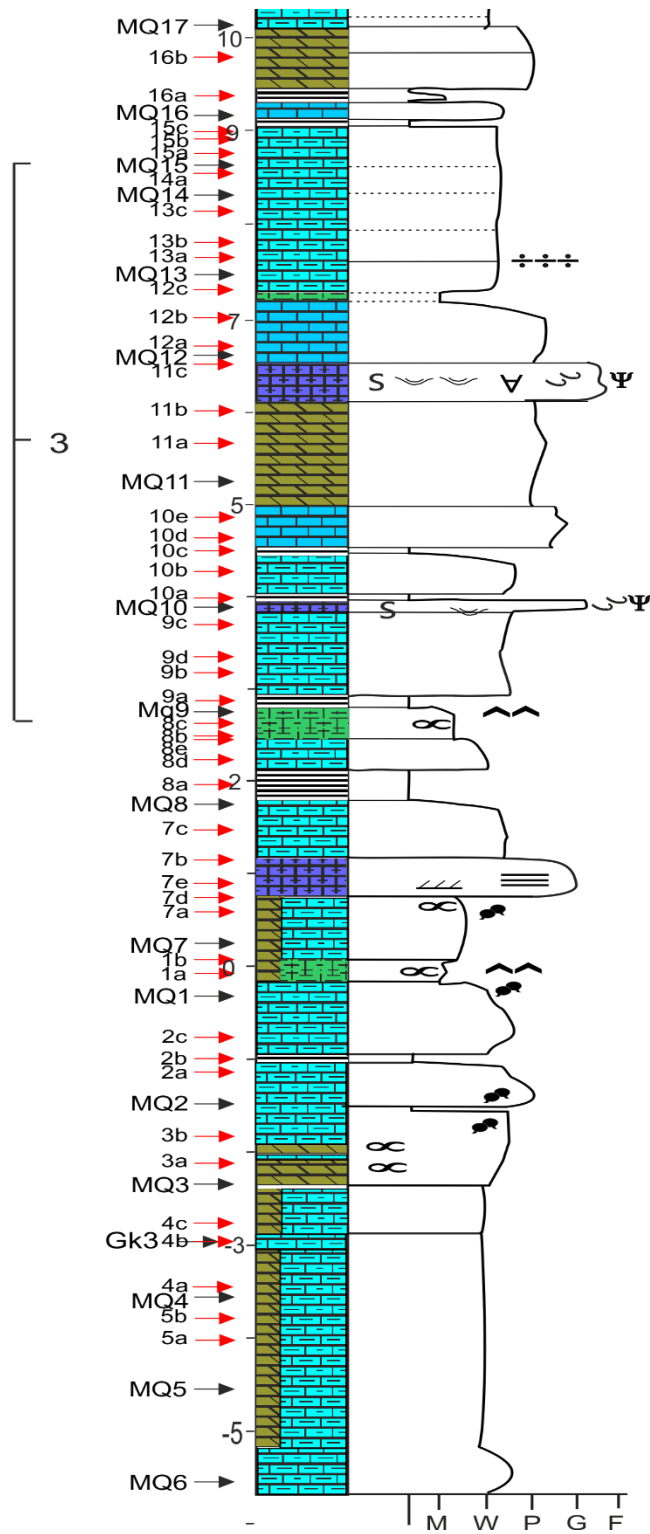


Figure 44

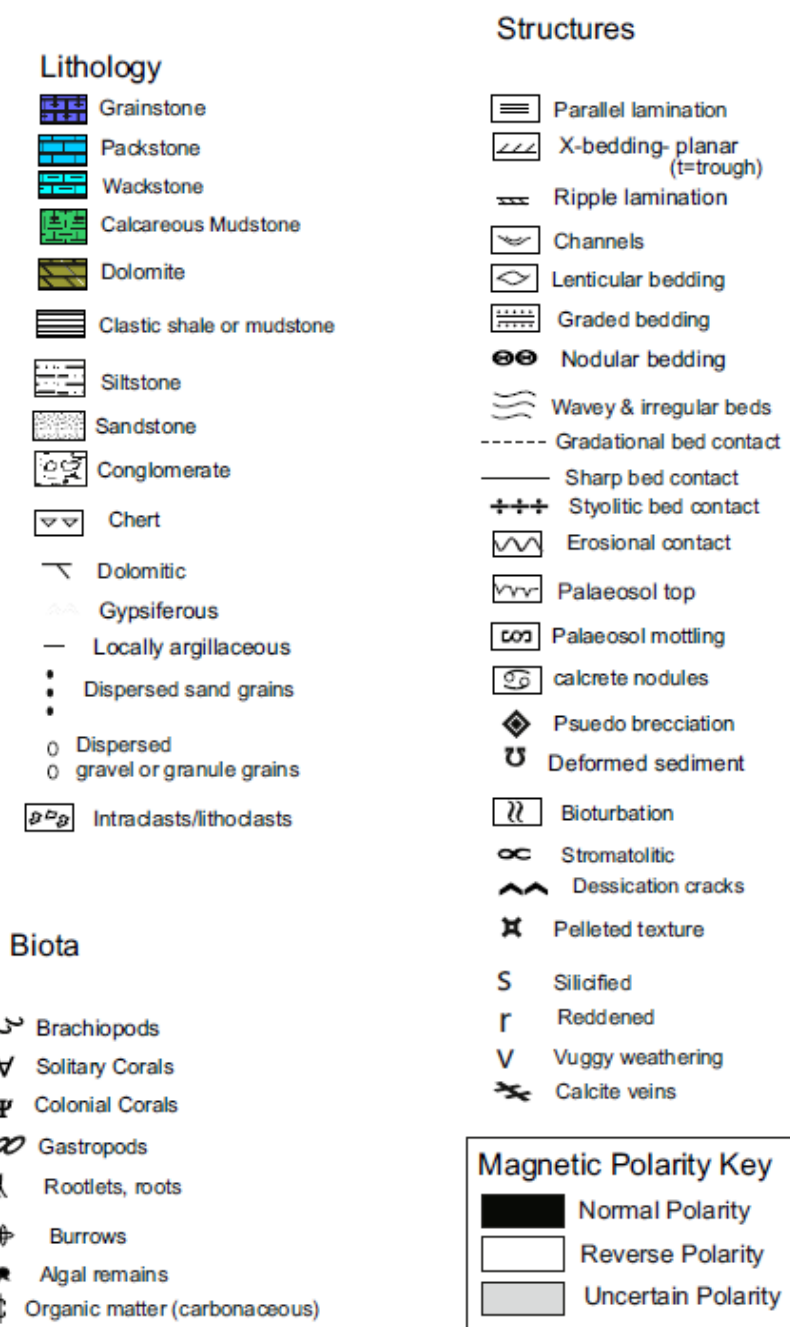


Figure 44 The Key for and log produced by our locality description, lithological description and bedding measurements.

4.1.1 Sedimentary description

The sedimentary log (Figure 44) of Meathop Quarry describing in total 50m.

The lower part, 0 to 25 meters are mostly wackstone varying in some parts with dolomite and grainstone. In the top part dominate the dolomite together with parts of grainstone, packstone and wackstone. In the position of 7 m, 17 m and 20 m can be found clastic shale or mudstone. The top 2,5 m is heavy dolomitized grainstone with the clastic dikes.

Fossil record is distributed to zones from 4 to 12m with stromatolihic record, algal remains. In the top of this section can be found silicified colonial corals and brachiopods. Section from 19 to 21m, the lower part has stromatolihic remains corresponding with the dolomitized shale, top part of this section has algal remains. Section from 23 to 25m has stromatolihic, algal and colonial coral remains, in the mid of this section is stylolithic bed contact. Section from 37 to 39m is has algal remains and dessication cracks. In the mid and top of this section is parallel lamination. The uppermost section, from 43 to 50m has algal remains, with parallel laminations and the top of this section has solitary and colonial corals.

4.1.2 Microfossil biostratigraphy

The sub-division of the Viséan follows the MFZ biozones (MFZ=Mississippian Foraminiferal Zone) characterisation as proposed by (Poty et al., 2006)

Meathop Quarry results are summarized in the (Figure 45). The higher part of the section at Meathop Quarry has mostly uniform algal and foraminiferal assemblages. Our findings corresponds with the findings of (Kalvoda and et al., 2011; Kalvoda *et al.*, 2012) in England, South Wales and Ireland in rocks of a similar age. (Figure 45) display the presence of foraminifera species on the right side. The most abundant on the fossils was intraclastic algal limestone and intraclastic oncoidal grainstone. By contrast sections dominated by dolomitized limestones, do not preserve any foraminifera, and due to this it is difficult to characterize this part. The fossils were probably washed out during the dolomitization process. Thus, section between meter 40 to 45 except to the borders, has no biostratigraphic data.

The occurrence of some foraminifera species indicates the possibility of this being part of the uppermost MFZ 8 or lowermost MFZ 9 (Figure 45). Due to the lack of data in the section in between meter 40 to 45, it is not possible to determine the boundary between those zones (MFZ). The boundary between the MFZ 8 and MFZ 9 are recognized as the chronostratigraphic border in between the Tournaisian and Viséan (Kalvoda and et al., 2011).

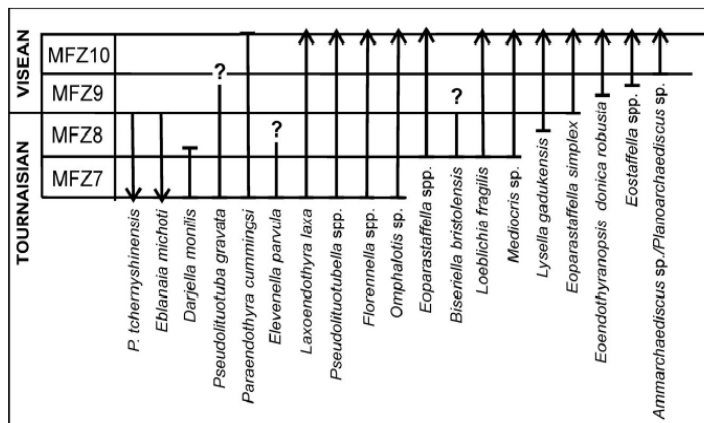
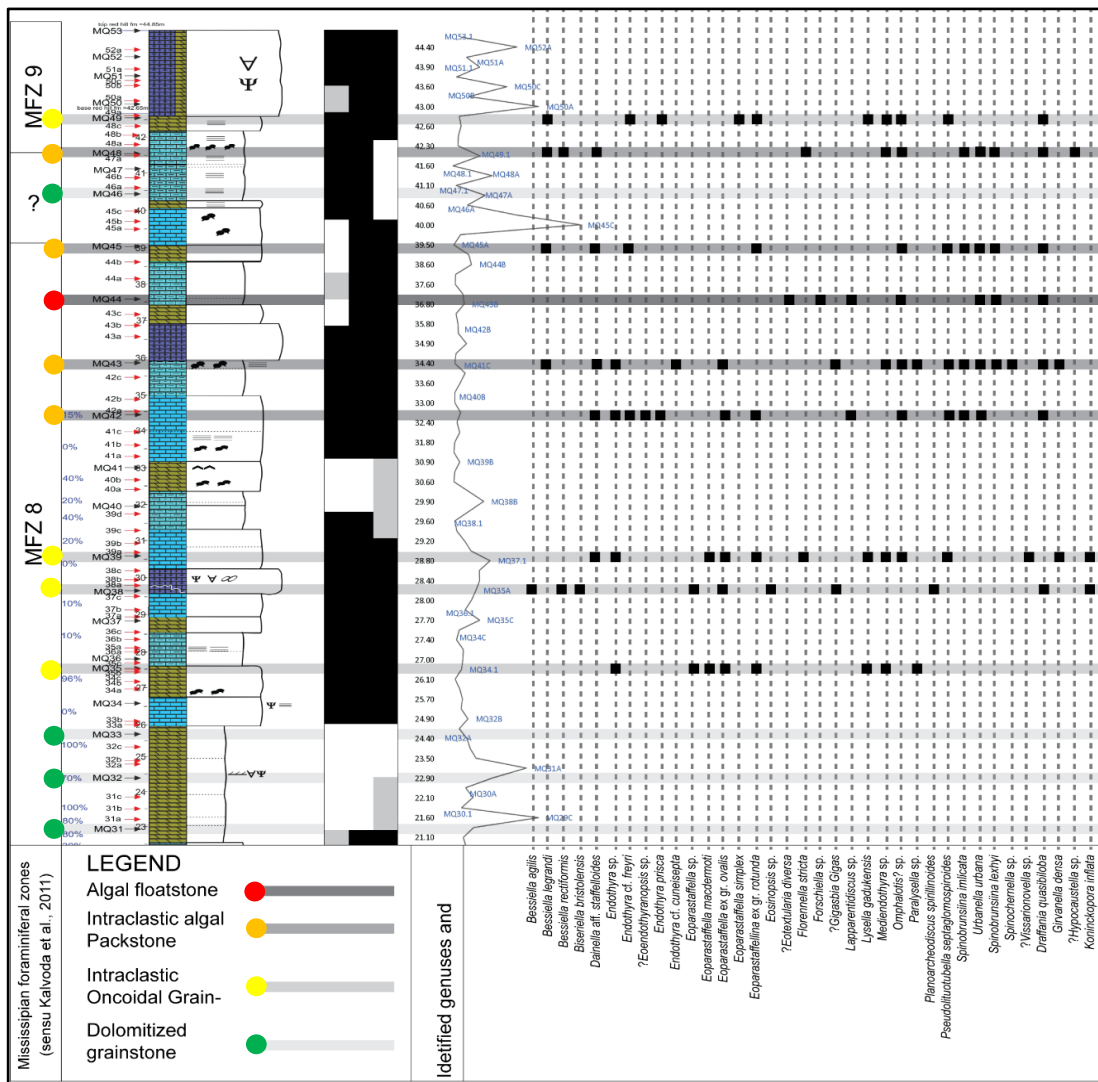


Figure 45 Upper: Meathop Quarry: The dataset of presence and absence of foraminifera assemblages. Bottom: The zonation of foraminifera by (Kalvoda and et al., 2011).

The top part of the section indicates a lowermost to Lower Visean age, which is characterized as Mississippiian foraminiferal zone MFZ8 and MFZ9 following Kalvoda et al. (2011).

4.1.3 Magnetostratigraphy, magnetic susceptibility and mineral origin of the magnetism

4.1.3.1 Magnetostratigraphy

52 samples from Meathop Quarry, with 3 or 4 measured specimens was undertaken to diminish the uncertainty in the polarity determination.

(Figure 46) shows how the data from Meathop Quarry fits in accordance with sampling at other sampling sites, which are ongoing projects described elsewhere. Meathop Quarry covers most of Chadian stage continuing into the lower part of the Arundian.

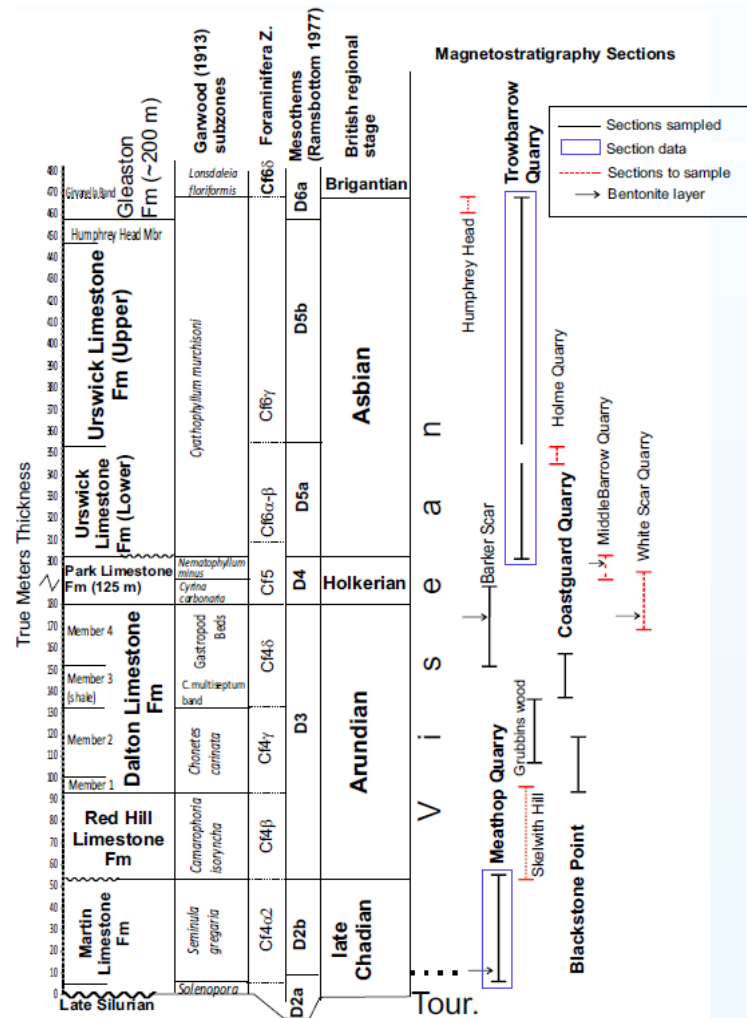


Figure 46 Shows the studied section Meathop Quarry with surrounding areas sampled for similar projects corresponding with time.

Processed paleomagnetic data shows, that many samples has been overprinted in the later period. The direction was southern with low inclination. That gave us insight that this overprint might be the Kiaman superchron from upper Carboniferous - upper Permian. This direction could be found quite often, the demagnetization has to be taken further in order to get rid of this overprint. The results of magnetic measurements show a dominance of a reverse polarity overprint from the later Kiaman superchron (Figure 47). This is visible in most specimens within the different parts of the section. Hence, the expectation was that the primary signal should be present at the highest demagnetisation temperature (depending on the magnetic carriers) and/or the larger AF demagnetization fields.

In some samples it was problematic to distinguish if any primary signal was recorded, other than the Kiaman component. This was typically a problem with the specimens having a strong Kiaman component, which was not fully demagnetized, so it was impossible to be confident if any primary signal remained in these cases. In that case, it was necessary to take a new specimen and do the whole measuring procedure again, continuing to a higher temperatures at or over 450°C and perform the AF demagnetization in more detail between 50-100 mT. Some results can be seen (Figure 48, Figure 49, Figure 50, Figure 51). The NRM magnitude is mostly less than 10mA/m it is weak magnetization. The NRM direction was variable from 341,4 Dec/10,4 Inc to 74,1 Dec/ - 74.9 Inc. The TVRM component shows from 0 (NRM) to 300, Kiaman component from 300 to 450 and the CHRM component from 450 to 550.

It was therefore finally necessary to measure from 3 to 4 specimens from each sample to have a reasonable confidence in finding a specimen that worked, or collectively showed similar behaviour.

The results were recorded into Excel with respect to stratigraphic height position in the profile and the magnetostratigraphic chart was so formed.

The results (Figure 47) show quite a few reversals of polarity within the section. Black correspond with normal polarity, white with reversed polarity and grey convey uncertainty in the polarity, half black half grey means uncertain, probably normal polarity. These uncertainties can be found at meter six, eight and thirty-two of the profile. One meter is estimated to be sedimented in about 30 000 yrs (based on duration of Visian and average thickness), and so on that basis shows that reversals were quite common. There are 7 reversed polarity zones in a dominant interval of normal polarity within the 50 m of the section. The dominant is normal polarity, intervals varies from 60 000 yrs to 360 000 years. The reversed polarity was significantly shorter, as the longest interval was 90 000 yrs and shortest 30 000 yrs. The reversal rate is 7 reversals to 1 500 000yrs it is roughly one reversal each 215 000 years during the lower Visian.

The (Figure 48, Figure 49, Figure 50, Figure 51) show the projections in Geographic coordinates, Tilt corrected and Zijderveld projection. Stereoscopic projection shows a Kiaman component and primary direction of normal or reversed polarity. Figures also have intensity chart for the different demagnetisation steps and magnetic susceptibility curve for each step. Those charts were created in Remasoft software after processing the data in GM4 edit software. The primary and Kiaman directions were visually detected on behalf of the comparison with the Carboniferous and Kiaman paleodirections.

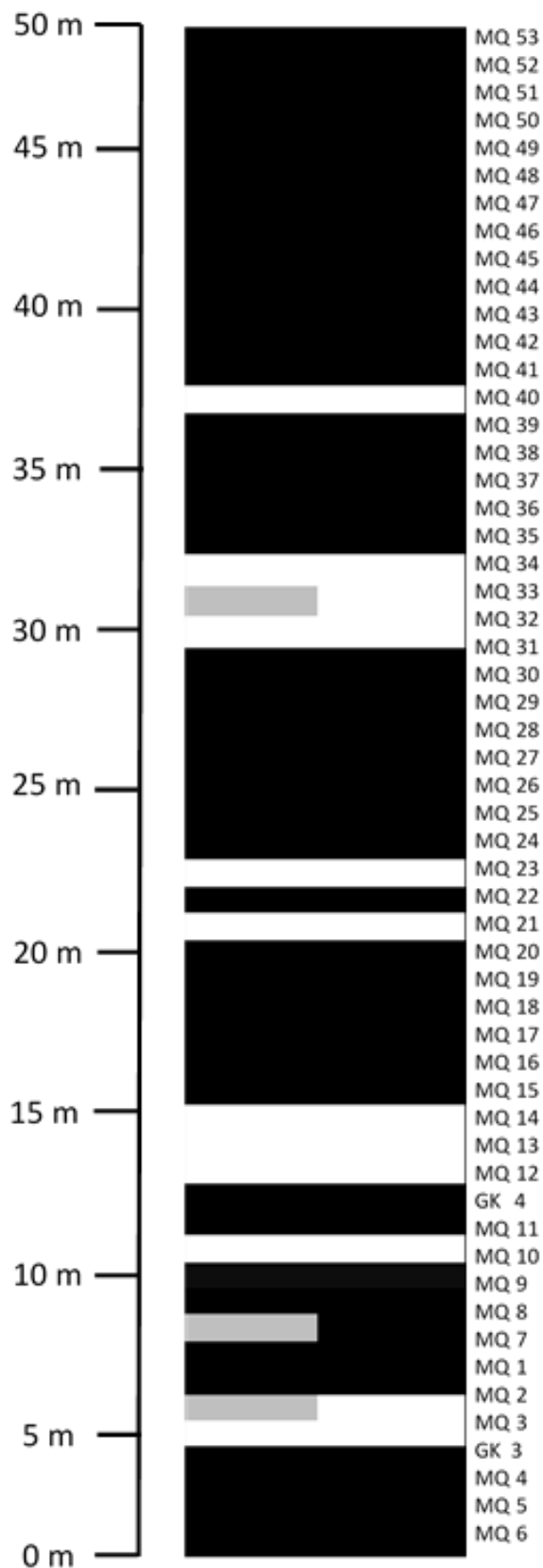


Figure 47 Results of magnetostratigraphic measurements form Meathop Quarry. Black stands for normal polarity and white for reversed polarity. Grey colour shows uncertainty of polarity.

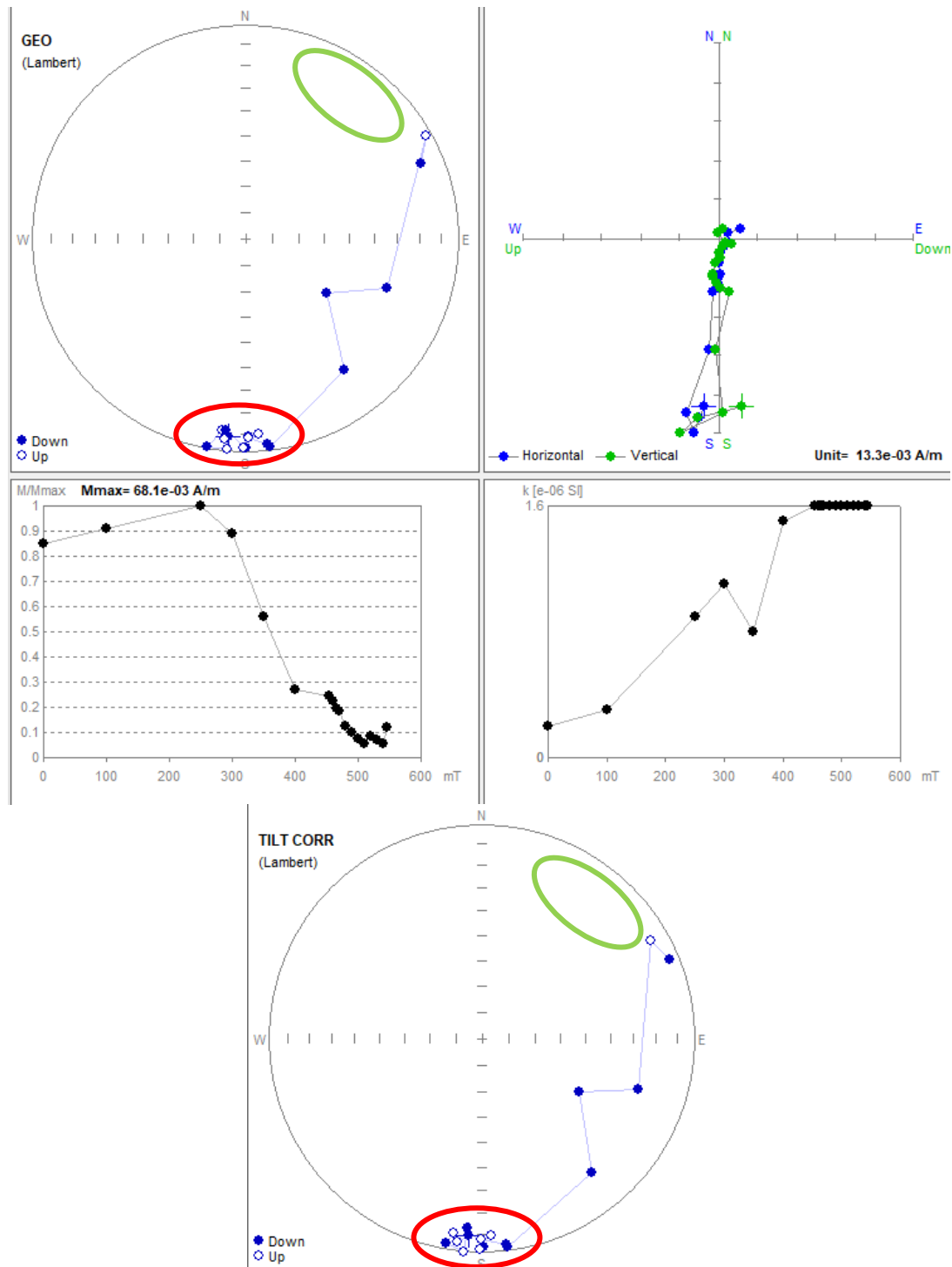


Figure 48 Sample MQ50.1. Upper: projections in Geographic coordinates and Tilt corrected on the lower part. On each, the right side is a Zijderveld projection. In the stereoscopic projection is a strong Kiaman component (red circle) and then further demagnetization trends towards the primary direction of Normal polarity (green circle). Left chart shows the intensity for the different demagnetisation steps. Right side: the magnetic susceptibility for each step.

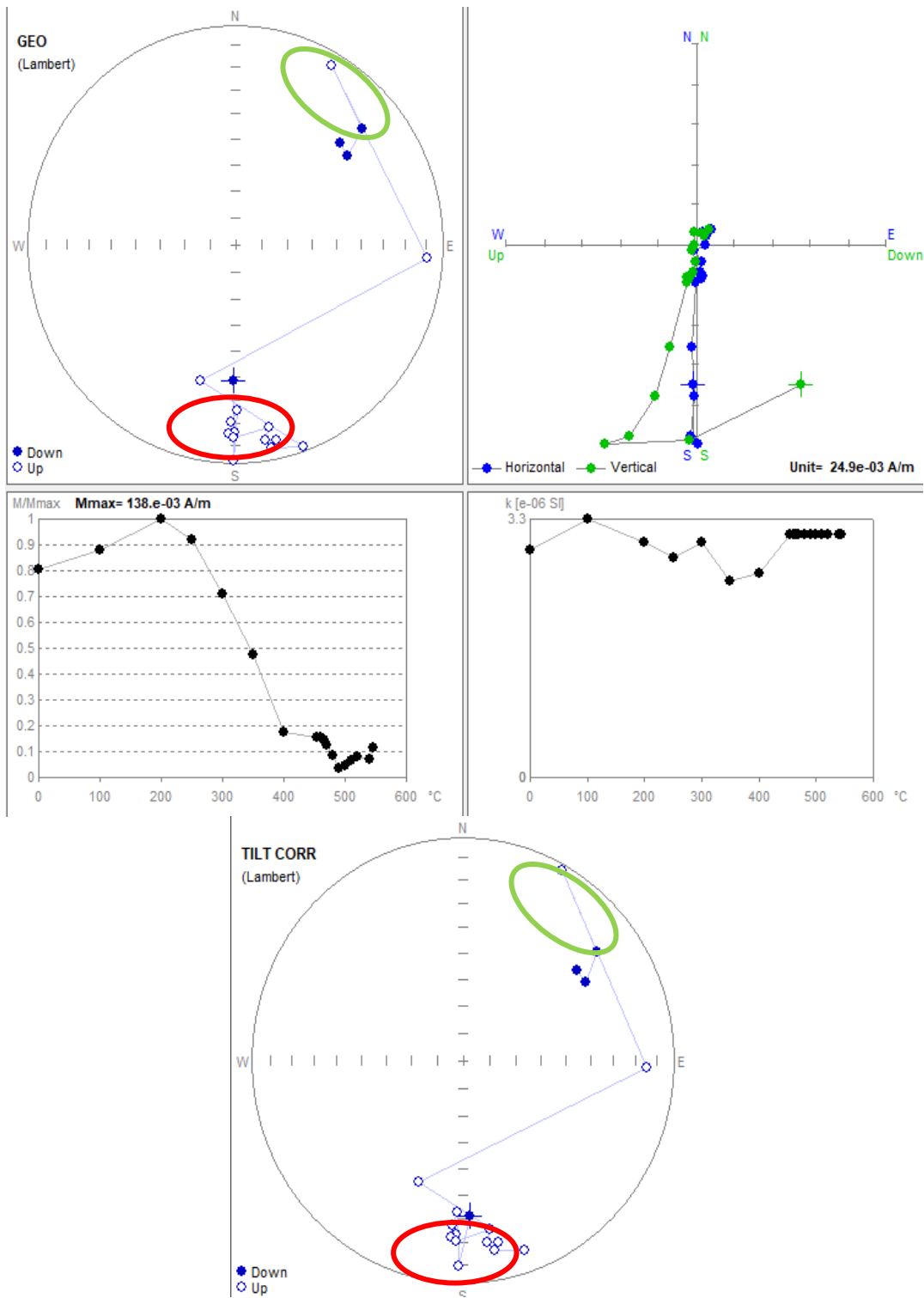


Figure 49 Sample MQ37.1. See (Fig 48) for details. In the stereoscopic projection is a strong Kiaman component (red circle) and then a further demagnetization trends towards the primary direction of normal polarity (green circle).

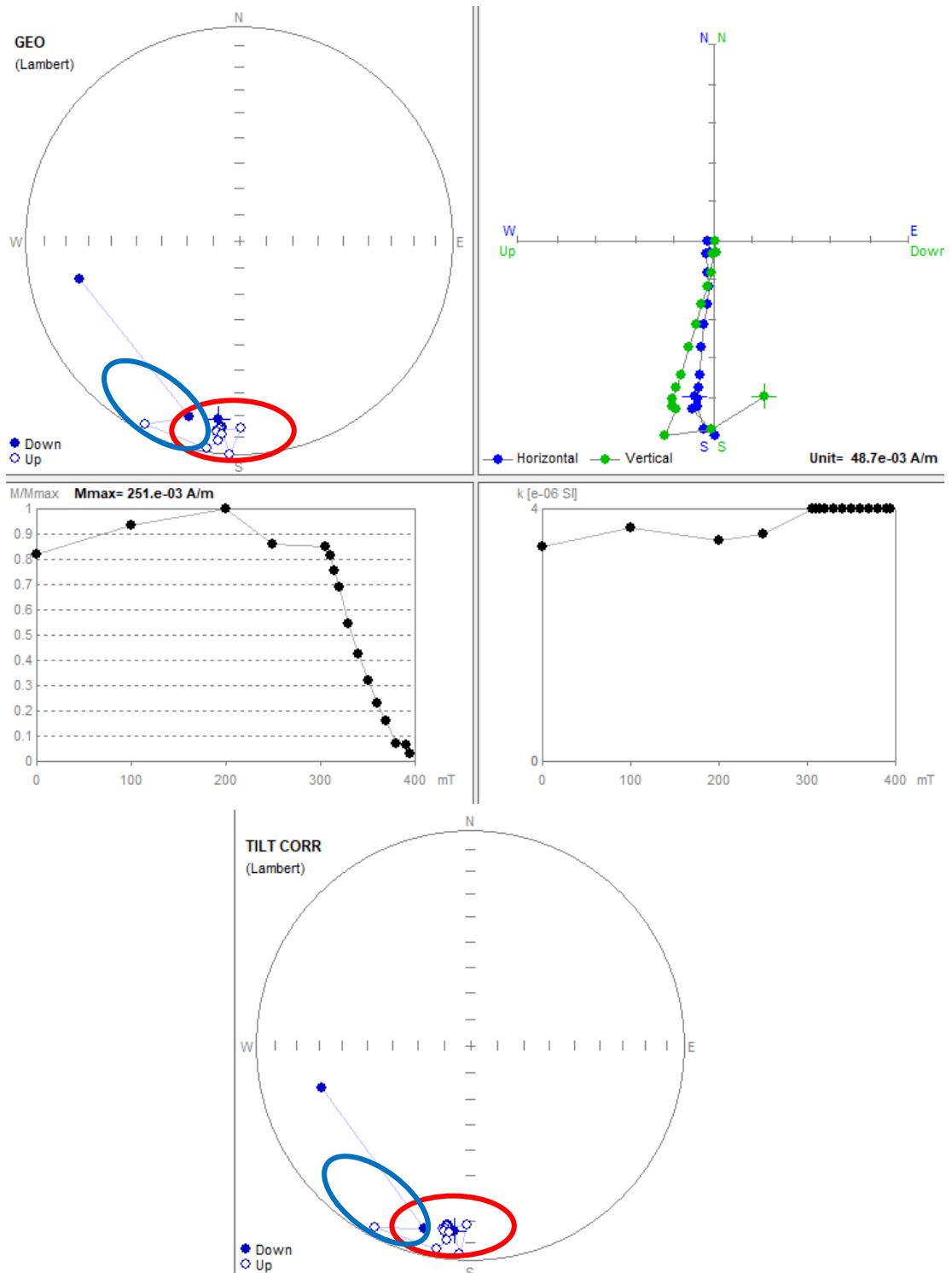


Figure 50 Sample MQ13.2. See (Fig 48) for details. In the stereoscopic projection is a strong Kiaman component (red circle) and then further demagnetization towards the primary direction of reverse polarity (blue circle).

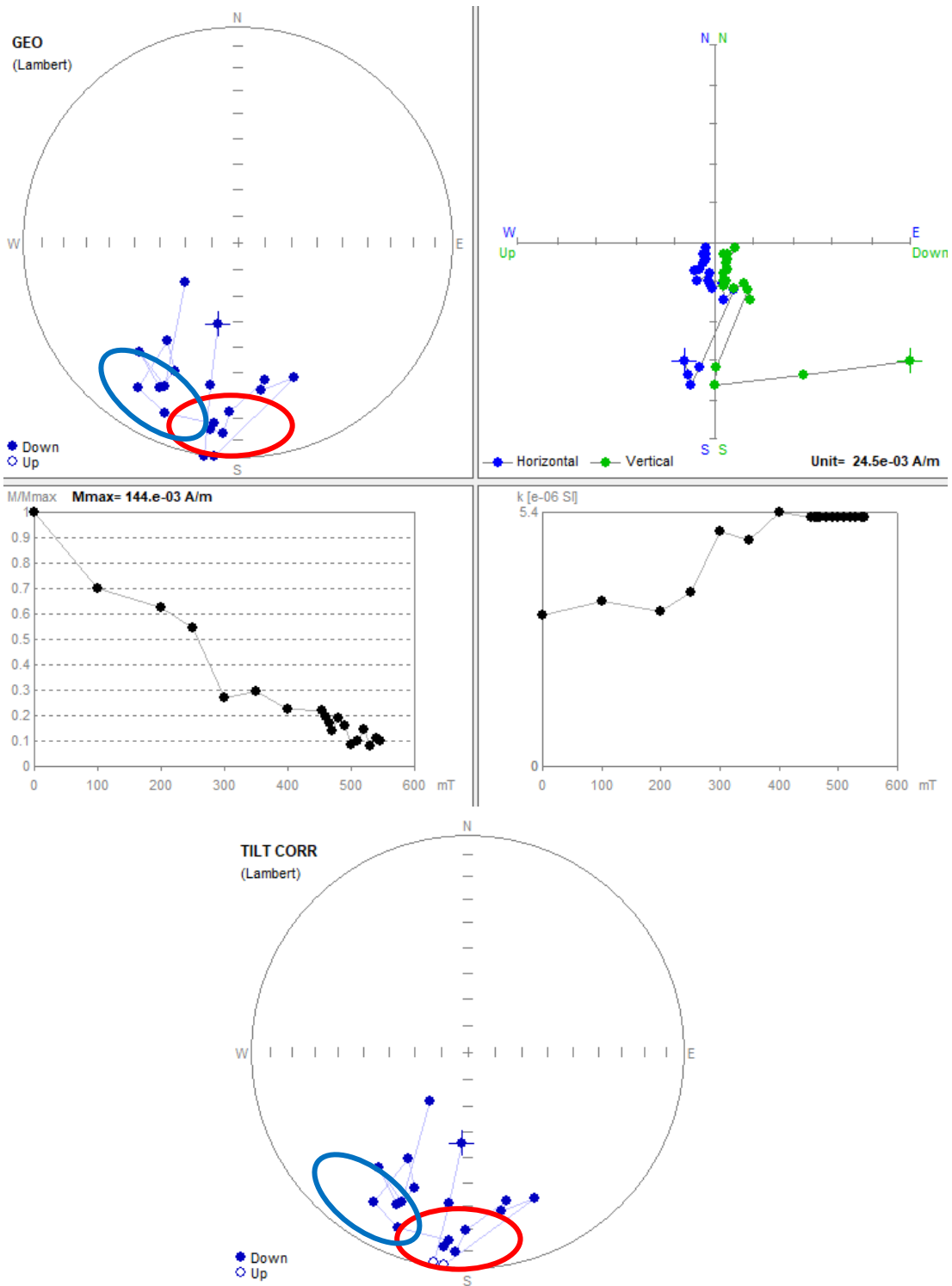


Figure 51 Sample MQ3.1. See (Fig 48) for details. In the stereoscopic projection is a strong Kiaman component (red circle) and then further demagnetization towards the primary direction of reverse polarity (blue circle).

4.1.3.2 Magnetic mineralogy

Demagnetisation results were assessed to find out if there was a polarity bias towards a particular magnetic mineral (Figure 52). This might be expected, say if the haematite was carrying a CRM. Specimen data were broken into three groups a) Samples that could be fully AF demagnetized suggesting magnetite (or a magnetic sulphide) as a magnetic carrier. b) Those that could not be AF demagnetization, indicating haematite or

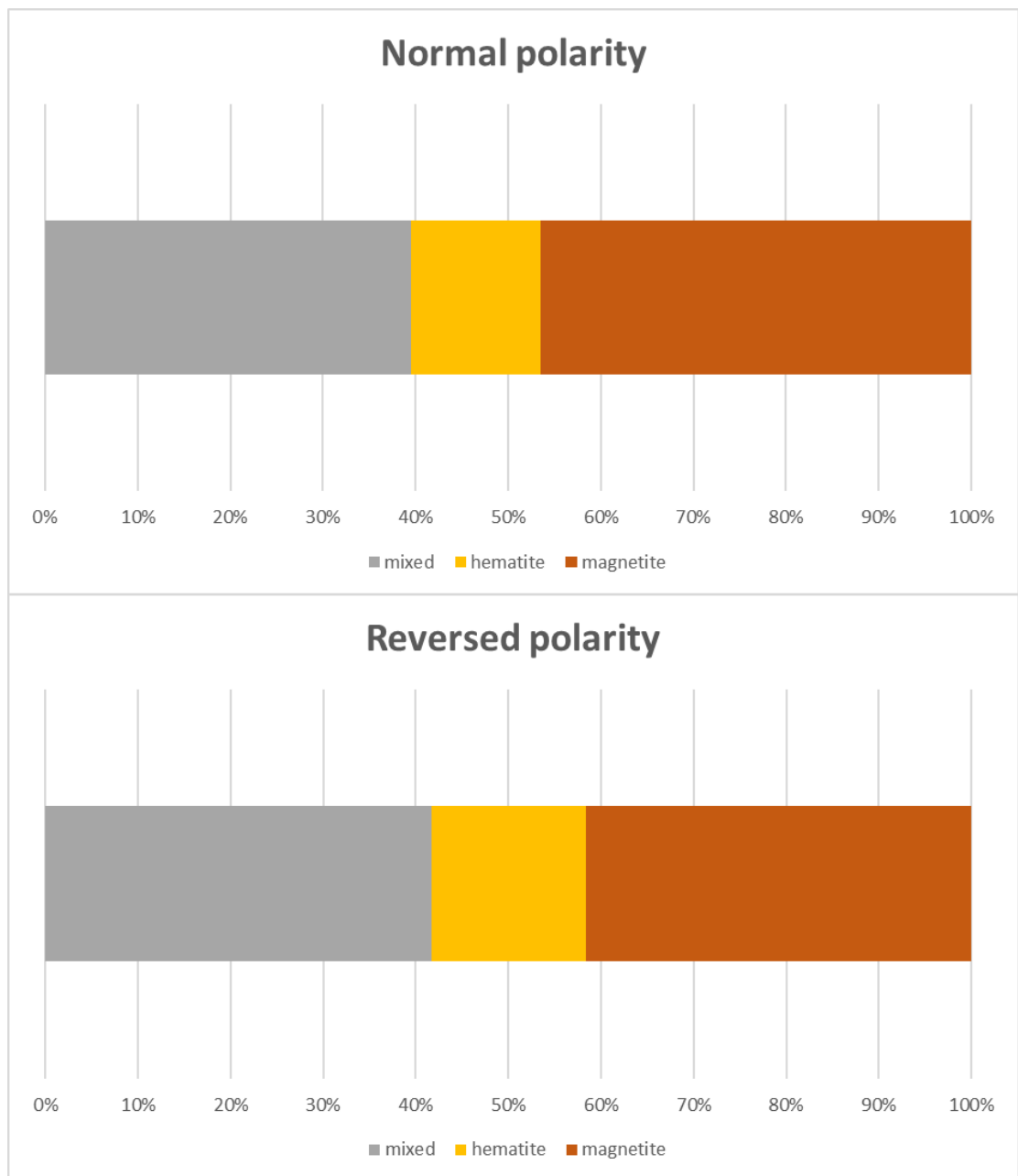


Figure 52 Percentage contribution of different minerals to inferred polarity. Normal polarity specimens have a slightly higher abundance of magnetite as a magnetic carrier than the reversed polarity.

goethite and c) samples which could be partially demagnetised, but had a high coercivity tail, so have mixed magnetic carriers. Generally, there is not a polarity bias based on their demagnetisation behaviour (Figure 53).

Magnetic susceptibility shows some variations along with the measured section. There is a peak in -3m (= 3m above road level), cluster of higher susceptibility between meter 4 and 14 (=10 and 20m above ground level) and in the top of the section around 40 m (Figure 53). The NRM intensity is quite similar to the magnetic susceptibility curve, with much variation in the lower levels (Figure 53).

4.1.3.3 Polarity interpretation

Each sample had up to 4 specimens measured, and each specimen was classified, based on the inferred primary polarity. Two classes of each polarity were assigned, with good (-1 and +1 code for reverse and normal) and -0.5 and +0.5 for poor reverse and normal respectively. A code of zero is for specimens in which a primary polarity component was not clear (Figure 52).

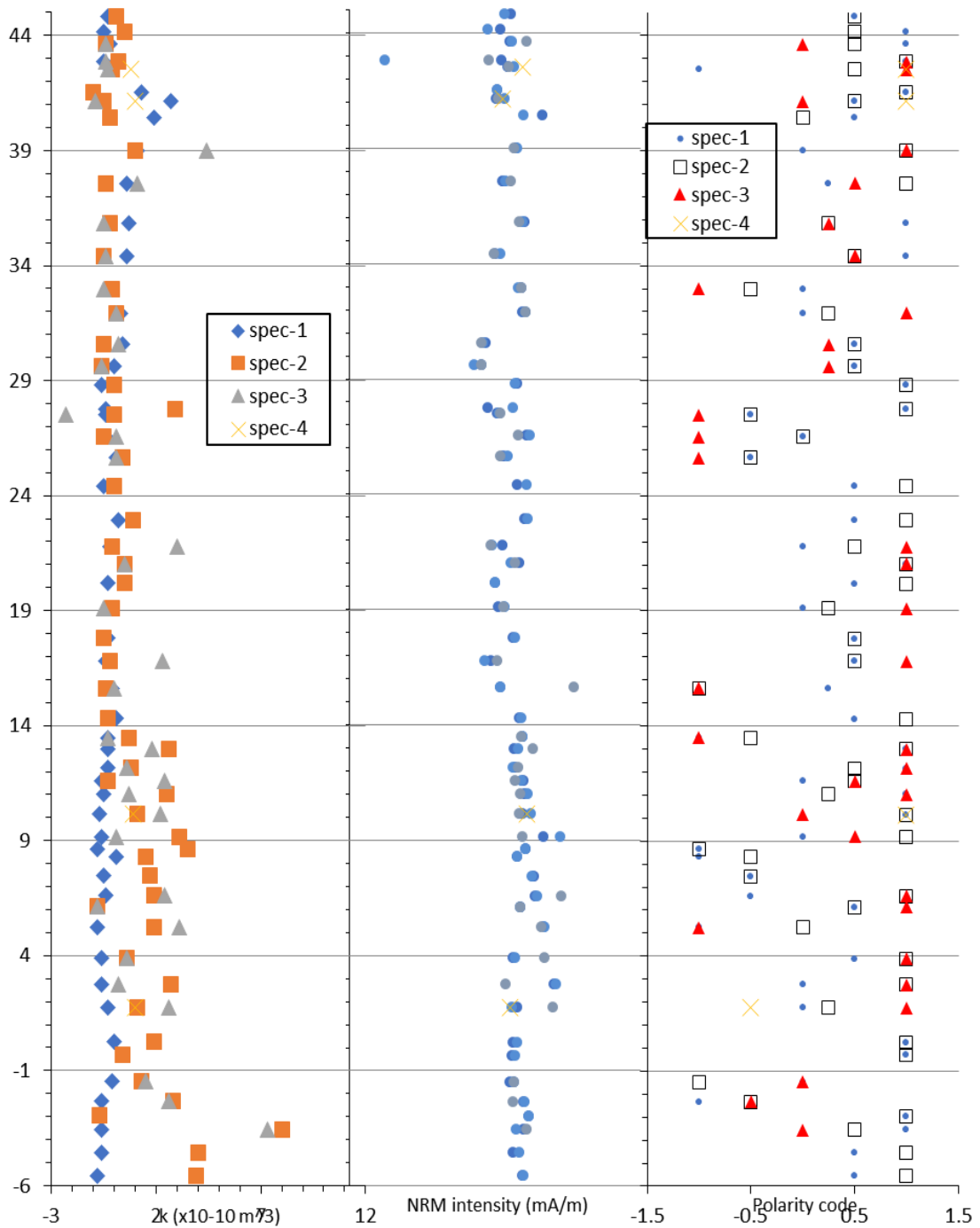


Figure 53 Summary of Meathop Quarry Magnetic susceptibility (left), NRM intensity (middle) and Magnetic polarity (right) on meter scale. Bottom -6m is equal to 0. There were measured 4 different specimens for each sample, which has the different colour and shape code.

4.2 Trowbarrow Quarry

4.2.1 Geological features and logs

Trowbarrow Quarry has a previously described lithological description derived from thin sections and logging by Horbury (1987). Horbury's log (Figure 54) was a primary source for sample locations in the quarry, even if his log was quite difficult to navigate sometimes. Some adjustments were made in thicknesses in parts where the section did not match well.

In total, the quarry has about 200 m of section. We sampled 174 levels, each sample having a minimum of 2 or 3 specimens, that were measured. Sampled locations were broken into the Upper and Lower Urswick Fm logs of Horbury and the Gleaston Fm log, which was newly constructed.

The mid part of the Urswick Fm has a shale unit, which was partly weathered out, and marked on the log as black. We sampled the shales just for susceptibility measurements since it was not possible to collect palaeomagnetic samples in the shale.

Most abundant lithologies were grainstones, packstones and wackestones. Most common fauna are brachiopods, solitary or colonial corals, roots and burrows. There are also a few locations with palaeosols, sometimes with possible volcanic ash altered to bentonite.

An interesting feature in Trowbarrow Quarry is the dramatic 'red-wall' palaeosol with holes left from tree roots (Figure 55), described by Horbury and Adams (1989). Some other features (Figure 56, Figure 57, Figure 58).

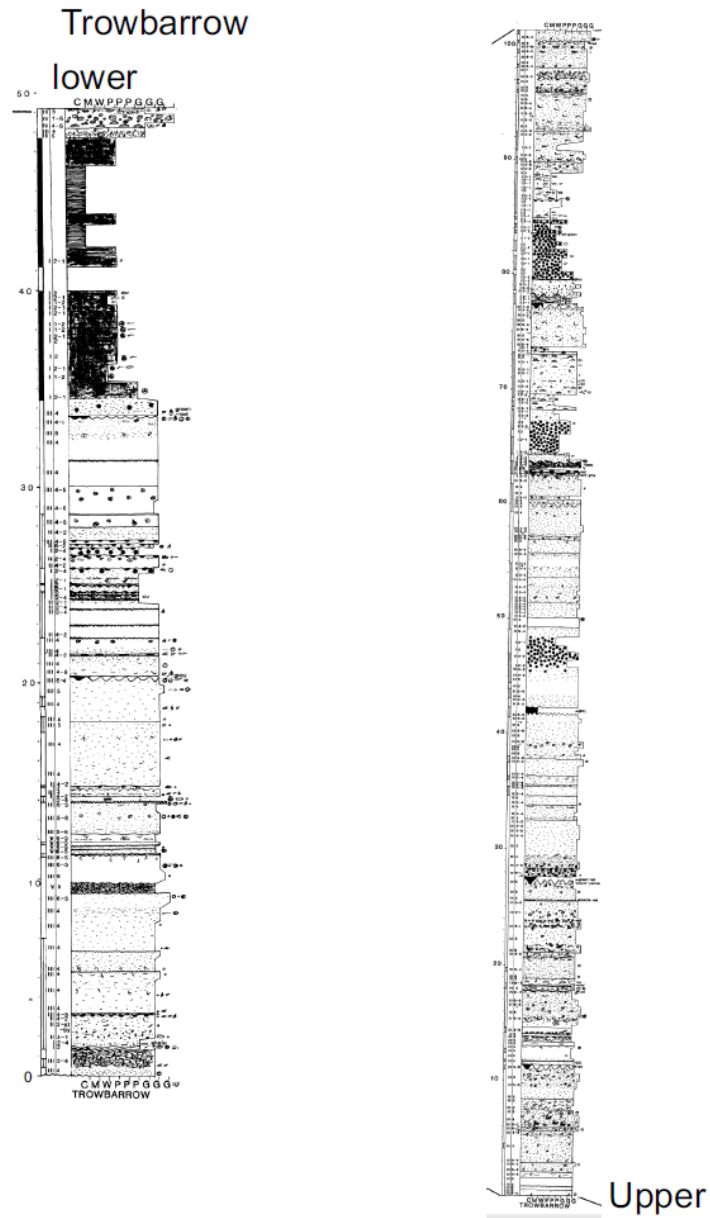


Figure 54 Original Trowbarrow Quarry logs from (Horbury, 1987) which were used as a preliminary information for logging.



Figure 55 Tree root structures in Trowbarrow Quarry, this site is exceptional for occurrence of this structures, which are perfectly visible due the vertical bedding. This part is protected, and it is used as a climbing wall, so the light marks are from climbing chalk.



Figure 56 Burrows in Trowbarrow Quarry are visible in multiple places, mainly the top part of the quarry.



Figure 57 Area with quite big burrows, very well visible the 2D architecture in the wall. Those burrows of different sizes are visible in multiple places in the top section of the quarry.



Figure 58 Rich fossil fauna, area with quite big fossils of brachiopods and other clastic residuals.

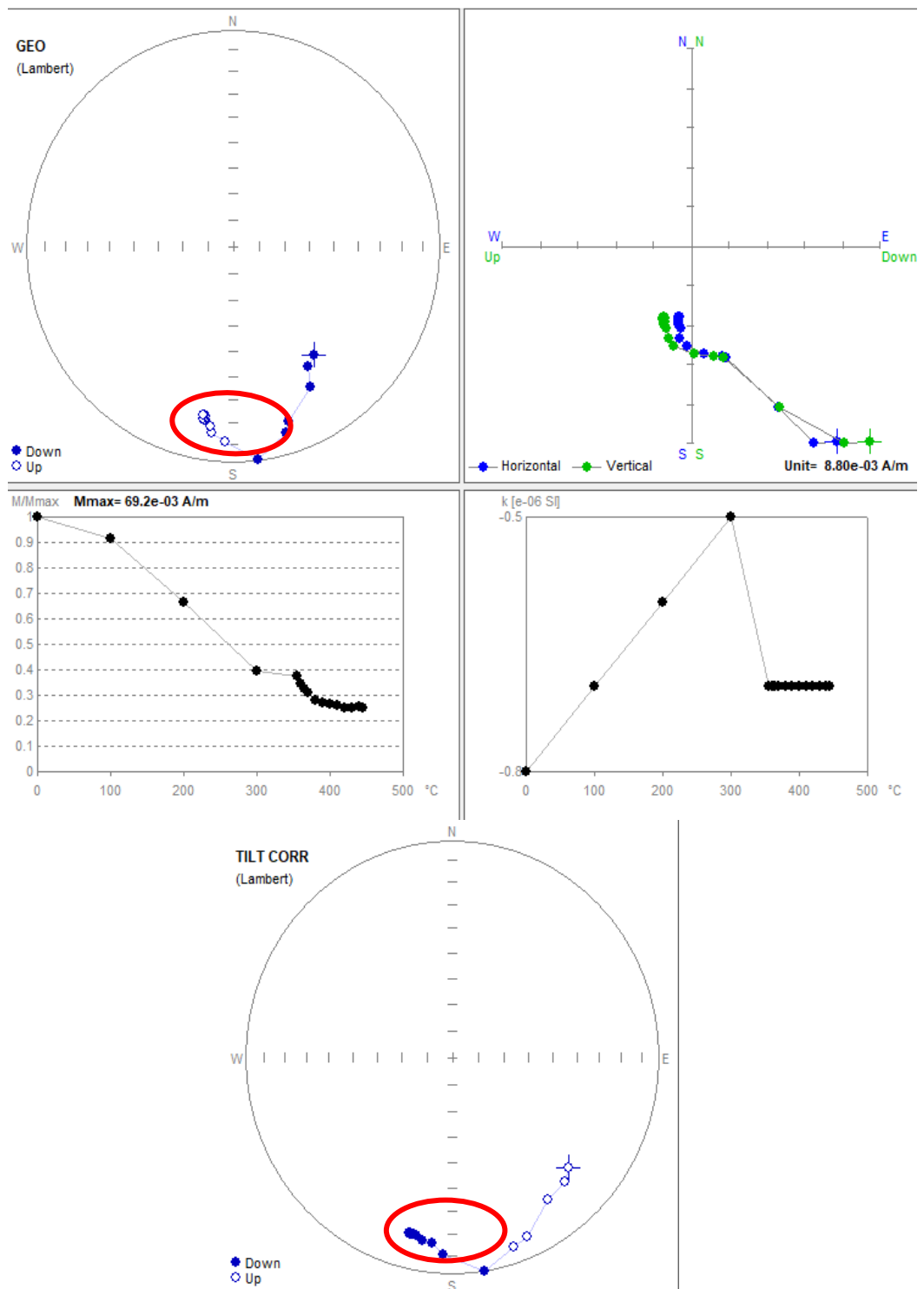


Figure 60 Sample TQ1.1. See (Figure 48) for details. In the stereoscopic projection is visible a demagnetization trend, towards inferred Kiaman remagnetisation (red circle).

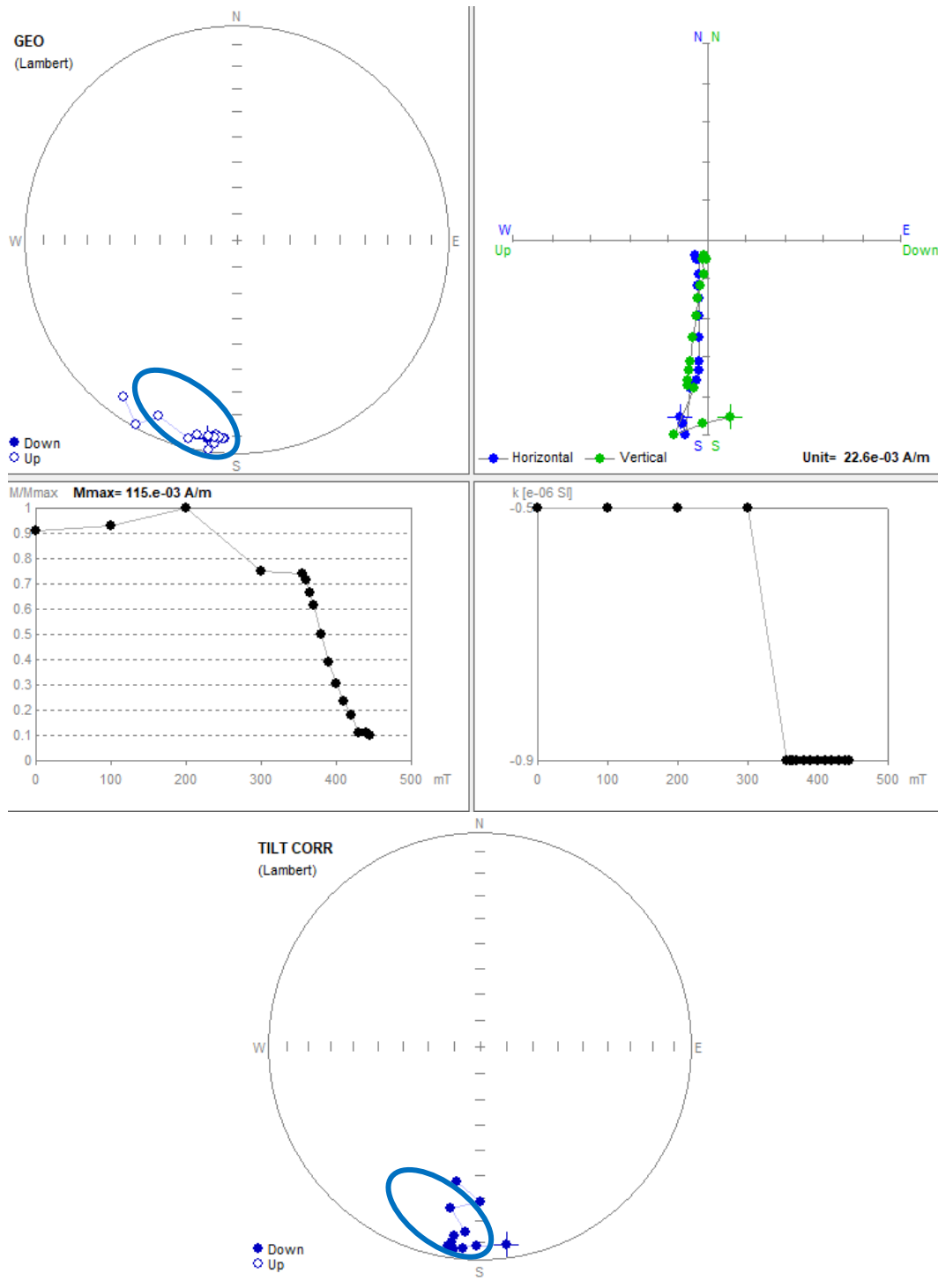


Figure 61 Sample TQ154.1. See (Figure 48) for details. In the stereoscopic projection is a demagnetization trend towards expected reversed polarity (blue circle).

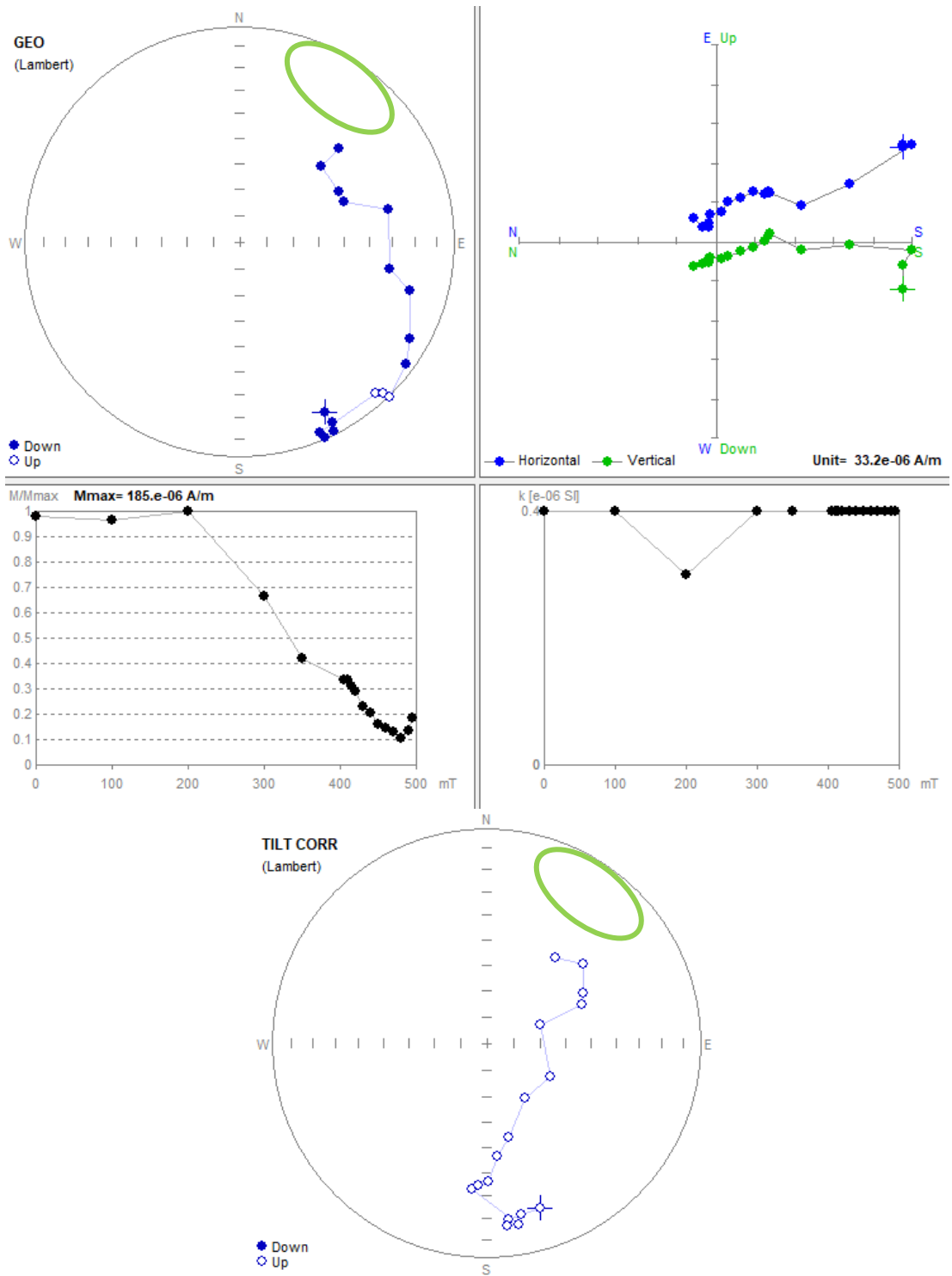


Figure 62 Sample TQ34.4. See (Figure 48) for details. In the stereoscopic projection is visible a demagnetization trend, towards expected normal polarity (green circle).

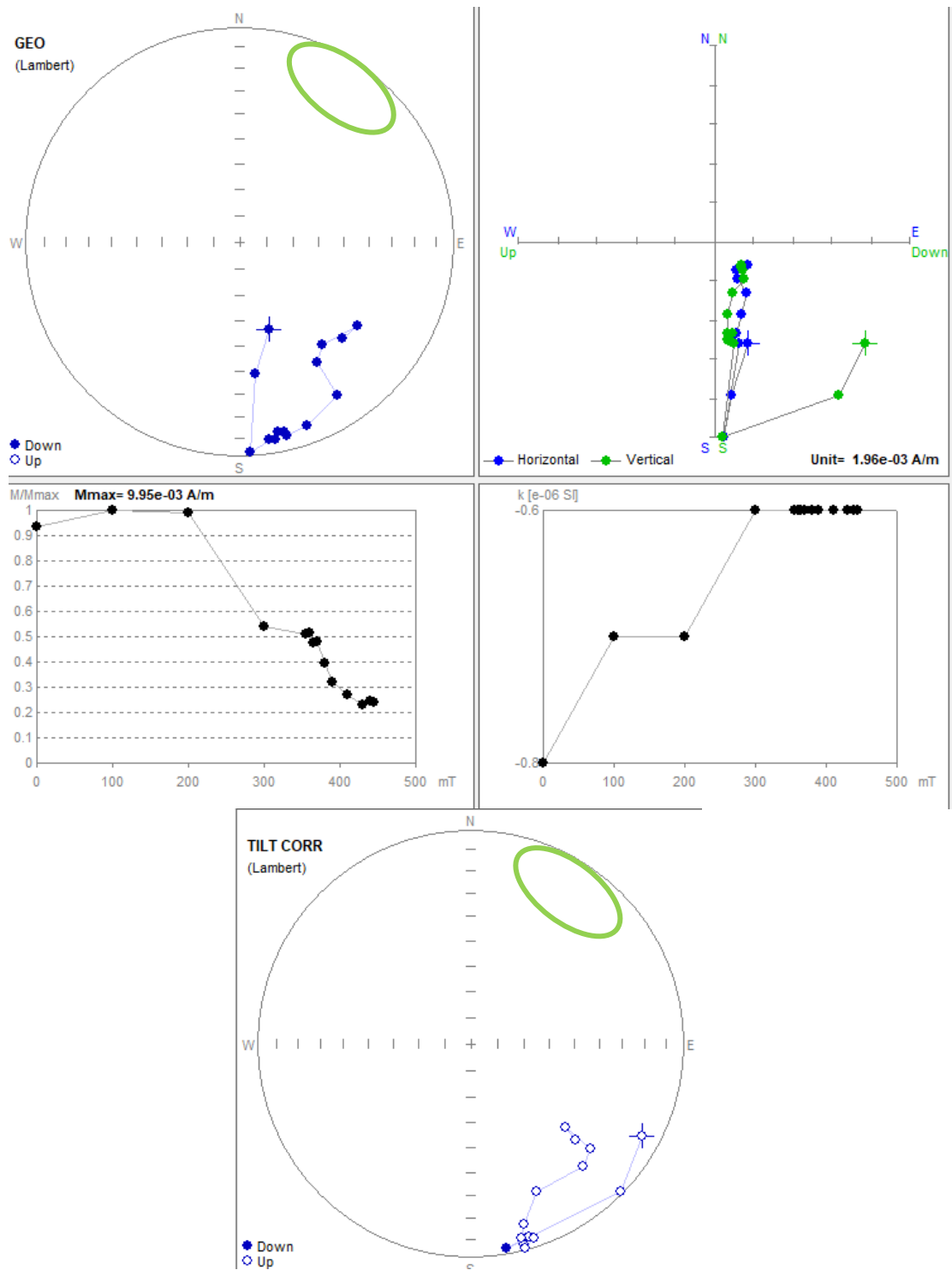


Figure 63: Sample TQ13.1. See (Figure 48) for details. Stereoscopic projection shows a partial demagnetization trend towards normal polarity (green circle).

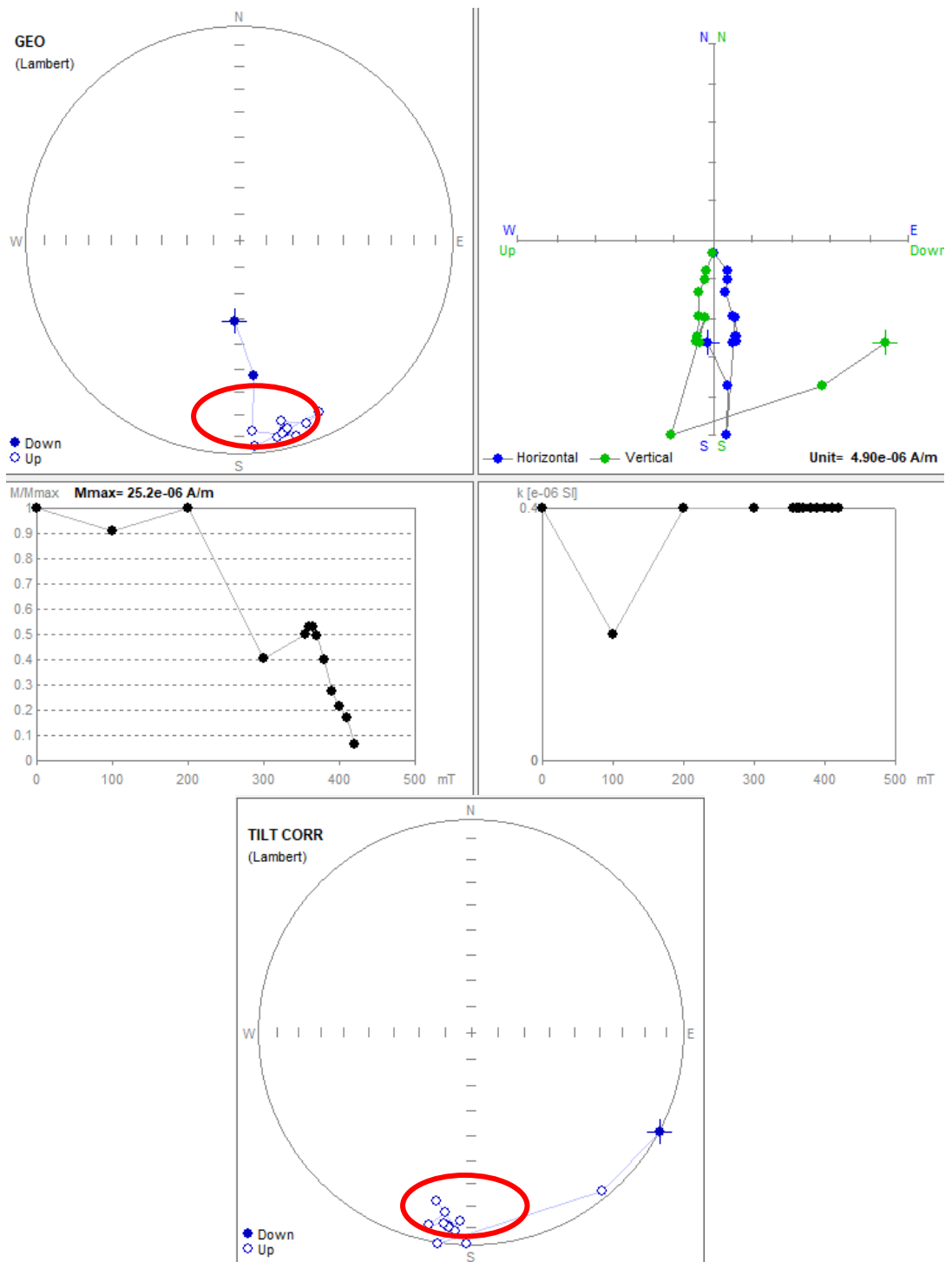


Figure 64 Sample TQ106.2. See (Figure 48) for details. Stereoscopic projection shows a strong Kiaman component (red circle), with no evidence of a primary Carboniferous component.

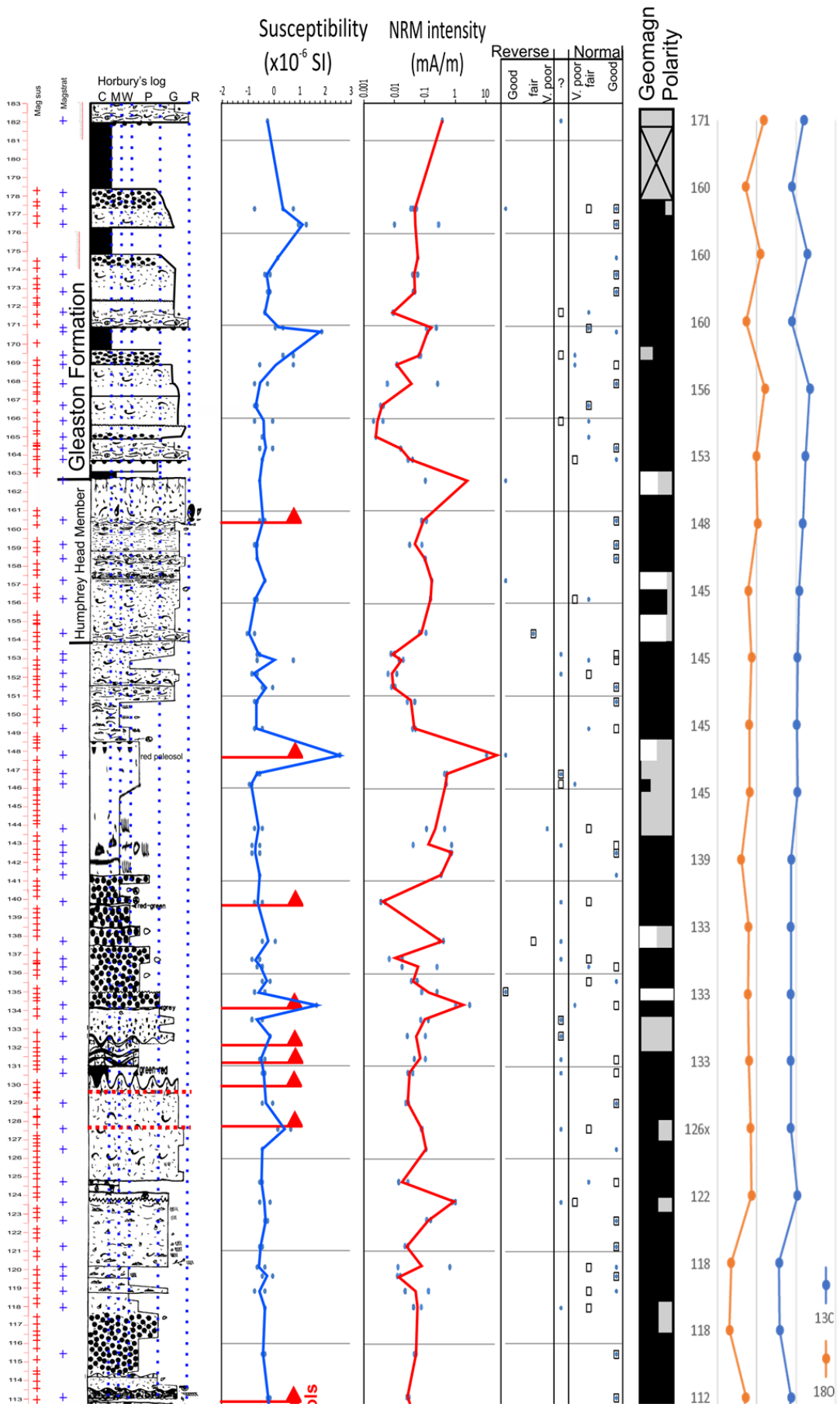


Figure 65

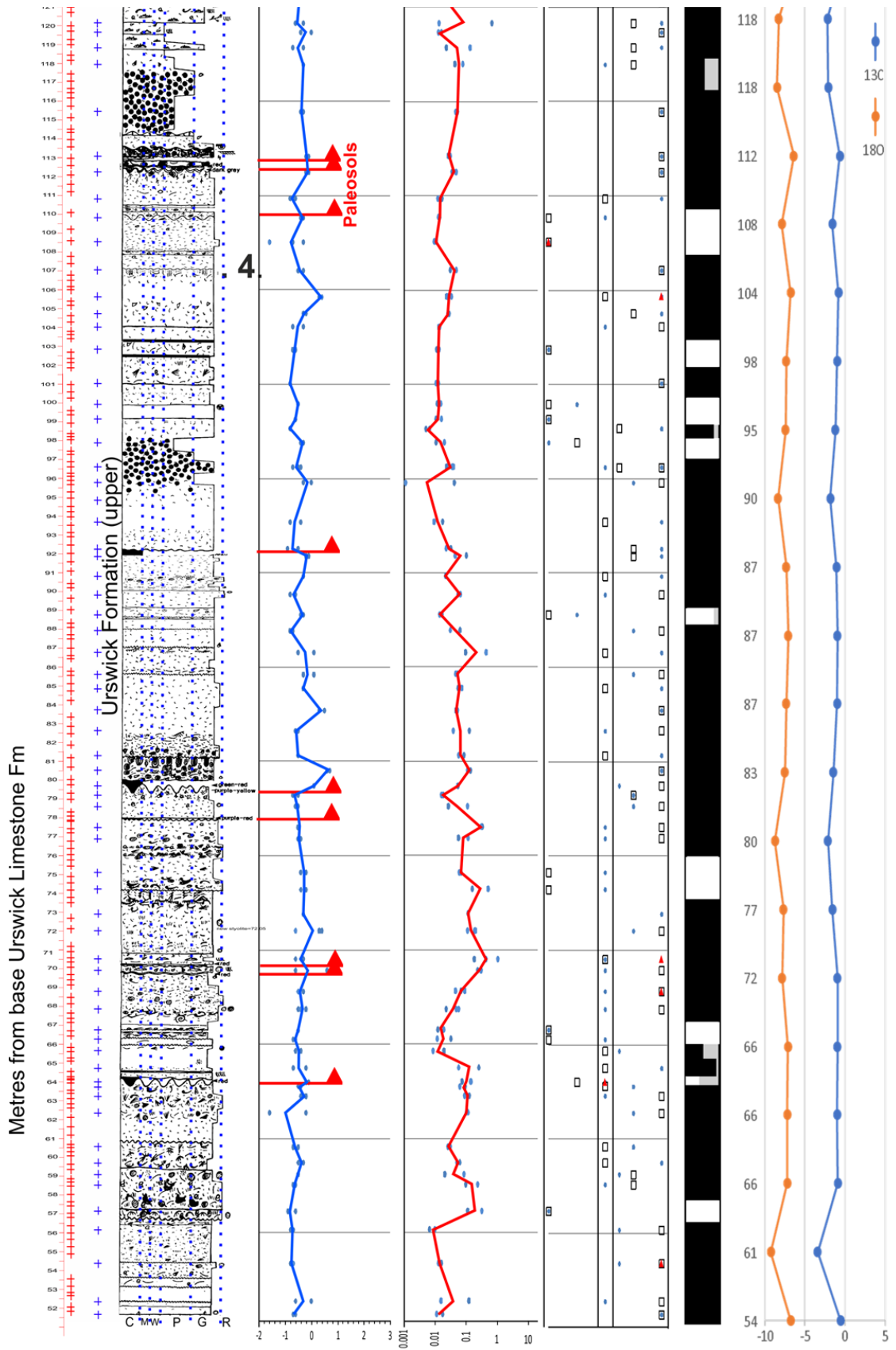


Figure 65

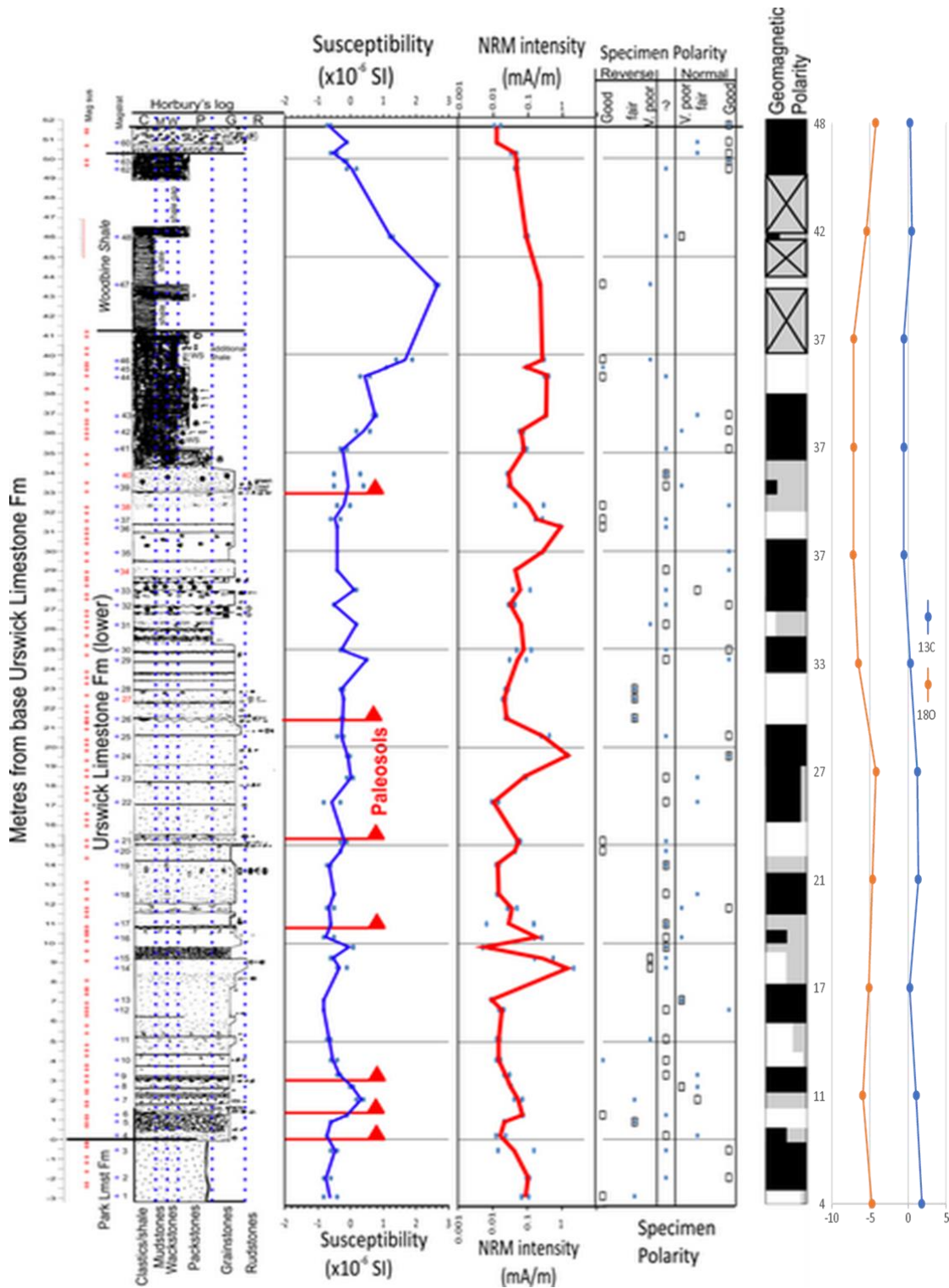


Figure 65 Summary of data from Trowbarrow Quarry, left column is log and lithologies, next column is magnetic susceptibility. Next column is NRM intensity, and next is specimen polarity classification (black stands for Normal polarity, white for Reversed polarity and grey for uncertain polarity. Far right column is results from carbon isotopes analysis. Orange is for, $\delta^{18}\text{O}$ and blue, $\delta^{13}\text{C}$.

4.2.2.2 Magnetic susceptibility

Magnetic susceptibility was measured similarly as the Meathop Quarry samples. (Figure 65) show the susceptibility variations along the NRM intensity and lithology. The susceptibility mostly corresponds with the NRM curve. However, Trowbarrow Quarry has high abundance of paleosols (iron rich horizons) influencing the magnetic susceptibility curve. Other major positive peak is around the Woodbine Shale horizon. Shales in general contain high amount ferromagnetic grains.

4.2.2.3 NRM intensity

The intensity of NRM is quite correspondent to the Magnetic susceptibility curve. It shows the variations in the lower level, (Figure 65). NRM intensity is corresponding to lithology, areas involving the paleosols (sampling method tried to avoid these, but some areas had radial veining from the paleosols outside) which can be the reason for those positive peaks.

4.2.2.4 Polarity code and polarity interpretation

(Figure 65) summarize the polarity of the measured specimens for each sample. Up to 4 specimens were measured for each sample, those are marked as a point in the chart. As further from the centre point is, the higher probability is, that the sample has normal or reversed polarity. Marks in the centre refers to uncertain orientation. That gives the valuable information together with the geomagnetic polarity chart (in the right column), black corresponds to normal polarity, white to reverse polarity, grey to uncertain polarity and crossed area to missing data (some areas were extremely weathered or were completely missing).

In the lower area, the reversal rate seems to be higher than the mid and top section where dominate mainly normal polarity with some areas of uncertain polarity. On behalf the Carbon isotopes the measured 180 meters correspond roughly to 6 000 000 yrs. Measured profile has 21 reversals. The reversal rate then corresponds to reversal every 285 000 yrs for the upper Viséan interval.

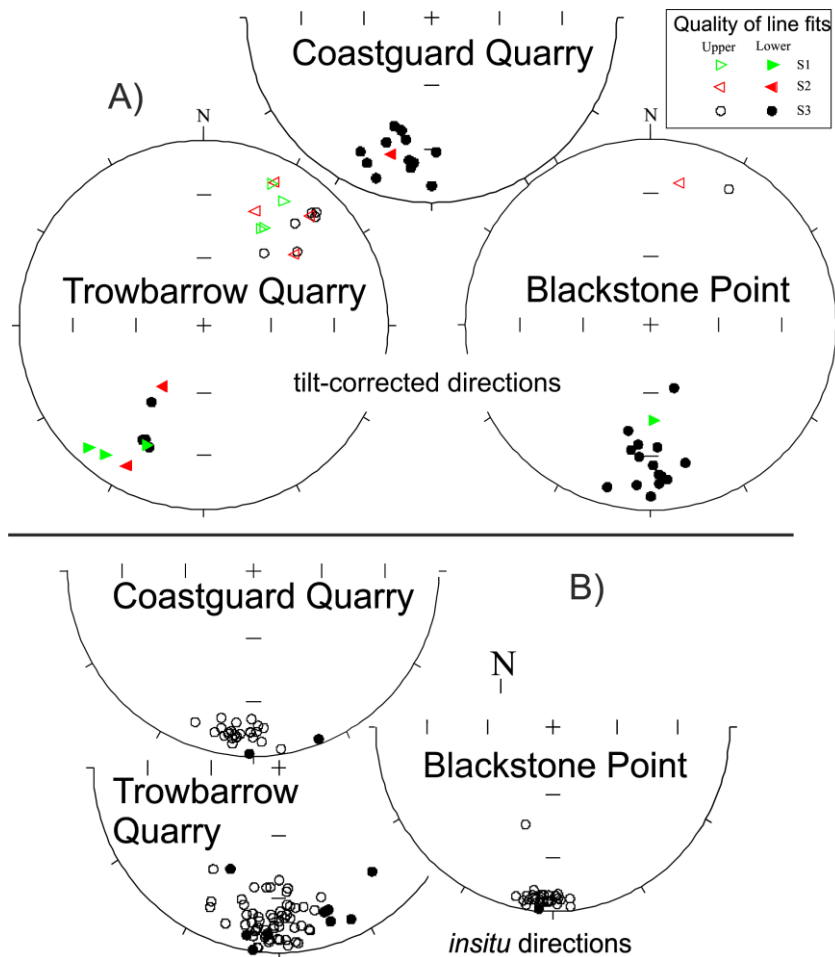


Figure 66 Mean paleo directions of the Trowbarrow Quarry: A) tilt-corrected directions, B) insitu directions (Kamenikova *et al.*, 2019).

The mean paleo directions are summarized in Figure 66). All three components for the reversed polarity have lower, south west orientation, hence the normal polarity has upper, north eastern orientation.

The Kiaman component is weaker comparing samples from Meathop Quarry. But in this location, seems there were more significant postdeposition processes as different fluid

intrusions. We found up to four different episodes of veining systems. Two red coloured , they might originated from south west Cumbria, there were found major deposits of hematite of Triassic age (Rowe et al., 1999), each spreading in different directions and intersecting each other, one black veining system (probably fluids were mixed with organic material) and one white calcite veins, with developed recognizable calcite grains.

4.2.2.5 Carbon Isotopes

The analysis of non-organic carbon ^{13}C together with ^{18}O which is a by-product of this analysis, is characterized in (Figure 67) which shows a decline in the Upper Urswick Fm corresponding to the drop of $\delta^{13}\text{C}$ in the late Visean (Liu *et al.*, 2015).

In the (Figure 67) is compared dataset with the actual Carboniferous data from (Saltzman and Thomas, 2012). Those data correspond with the great negative peak in upper Visean, they show tight fit in the surrounding areas (negative and positive peaks) with the published global dataset as well. The analysed area covers 6 myrs long period and the top of the Trowbarrow Quarry corresponds with the border in between middle and upper Mississippian (Saltzman and Thomas, 2012).

The negative excursions are corresponding, from the paleoclimatology perspective, to the high level of atmospheric dioxide at the other hand, the positive excursion are sign of low level of atmospheric dioxide (Torsvik and Cocks, 2017).

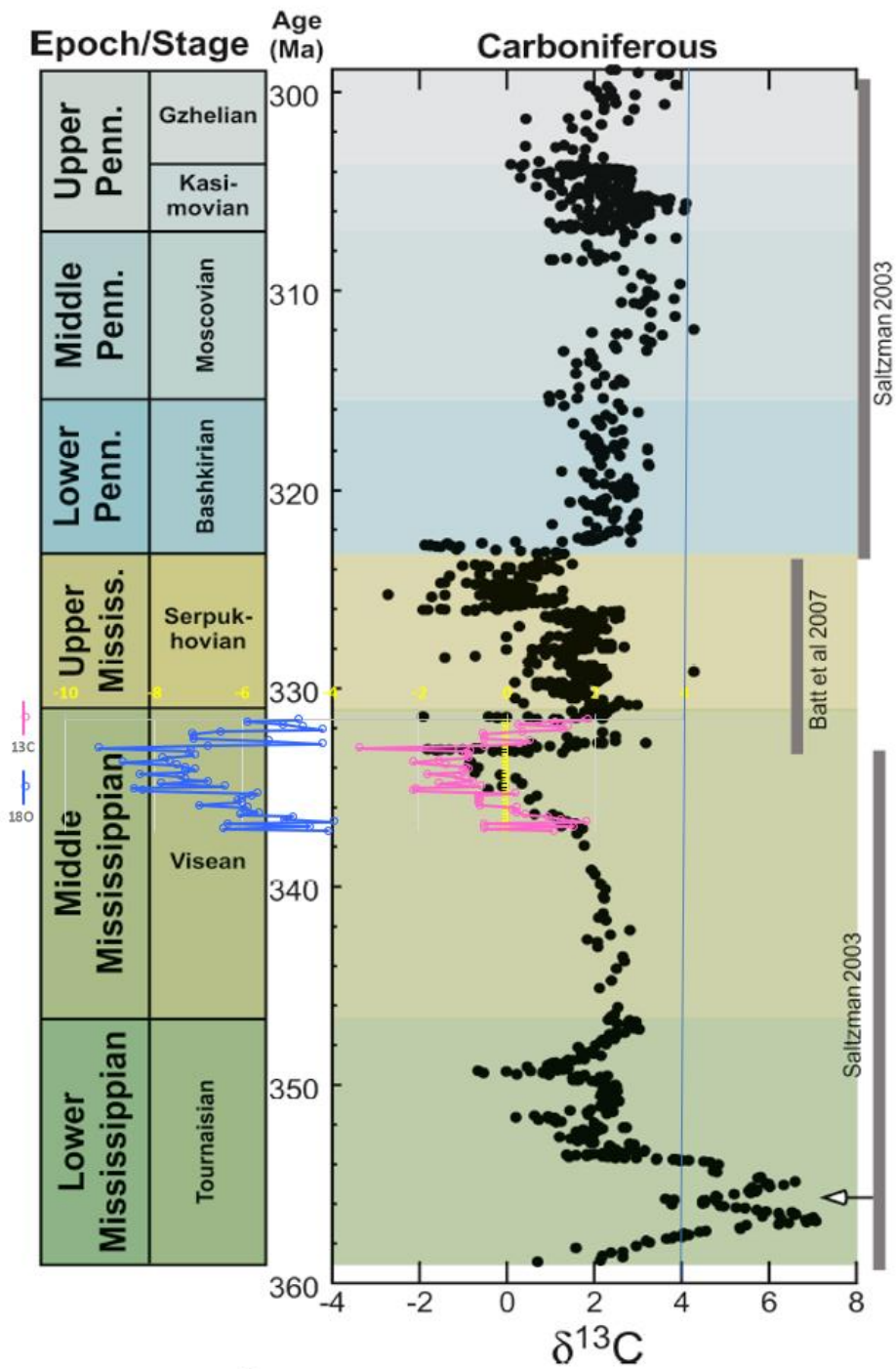


Figure 67 The results of isotope measurements. Pink curve marks our ^{13}C results compared with global isotopic curve for upper Visean (Saltzman and Thomas, 2012).

4.2.2.6 Magnetic mineralogy

Like the Meathop Quarry data (section 4.3.2), demagnetisation data was classified to identify possible mineralogical bias in the polarity (Figure 68). Overall, there is evidence of some bias of haematite in the normal polarity interpreted specimens.

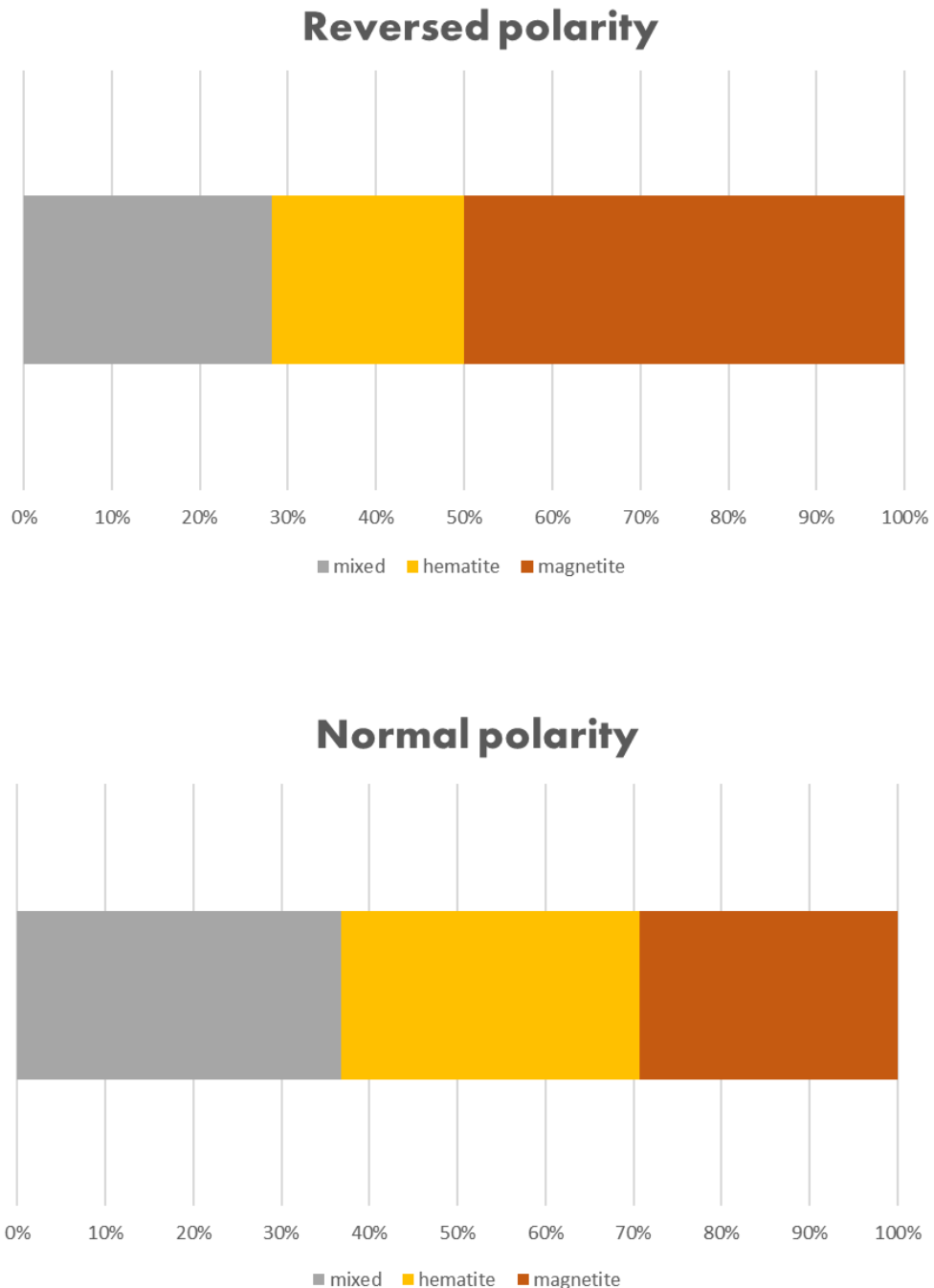


Figure 68 Percentage contribution of different minerals to polarity. Normal polarity specimens have lower abundance of magnetite as a magnetic carrier than the reversed polarity.

5 Discussion

First, main motivation of this work is to fill the gap in understanding the Viséan paleomagnetic field. The second aim is to find out what is the frequency of the Viséan paleomagnetic field reversal.

5.1 Filling “The gap”

It seems that with the modern techniques of paleomagnetic measurements, mass spectroscopy and biostratigraphic correlations, it is possible to obtain much better data than the previous generations of scientist without access to these modern methods combined with the better understanding of secondary remagnetisation and nature of the studied material, it is possible to perform such detailed magnetostratigraphic research.

The data confirms that it is possible to extract a dual polarity of Mississippian age from the studied limestones. The primary signal is present beneath a usually much stronger Kiaman component. Results from the late Chandian (Martin Limestone Fm) suggest that normal polarity was dominant within this interval, but with seven reverse magnetozones. The Asbian, Urswick Limestone Fm, is also largely normal polarity, but the early Asbian has a higher reversal rate than the late Asbian, in total there was twenty-one reverse magnetozones. The Martin Limestone Fm, in general, has a stronger Kiaman component, than the Urswick Limestone Fm, which in some cases has the Kiaman component missing, and weaker than in the Martin Limestone Fm. This is an interesting feature, since overly the lithologies in the Urswick Limestone have more complicated depositional and diagenetic history than the Martin Limestone. The Urswick Limestone has up to four

different veining systems of different components and directions, crossing each other. At least some of this veining might be explained related to the haematite genesis in SW Cumbria (Rose *et al.*, 1977). It seems that some sections might be slightly remagnetised (those relate to the grey zones in the profile, where the signal was not unambiguous).

The characteristic remanent magnetization (ChRM) seems to be carried equally by magnetite and haematite. The mineralogical dominance of ChRM carriers for each polarity is rather homogenous, although rather more normal polarity is carried by haematite at Trowbarrow Quarry. The source of the haematite in the sediments might be from Carboniferous terrestrial land sources from Southern Scotland or the Lake District hills, being, in-washed or windblown. The major haematite component at Trowbarrow is from the red-paleosols, and therefore may be near depositional in origin. The source of the magnetite is unknown but is presumably like the detrital haematite.

As no one else has examined Viséan magnetostratigraphy in such detail, overall correlation with other data is difficult. More work needs to be done to cover Viséan period being able to correlate the magnetostratigraphic dataset.

Foraminifera biostratigraphy data show, that the Meathop Quarry profile unambiguously covering the Tournaisian-Viséan boundary. Occurrence of foraminifera indicate that the top part of Meathop Quarry (between meter 40 to 45) is part of the MFZ 8 and MFZ 9 boundary which corresponds with the Tournaisian-Viséan boundary. However, it is not certain where exactly this boundary is. We know for sure, that it is located in between meter 40 and meter 45 in the sampled area, corresponding with the log, unfortunately the sediments in this gap did not retain any foraminifera markers.

Carbonate isotopes from Trowbarrow Quarry shown that the dataset peaks correspond with the global minimum peak in uppermost middle Mississippian. The dataset is looking very much as the ^{13}C global data from (Saltzman and Thomas, 2012). Trowbarrow Quarry

covers almost six million years. The topmost part of the profile corresponds with middle to upper Mississippian boundary.

This work brings the first detailed magnetostratigraphy for the British regional stages of the Viséan, so future work will be needed to continue this on the remaining Holkerian and Arundian, as well as to deliver a continuous dataset for a complete Viséan to fill the gap in our knowledge.

5.2 Reversal frequency

As discussed at the beginning, the reversal frequency of the paleomagnetic field is an important tool for understanding the geodynamo and Carboniferous magnetic field manner.

Meathop Quarry profile is 52 m long and the sedimentation rate was estimated for 30 000 yrs per m. Then MQ is covering 1 500 000 yrs. Hence the paleomagnetic profile has seven reversals in total, the reversal rate frequency is $4.6/\text{Myrs}^{-1}$.

Trowbarrow Quarry profile is 183 m long, which on behalf of the isotopic measurements was averaged as 6 000 000 yrs, then the sedimentation rate is about 32 000 yrs per m. Hence the paleomagnetic profile has twenty-one reversals in total, the reversal rate frequency is $3.5/\text{Myrs}^{-1}$.

Then reversal rate frequency in upper Viséan was lower than in the lower Viséan, this might have connection with the dynamic changes of the tectonic setting during the early Variscan orogeny involving plate subductions and other major tectonic changes.

6 Conclusion

The results show the first detailed Visian magnetostratigraphy indicate that it is possible to extract the original magnetic polarity from Carboniferous limestones. Similar aged rocks in the Craven Basin was previously assessed for this purpose but due to later remagnetisation in the Permian, the original signal was not clearly seen or identified (McCabe and Channell, 1994). This provides initial critical knowledge about how to correlate this interval with other locations spread over the world.

This research indicates that limestones from South Cumbria and North Lancashire, specifically the Martin Limestone Fm in Meathop Quarry and Urswick Limestone Fm in Trowbarrow Quarry, are suitable for palaeomagnetic research as they preserve some of the original geomagnetic signal from the Visian. The magnetic carrier for both normal and reversed polarities are equally haematite and magnetite.

It is possible to distinguish differing reversal rates estimates for the different regional stages. The magnetostratigraphic data are linked to a biostratigraphy and carbon isotopic record, allowing connections with the other sections of this time interval. Those methods showed that top section of Meathop Quarry corresponds with the Tournaisian-Visian boundary. And that Trowbarrow Quarry top section is corresponding with middle to upper Mississippian boundary.

The method using combined thermal and AF demagnetization was successful in isolating primary Mississippian data from limestones and dolostones and allowing partial separation from the much stronger Kiaman remagnetisation. It might be useful to sample some other locations with the same method, and so develop a continuous

magnetostratigraphic dataset through the Viséan. The limitations are that the signal is very weak and, in some cases, approaches the magnetometer noise level, which makes the signal all the more difficult to extract. However, the study of these sediments cannot provide relative palaeointensity information which would be useful for geomagnetic field modelling purposes.

7 References

Adams, A. E. and Cossey, P. J. (1981) 'Calcrete development at the junction between the Martin limestone and the Red Hill Oolite (Lower Carboniferous), South Cumbria', *Proceedings of the Yorkshire Geological Society*, 43(23), pp. 411–431.

Adams, A. E., Horbury, A. D. and Abdel Aziz, A. A. (1990) 'Controls on Dinantian sedimentation in south Cumbria and surrounding areas of northwest England', *Proceedings of the Geologists' Association*. The Geologists' Association, 101(1), pp. 19–30. doi: 10.1016/S0016-7878(08)80203-9.

AONB Unit (2009) 'The Bittern: Arnside and Silverdale Guide'.

Armstrong, H. and Purnell, M. (1993) 'Thermal maturation of the Lower Carboniferous strata of the Northumberland Trough and Tweed Basin from conodont colour alteration index (CAI) data', *Proceedings of the Yorkshire Geological Society*. Available at: <https://pygs.lyellcollection.org/content/49/4/335.short> (Accessed: 31 October 2019).

ARTHAUD, F. and MATTE, P. (1977) 'Late Paleozoic strike-slip faulting in southern Europe and northern Africa: Result of a right-lateral shear zone between the Appalachians and the Urals', *GSA Bulletin*. GeoScienceWorld, 88(9), pp. 1305–1320. doi: 10.1130/0016-7606(1977)88<1305:lpsfis>2.0.co;2.

Athersuch, J. and Strank, A. R. (1989) 'Foraminifera and Ostracods from the Dinantian Woodbine Shale and Urswick Limestone, South Cumbria, U.K', *J.Micropaleontology*, 8(1), pp. 9–21. doi: 10.1144/jm.8.1.9.

Bathurst, R. G. C. (1971) *Carbonate Sediments and Their Diagenesis*.

Belshe, J. C. (1957) 'Paleomagnetic investigations of carboniferous rocks in England and Wales', *Advanced Physics*, 6, pp. 187–91.

Berner, R. a (1990) 'Atmospheric Carbon Dioxide Levels', *Science*. JSTOR, 249, pp. 1382–1386. doi: 10.1016/0165-0572(78)90006-3.

Besly, B. M. and Turner, P. (1983) 'Origin of red beds in a moist tropical climate (Etruria Formation, Upper Carboniferous, UK). In: Residual Deposits: Surface Related Weathering Processes and Materials (Wilson RCL, ed.)', *Geological Society, London, Special Publications*, 11, pp. 131–147.

Bonadonna, D. (2018) *Conodonts: 520 Million Years Long in the Tooth*, *Pteroformer*. Available at: <https://pteroformer.blogspot.com/2016/07/conodonts-520-million-years-long-in.html> (Accessed: 31 December 2018).

Brand, W. A. *et al.* (2014) 'Assessment of international reference materials for isotope-ratio analysis (IUPAC Technical Report) in: Pure and Applied Chemistry Volume 86 Issue 3 (2014)', *Pure and Applied Chemistry*, 86(3). Available at: <https://www.degruyter.com/view/journals/pac/86/3/article-p425.xml> (Accessed: 27 April 2020).

Burnett, R. D. (1987) 'Regional maturation patterns for late Visean (Carboniferous, Dinantian) rocks of northern England based on mapping of conodont colour', *Irish Journal of Earth*. Available at: <https://www.jstor.org/stable/30002529> (Accessed: 31 October 2019).

Butler, R. F. (1992) 'Paleomagnetism: magnetic domains to geologic terranes', *Paleomagnetism: magnetic domains to geologic terranes*. Blackwell Scientific. doi: 10.5860/choice.29-5708.

Clement, B. (2004) *How Long Does It Take for Earth's Magnetic Field to Reverse?* / NSF - National Science Foundation. Available at: https://www.nsf.gov/news/news_summ.jsp?cntn_id=100358 (Accessed: 31 October 2019).

Cohen, K. M. *et al.* (2018) *The ICS International Chronostratigraphic Chart*. Available at: <http://www.stratigraphy.org/ICSchart/ChronostratChart2018-08.jpg> (Accessed: 13 December 2018).

Conodont collection, Natural History Museum (2018). Available at: <http://www.nhm.ac.uk/our-science/collections/palaeontology-collections/conodont-collection.html> (Accessed: 31 December 2018).

Cózar, P. and Somerville, I. D. (2016) 'Problems correlating the late Brigantian-Arnsbergian Western European substages within northern England', *Geological Journal*. John Wiley & Sons, Ltd, 51(5), pp. 817–840. doi: 10.1002/gj.2700.

Creer, K. M., Irving, E. and Nairn, A. E. M. (1959) 'Paleomagnetism of the Great Whin sill.', *Geophysical J. Roy. astronomical society*, 2, pp. 306–23.

Crowley, S. F. *et al.* (2014) 'Palaeomagnetic evidence for the age of the Cumbrian and Manx hematite ore deposits: Implications for the origin of hematite mineralization at the margins of the East Irish Sea Basin, UK', *Journal of the Geological Society*, 171(1). doi: 10.1144/jgs2013-004.

Dean, M. T. T. *et al.* (2011) *A lithostratigraphical framework for the Carboniferous successions of northern Great Britain (onshore)*, *British Geological Survey Research Report RR/09/01*. Available at: <http://nora.nerc.ac.uk/id/eprint/13985/> (Accessed: 24 September 2018).

Dearing, J. (1994) *Environmental magnetic susceptibility: using the Bartington MS2 system*. Kenilworth: Chi Pub. Available at: <https://www.worldcat.org/title/environmental-magnetic-susceptibility-using-the-bartington-ms2-system/oclc/31937476> (Accessed: 15 August 2019).

Divenere, V. J. and Opdyke, N. D. (1990) 'Paleomagnetism of the Maringouin and Shepody formation, New Brunswick: A Namurian magnetic stratigraphy', *Canadian Journal Earth Sciences*, 27, pp. 803–810.

Divenere, V. J. and Opdyke, N. D. (1991a) 'Magnetic polarity stratigraphy and Carboniferous paleopole position from the Joggins Section, Cumberland Basin, Nova Scotia', *Journal of Geophysical Research*, 96, pp. 4051–4064.

Divenere, V. J. and Opdyke, N. D. (1991b) 'Magnetic polarity stratigraphy in the uppermost Mississippian Mauch Chunk Formation, Pottsville, Pennsylvania', *Geology*, 19(2), pp. 127–130. doi: 10.1130/0091-7613(1991)019<0127:MPSITU>2.3.CO;2.

Dunlop, D. J. and Özdemir, O. (1997) *Rock magnetism: fundamentals and frontiers*. Cambridge University Press.

Ebdon, C. C. *et al.* (1990) *The Dinantian stratigraphy of the East Midlands: a seismostratigraphic approach*, *Journal of the Geological Society*. Available at: <http://jgs.lyellcollection.org/> (Accessed: 27 September 2018).

Epstein, A. G., Epstein, J. B. and Harris, L. D. (1977) 'Conodont color alteration - an index to organic metamorphism', *USGS Professional Paper*, 995, p. 27pp. doi: 10.1130/0016-7606(1987)99<471:CCATAA>2.0.CO;2.

Fielding, C. R. *et al.* (2008) 'Stratigraphic imprint of the Late Palaeozoic Ice Age in eastern Australia: A record of alternating glacial and nonglacial climate regime', *Journal*

of the Geological Society, 165(1), pp. 129–140. doi: 10.1144/0016-76492007-036.

Fraser, A. J. *et al.* (1990) ‘A regional assessment of the intra-Carboniferous play of Northern England’, *Geological Society, London, Special Publications*. Geological Society of London, 50(1), pp. 417–440. doi: 10.1144/GSL.SP.1990.050.01.26.

Garwood, E. J. (1907) ‘Notes and faunal succession in the Carboniferous Limestone of Westmoreland and neighbouring areas.’, *Geological Magazine*, 4, pp. 70–74.

Garwood, E. J. (1910) ‘VII.—On the Horizon of the Lower Carboniferous Beds containing *Archæosigillaria Vanuxemi* (Göppert) at Meathop Fell’, *Geological Magazine*, 7(3), pp. 117–119. doi: 10.1017/S0016756800132996.

Garwood, E. J. (1913) ‘The Lower Carboniferous succession in the Northwest of England.’, *Quarterly Journal of the Geological Society*, 68, pp. 449–596.

Garwood, E. J. (1916) ‘The faunal succession in the lower Carboniferous rocks of Westmorland and north Lancashire’, *Proceedings of the Geologists’ Association*. The Geologists’ Association, 27(1), pp. IN1–IN18. doi: 10.1016/S0016-7878(16)80001-2.

Gawthorpe, K. C., Gutteridge, P. and Leeder, M. R. (1989) ‘Late Devonian and Dinatian basin evolution in northern England and North Wales’. Yorkshire Geological Society Occasional Publication 6, pp. 1–23. Available at: https://books.google.co.uk/books?id=FCPxDyHJ-zIC&pg=PA202&lpg=PA202&dq=1989+Late+devonian+and+dinatian+basin+evolution+in+northern+england&source=bl&ots=gZ_wVT11C_&sig=ElxbWy7I285pmr93hagWz6ar2DY&hl=cs&sa=X&ved=2ahUKEwiV-YmLntvdAhURM8AKHQAC4wQ6AEwBXoECAY (Accessed: 27 September 2018).

Geological Survey of Canada (2018) *Natural Resources Canada, 2018*. Available at:

http://geomag.nrcan.gc.ca/mag_fld/sec-en.php (Accessed: 30 November 2018).

Google Maps (2019). Available at: <https://www.google.com/maps/@50.0628891,14.7087554,14z> (Accessed: 18 August 2019).

Horbury, A. D. (1987) *Sedimentology of the Urswick Limestone in South Cumbria and North Lancashire*. University of Manchester.

Horbury, A. D. (1989) 'The relative roles of tectonism and eustacy in the deposition of the Urswick Limestone in south Cumbria and north Lancashire', *Proceedings of the Yorkshire Geological Society*, (6), pp. 153–169. Available at: https://www.cambridgecarbonates.com/assets/horbury_1989.pdf (Accessed: 27 September 2018).

Horbury, A. D. and Adams, A. E. (1989) 'Tree root structures on a Dinantian palaeokarst, Urswick Limestone, south Cumbria', pp. 345–348.

Hounslow, M. W. *et al.* (2004) *Magnetostratigraphy of the Carboniferous: a review and future prospects*, *From Newsletter On Carboniferous Stratigraphy*. Available at: https://s3.amazonaws.com/academia.edu.documents/46482617/Magnetostratigraphy_of_the_Carboniferous20160614-22372-1cz2l3b.pdf?AWSAccessKeyId=AKIAIWOWYYGZ2Y53UL3A&Expires=1538054003&Signature=bz1%2BmouR2%2FIrfspgkqnJ0U4wLys%3D&response-content-disposition=in (Accessed: 27 September 2018).

Hounslow, M. W. (2016) 'Geomagnetic reversal rates following Palaeozoic superchrons have a fast restart mechanism', *Nature Communications*. Nature Publishing Group, 7. doi: 10.1038/ncomms12507.

Hounslow, M. W. and Balabanov, Y. P. (2018) 'A geomagnetic polarity timescale for the Permian, calibrated to stage boundaries', in *Geological Society Special Publication*. Geological Society of London, pp. 61–103. doi: 10.1144/SP450.8.

Hounslow, M. W., Domeier, M. and Biggin, A. J. (2018) 'Subduction flux modulates the geomagnetic polarity reversal rate', *Tectonophysics*, 742–743, pp. 34–49. doi: 10.1016/j.tectonophysics.2018.06.027.

ICS - Chart/Time Scale (2019). Available at: <http://www.stratigraphy.org/index.php/ics-chart-timescale> (Accessed: 30 October 2019).

Ineson, P. R. and Mitchell, J. G. (1972) 'Isotopic age determinations on clay minerals from lavas and tuffs of the Derbyshire orefield', *Geological Magazine*, 109(06), p. 501. doi: 10.1017/S0016756800042783.

Iosifidi, A. G. *et al.* (2019) 'Carboniferous of the Russian Platform: Paleomagnetic Data', in, pp. 37–54. doi: 10.1007/978-3-319-90437-5_4.

Irving, E. and Parry, L. G. (1963) 'The magnetism of some Permian rocks from New South Wales', *Geophysical J. Roy. astronomical society*, 7, pp. 395–411.

Kalvoda, J. *et al.* (2012) 'High resolution biostratigraphy of the Tournaisian-Viséan boundary interval in the North Staffordshire Basin and correlation with the South Wales-Mendip Shelf', *Bulletin of Geosciences*, pp. 497–541. doi: 10.3140/bull.geosci.1338.

Kalvoda, J. and *et al.* (2011) *Biostratigraphy, sequence stratigraphy and gamma-ray spectrometry of the Tournaisian-Viséan boundary interval in the Dublin Basin*, *Bulletin of Geosciences*. Available at: <http://www.geology.cz/bulletin/contents/art1265> (Accessed: 21 October 2019).

Kamenikova, T. *et al.* (2019) 'Tournaisian-Viséan magnetostratigraphy: new data from

- British and Polish limestones', in *3rd International Congress on Stratigraphy*, p. 206.
- Kent, D. V. (1973) 'Post-depositional remanent magnetisation in deep-sea sediment', *Nature*, 246(5427), pp. 32–34. doi: 10.1038/246032a0.
- Khattak, O. (2018) *Paleomagnetism and the Proof of Continental Drift, 2018*. Available at: <https://geologylearn.blogspot.com/2016/02/paleomagnetism-and-proof-of-continental.html> (Accessed: 30 November 2018).
- Khramov, A. N. (1963) 'Paleomagnetism of Paleozoic', *Transactions of VNIGRI*, p. 283.
- Khramov, A. N. *et al.* (1974) 'Paleozoic Paleomagnetism', *Transactions of VNIGRI*, pp. 1–238.
- Khramov, A. N. and Rodionov, R. (1981) 'The geomagnetic field during Paleozoic time.', *Earth and Planetary Sciences*, 10, pp. 99–116.
- Khramov, A. N. and Rodionov, V. P. (1980) 'Palaeomagnetism and Reconstruction of Palaeogeographic Positions of the Siberian and Russian Plates during the Late Proterozoic and Palaeozoic', *Journal of geomagnetism and geoelectricity*, 32, pp. SIII23–SIII37. doi: 10.5636/jgg.32.Supplement3_SIII23.
- King, H. M. (2018) *Limestone*. Available at: <https://geology.com/rocks/limestone.shtml> (Accessed: 7 December 2018).
- Kirschvink, J. L. *et al.* (2008) 'Rapid, precise, and high-sensitivity acquisition of paleomagnetic and rock-magnetic data: Development of a low-noise automatic sample changing system for superconducting rock magnetometers', *Geochemistry, Geophysics, Geosystems*, 9(5), pp. 1–20. doi: 10.1029/2007GC001856.
- Kodama, K. P. (2013) *Paleomagnetism of sedimentary rocks : process and interpretation*.

Wiley-Blackwell.

Kombrink, H. *et al.* (2008) 'Late Carboniferous foreland basin formation and Early Carboniferous stretching in Northwestern Europe: inferences from quantitative subsidence analyses in the Netherlands', *Basin Research*. Blackwell Publishing Ltd, 20(3), pp. 377–395. doi: 10.1111/j.1365-2117.2008.00353.x.

Kopp, R. E. and Kirschvink, J. L. (2008) 'The identification and biogeochemical interpretation of fossil magnetotactic bacteria', *Earth-Science Reviews*, 86(1–4), pp. 42–61. doi: 10.1016/j.earscirev.2007.08.001.

Lang, K. (2010) *NASA's Cosmos*, Tufts University. Available at: https://ase.tufts.edu/cosmos/view_picture.asp?id=107 (Accessed: 27 November 2018).

Langereis, C. G. *et al.* (1989) *Encyclopedia of Solid Earth Geophysics*. Edited by David E. James. New York: Springer Netherlands (Encyclopedia of Earth Sciences Series). doi: 10.1007/978-90-481-8702-7.

Lecoanet, H., Lévêque, F. and Segura, S. (1999) 'Magnetic susceptibility in environmental applications: comparison of field probes', *Physics of the Earth and Planetary Interiors*. Elsevier, 115(3–4), pp. 191–204. doi: 10.1016/S0031-9201(99)00066-7.

Leeder, M. R. and Hardman, M. (1990) 'Carboniferous geology of the Southern North Sea Basin and controls on hydrocarbon prospectivity', *Geological Society Special Publication*, 55, pp. 87–105. doi: 10.1144/GSL.SP.1990.055.01.04.

Leviston, D. (1979) 'A study of four localities, the Martin Limestone (Lower Carboniferous, Dinantian) of Furness and Grange-over-Sands.', *Proceedings of the Cumberland Geological Society*.

Liu, C. *et al.* (2015) 'Microfacies and carbon isotope records of Mississippian carbonates from the isolated Bama Platform of Youjiang Basin, South China: Possible responses to climate-driven upwelling', *Palaeogeography, Palaeoclimatology, Palaeoecology*. Elsevier, 438, pp. 96–112. doi: 10.1016/j.palaeo.2015.07.048.

Lovlie, R., Lowrie, W. and Jacobs, M. (1971) 'Magnetic properties and mineralogy of four deep-sea cores', *Earth and Planetary Science Letters*, 15(157–168).

Lowrie, W. (2007) *Fundamentals of geophysics*. Cambridge University Press. Available at: <http://www.cambridge.org/cz/academic/subjects/earth-and-environmental-science/solid-earth-geophysics/fundamentals-geophysics-2nd-edition?format=PB&isbn=9780521675963> (Accessed: 10 April 2017).

Lowrie, W. and Heller, F. (1982) 'Magnetic properties of marine limestones', *Reviews of Geophysics*, 20(2), p. 171. doi: 10.1029/RG020i002p00171.

McCabe, C. and Channell, J. E. T. (1994) 'Late Palaeozoic remagnetisation during in limestones of the Craven Basin (Northern England) and rock magnetic fingerprinting of remagnetised carbonates.', *Journal of Geophysical Research*, 99, pp. 4603–4612.

McCabe, C. and Elmore, R. D. (1989) 'The occurrence and origin of Late Paleozoic remagnetization in the sedimentary rocks of North America', *Reviews of Geophysics*, 27(4), p. 471. doi: 10.1029/RG027i004p00471.

McElhinny, M. W. (1973) *Palaeomagnetism and plate tectonics*. University Press. Available at: <https://catalogue.nla.gov.au/Record/445176> (Accessed: 30 November 2018).

Meathop Woods and Quarry | Protected Planet (2019). Available at: <https://www.protectedplanet.net/meathop-woods-and-quarry-site-of-special-scientific->

interest-gb (Accessed: 18 August 2019).

Merrill, R. T. (2010) *Our Magnetic Earth: The Science of Geomagnetism*, by Ronald T. Merrill, The University of Chicago Press.

Miller, C. B. and Wheeler, P. (2012) *Biological oceanography*.

Molostovskii, E. A., Pechersky, D. M. and Frolov, I. Y. (2007) 'Magnetostratigraphic timescale of the Phanerozoic and its description using a cumulative distribution function', *Izvestiya, Physics of the Solid Earth*, 43(10), pp. 811–818. doi: 10.1134/S1069351307100035.

Mook, W. G. and Tan, F. C. (1991) *Stable carbon isotopes in rivers and estuaries* . Available at: <https://library.wur.nl/WebQuery/titel/864334> (Accessed: 27 April 2020).

Ogg, J. G. *et al.* (2008) 'Paleozoic Time Scale and Sea-Level History', *Time*, (1985), p. 416.

Opdyke, N. D. (1995) 'Magnetostratigraphy of Permo-Carboniferous time', *Geochronology, time scale and global stratigraphic correlation*, 54, pp. 42–47.

Opdyke, N. D. *et al.* (2000) 'Base of the Kiaman: Its definition and global stratigraphic significance', *Bulletin of the Geological Society of America*, 112(9), pp. 1315–1341. doi: 10.1130/0016-7606(2000)112<1315:BOTKID>2.0.CO;2.

Opdyke, N. D. and Channell, J. E. T. (1996) *Magnetic stratigraphy*. San Diego: Academic Press.

Opdyke, N. D. and Divenere, V. J. (2004) 'The magnetic polarity stratigraphy of the Mauch Chunk Formation, Pennsylvania', 101(37), pp. 13423–13427. doi: 10.1073/pnas.0403786101.

Opdyke, N. D., Giles, P. S. and Utting, J. (2014) 'Magnetic polarity stratigraphy and palynostratigraphy of the Mississippian-Pennsylvanian boundary interval in eastern North America and the age of the beginning of the Kiaman', *Bulletin of the Geological Society of America*, 126(7–8), pp. 1068–1083. doi: 10.1130/B30953.1.

Oppenheim, M. J., Piper, J. D. A. and Rolph, T. C. (1994) 'A palaeointensity study of the Lower Carboniferous transitional geomagnetic field directions: the Cockermouth lavas, northern England.', *Physics of the Earth and Planetary Interiors*, 82, pp. 65–74.

Palmer, J. A. (1987) *Carboniferous magnetostratigraphy*. Newcastle upon Tyne.

Palmer, J. A., Perry, S. P. G. and Tarling, D. H. (1985) 'Carboniferous magnetostratigraphy', *Journal of the Geological Society*, 142(6), pp. 945–955. doi: 10.1144/gsjgs.142.6.0945.

Piper, J. D. A. *et al.* (1991) 'Palaeomagnetic study of the Derbyshire lavas and intrusions, central England: definition of Carboniferous apparent polar wander', *Physics of the Earth and Planetary Interiors*, 69(1–2), pp. 37–55. doi: 10.1016/0031-9201(91)90152-8.

Postgraduate Unit of Micropalaeontology, U. C. L. (2002) 'Foraminifera', *various*. Postgraduate Unit of Micropalaeontology, Department of Earth Sciences, University College London, Gower Street, London, WC1E 6BT. Available at: <https://www.ucl.ac.uk/GeolSci/micropal/foram.html#intro> (Accessed: 31 December 2018).

Poty, E., Devuyt, F. X. and Hance, L. (2006) 'Upper Devonian and Mississippian foraminiferal and rugose coral zonations of Belgium and northern France: A tool for Eurasian correlations', *Geological Magazine*, 143(6), pp. 829–857. doi: 10.1017/S0016756806002457.

Ramsbottom, W. and Aithenhead, N. (1981) *Field guide to the Boundary stratotypes of the Carboniferous stages in Britain: 25 August - 1 September, 1981*. Leeds: Subcommission on Carboniferous Stratigraphy. Available at: <https://www.worldcat.org/title/field-guide-to-the-boundary-stratotypes-of-the-carboniferous-stages-in-britain-25-august-1-september-1981/oclc/46438344> (Accessed: 5 August 2019).

Ramsbottom, W. H. (1973) 'Transgressions and regressions in the Dinantian: a new synthesis of British Dinantian stratigraphy.', *Proceedings of the Yorkshire Geological Society*, 39(4), pp. 567–607.

Rejebian, V. A., Harris, A. G. and Huebner, J. S. (1987) 'Conodont color and textural alteration: An index to regional metamorphism, contact metamorphism, and hydrothermal alteration', *GSA Bulletin*, 99(4), pp. 471–479.

Riley, N. J. (1993) 'Dinantian (Lower Carboniferous) biostratigraphy and chronostratigraphy in the British Isles', *Journal of the Geological Society, London*, 150, pp. 227–241.

Rose, W. C. C. *et al.* (1977) *Geology and hematite deposits of south Cumbria : Economic memoir for 1:50,000*. London. Available at: <https://www.bgs.ac.uk/data/publications/pubs.cfc?method=viewRecord&publnId=19864678> (Accessed: 27 September 2018).

Rowe, J., Turner, P. and Burley, S. (1998) 'Palaeomagnetic dating of the west Cumbrian hematite deposits and implications for their mode of formation', *Proceedings of the Yorkshire Geological Society*, 52(1), pp. 59–71. doi: 10.1144/pygs.52.1.59.

Rowe, J., Turner, P. and Burley, S. (1999) 'Palaeomagnetic dating of the west cumbrian hematite deposits and implications for their mode of formation', *Proceedings of the*

Yorkshire Geological Society, 52(1), pp. 59–71. doi: 10.1144/pygs.52.1.59.

Roy, J. L. and Morris, W. A. (1983) ‘A review of paleomagnetic results from the Carboniferous of North America; the concept of Carboniferous geomagnetic field horizon markers.’, *Earth and Planetary Science Letters*, 65, pp. 167–181.

Saltzman, M. R. (2003) ‘Late Paleozoic ice age: Oceanic gateway or pCO₂?’, *Geology*. GeoScienceWorld, 31(2), pp. 151–154. doi: 10.1130/0091-7613(2003)031<0151:lpiaog>2.0.co;2.

Saltzman, M. R. and Thomas, E. (2012) ‘Carbon Isotope Stratigraphy’, *The Geologic Time Scale 2012*, 1–2(July), pp. 207–232. doi: 10.1016/B978-0-444-59425-9.00011-1.

Scotese, C. (2002) *Early Carboniferous*. Available at: <http://www.scotese.com/newpage4.htm> (Accessed: 29 April 2020).

SENCKENBERG world of biodiversity (2018). Available at: http://www.senckenberg.de/root/index.php?page_id=875 (Accessed: 31 December 2018).

Sleep, N. H. and Fujita, K. (Kazuya) (1997) *Principles of geophysics*. Malden Mass. USA: Blackwell Science. Available at: <https://www.worldcat.org/title/principles-of-geophysics/oclc/35646456> (Accessed: 27 November 2018).

Smethurst, M. A. and Khramov, A. N. (1992) ‘A new Devonian palaeomagnetic pole for the Russian Platform and Baltica, and related apparent polar wander’, *Geophysical Journal International*, 108, pp. 179–192.

Smit, J., van Wees, J. D. and Cloetingh, S. (2018) ‘Early Carboniferous extension in East Avalonia: 350 My record of lithospheric memory’, *Marine and Petroleum Geology*. Elsevier Ltd, pp. 1010–1027. doi: 10.1016/j.marpetgeo.2018.01.004.

Stephenson, A. (1981) 'Gyroremanent magnetization in a weakly anisotropic rock sample', *Physics of the Earth and Planetary Interiors*. Elsevier, 25(2), pp. 163–166. doi: 10.1016/0031-9201(81)90149-7.

Stolz, J. F., Chang, S. B. R. and Kirschvink, J. L. (1986) 'Magnetotactic bacteria and single-domain magnetite in hemipelagic sediments', *Nature*, 321(6073), pp. 849–851. doi: 10.1038/321849a0.

Strank, A. R. E. (1982) 'New Stratigraphically Significant Foraminifera From the Dinantian of Great Britain'. *Palaentology*, pp. 435–442.

Sweet, W. C. and Donoghue, P. C. J. (2001) 'Conodonts: Past, present, future', *Journal of Paleontology*. Paleontological Society, pp. 1174–1184. doi: 10.1017/S0022336000017224.

Tauxe, L. (2002) *Paleomagnetic principles and practice*. Kluwer Academic Publishers.

Tauxe, L. (2005) *Lectures in Paleomagnetism*. Available at: https://books.google.co.uk/books/about/Lectures_in_Paleomagnetism_2005.html?id=gx4nMwEACAAJ&redir_esc=y (Accessed: 27 November 2018).

Tauxe, L. *et al.* (2010) *Essentials of paleomagnetism*. University of California Press. Available at: <https://www.ucpress.edu/book/9780520260313/essentials-of-paleomagnetism> (Accessed: 3 December 2018).

Tauxe, L., Steindorf, J. and Harris, A. (2006) *Depositional remanent magnetization: Toward an improved theoretical and experimental foundation*, *Earth and Planetary Science Letters*. Available at: <http://scrippsscholars.ucsd.edu/ltauxe/content/depositional-remanent-magnetization-toward-improved-theoretical-and-experimental-foundation> (Accessed: 30 October 2019).

Tercyak, R. (2015) *Brachiopods*. Available at: <https://paleosoc.org/wp-content/uploads/2015/08/Brachiopods.pdf> (Accessed: 31 December 2018).

Thomas, P. R. *et al.* (2005) *Geology of the area between Lindale and Witherslack*.

Thominski, H. P., Wohlenberg, J. and Bleil, U. (1993) 'The remagnetization of Devonian-Carboniferous sediments from the Ardenno-Rhenish Massif', *Tectonophysics*, 225(4), pp. 411–431. doi: 10.1016/0040-1951(93)90307-6.

Thompson, A. and Poole, J. S. (2018) *Landscape Monitoring Project - Geology Audit and Assessment*.

Torsvik, T. H. *et al.* (1989) 'Palaeozoic palaeomagnetic results from Scotland and their bearing on the British apparent polar wander path', *Physics of the Earth and Planetary Interiors*, 55(1–2), pp. 93–105. doi: 10.1016/0031-9201(89)90236-7.

Torsvik, T. H. and Cocks, R. M. (2017) *Earth History and Palaeogeography*. Available at:

[https://books.google.cz/books?id=j6hsDQAAQBAJ&pg=PA271&lpg=PA271&dq=torsvik+climates+past+and+present&source=bl&ots=cFt_FeWzh4&sig=ACfU3U3SaeFPT7TM1zwjiiDdv4pel7_pEA&hl=cs&sa=X&ved=2ahUKEwj60qG2r4fpAhWUQEEAHanoAucQ6AEwAXoECAkQAQ#v=onepage&q=torsvik climates past and present&f=false](https://books.google.cz/books?id=j6hsDQAAQBAJ&pg=PA271&lpg=PA271&dq=torsvik+climates+past+and+present&source=bl&ots=cFt_FeWzh4&sig=ACfU3U3SaeFPT7TM1zwjiiDdv4pel7_pEA&hl=cs&sa=X&ved=2ahUKEwj60qG2r4fpAhWUQEEAHanoAucQ6AEwAXoECAkQAQ#v=onepage&q=torsvik%20climates%20past%20and%20present&f=false) (Accessed: 27 April 2020).

Turner, P., Metcalfe, I. and Tarling, D. H. (1979) 'Paleomagnetic studies of some Dinatian limestones from the Craven basin and a contribution to Asbian magnetostratigraphy', *Proceedings of the Yorkshire Geological Society*, 42, pp. 371–396.

Vachard, D. and Arefifard, S. (2015) 'Foraminifers and algae of the late Tournaisian-early Viséan boundary interval (MFZ8-9) in the Gachal Formation (Central Iran)', *Revue*

de Micropaleontologie. Elsevier Masson SAS, 58(3), pp. 185–216. doi: 10.1016/j.revmic.2015.07.001.

Van der Voo, R. (1993) *Paleomagnetism of the Atlantic, Tethys, and Iapetus oceans*. Cambridge University Press.

van der Voo, R. and Torsvik, T. H. (2012) ‘The history of remagnetization of sedimentary rocks: Deceptions, developments and discoveries’, *Geological Society Special Publication*. Geological Society of London, 371(1), pp. 23–53. doi: 10.1144/SP371.2.

Waters, C. N. *et al.* (2012) ‘Cumbria and the northern Pennines’, (2017), pp. 1–9.

Waters, C. N. *et al.* (2017) ‘Lithostratigraphy and biostratigraphy of the Lower Carboniferous (Mississippian) carbonates of the southern Askrigg Block, North Yorkshire, UK’, *Geological Magazine*, 154(2), pp. 305–333. doi: 10.1017/S0016756815000989.

Waters, C. N. and *et al.* (2011) *A Revised Correlation of Carboniferous Rocks in the British Isles* - C. N. Waters - *Knihy Google*. Bath. Available at: https://books.google.cz/books?hl=cs&lr=&id=B-anbPLFd7QC&oi=fnd&pg=PP5&dq=Waters+C.+N.+et+al+2011&ots=FMOA7f22Hy&sig=lqaL7clnvwoCdn_NMjjBkGCw2WM&redir_esc=y#v=onepage&q=Waters C. N. et al 2011&f=false (Accessed: 3 August 2019).

Wilson, R. L. and Everitt, C. W. F. (1963) ‘Thermal demagnetisation of some Carboniferous lavas for paleomagnetic purposes’, *Geophysical J. Roy. astronomical society*, 8, pp. 149–64.

Woodcock, N. H. and Strachan, R. A. (2012) *Geological history of Britain and Ireland*. John Wiley & Sons. Available at: <https://www.wiley.com/en->

us/Geological+History+of+Britain+and+Ireland%2C+2nd+Edition-p-9781405193825

(Accessed: 12 December 2018).

Worm, H. -U and Jackson, M. (1988) 'Theoretical time-temperature relationships of magnetization for distributions of single domain magnetite grains', *Geophysical Research Letters*, 15(10), pp. 1093–1096. doi: 10.1029/GL015i010p01093.

Zegers, T. E., Dekkers, M. J. and Bailly, S. (2003) 'Late Carboniferous to Permian remagnetization of Devonian limestones in the Ardennes: Role of temperature, fluids, and deformation', *Journal of Geophysical Research: Solid Earth*. American Geophysical Union (AGU), 108(B7). doi: 10.1029/2002jb002213.

